Mechanisms of amyloid fibril formation by proteins

Jayant Udgaonkar
National Centre for Biological Sciences
Tata Institute of Fundamental research
Bangalore, India

How do proteins fold, unfold and misfold?

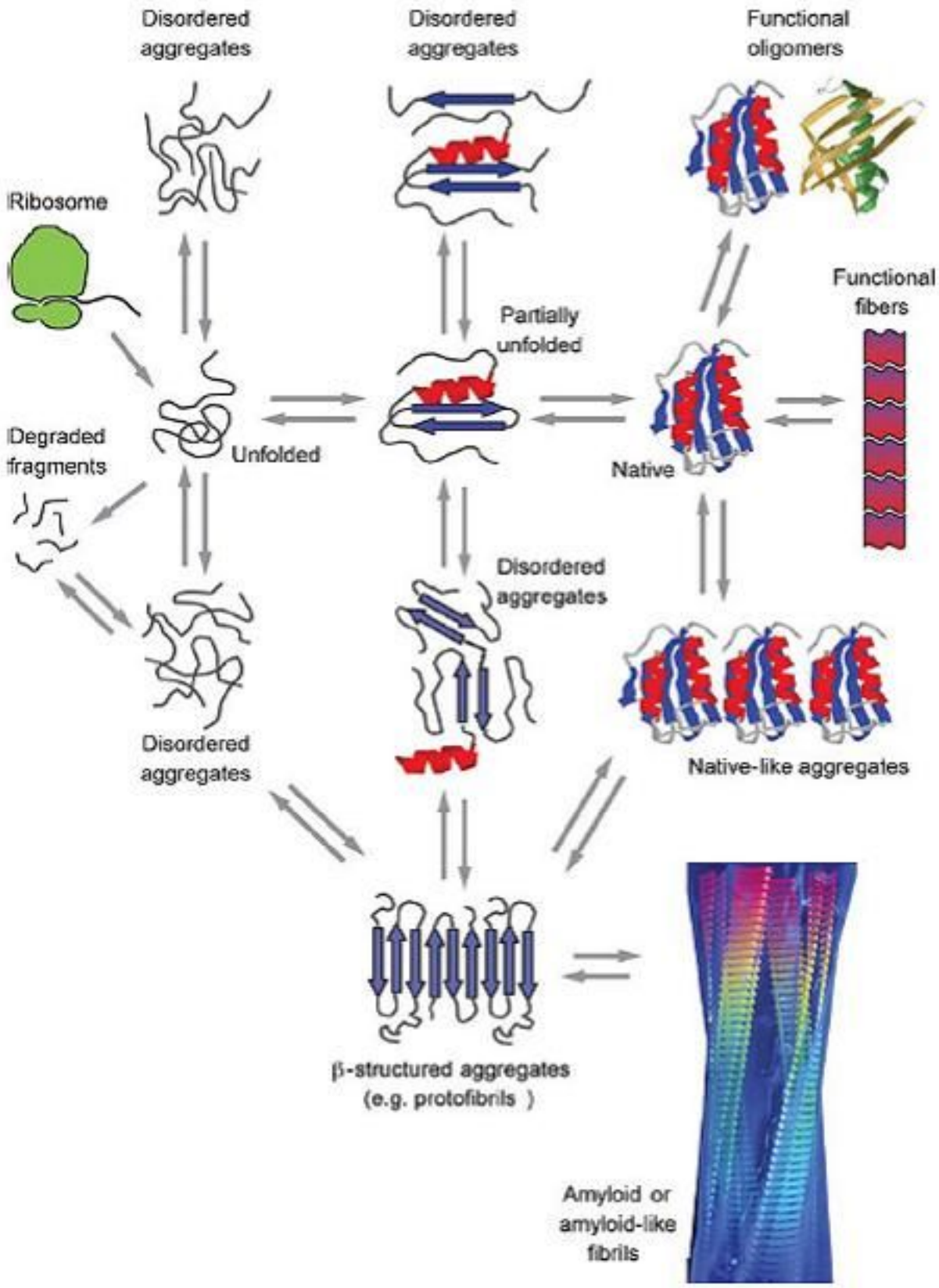

MOLECULAR PLAYERS IN THE LABORATORY

Barstar
Thioredoxin
Monellin
PI3K SH3 domain
GroEL
α-synuclein
Prion protein
Tau protein

Ribonuclease A
Cytochrome *c*
GFP
Barnase

Transient protein aggregation can be a problem

during protein folding as well as during protein unfolding

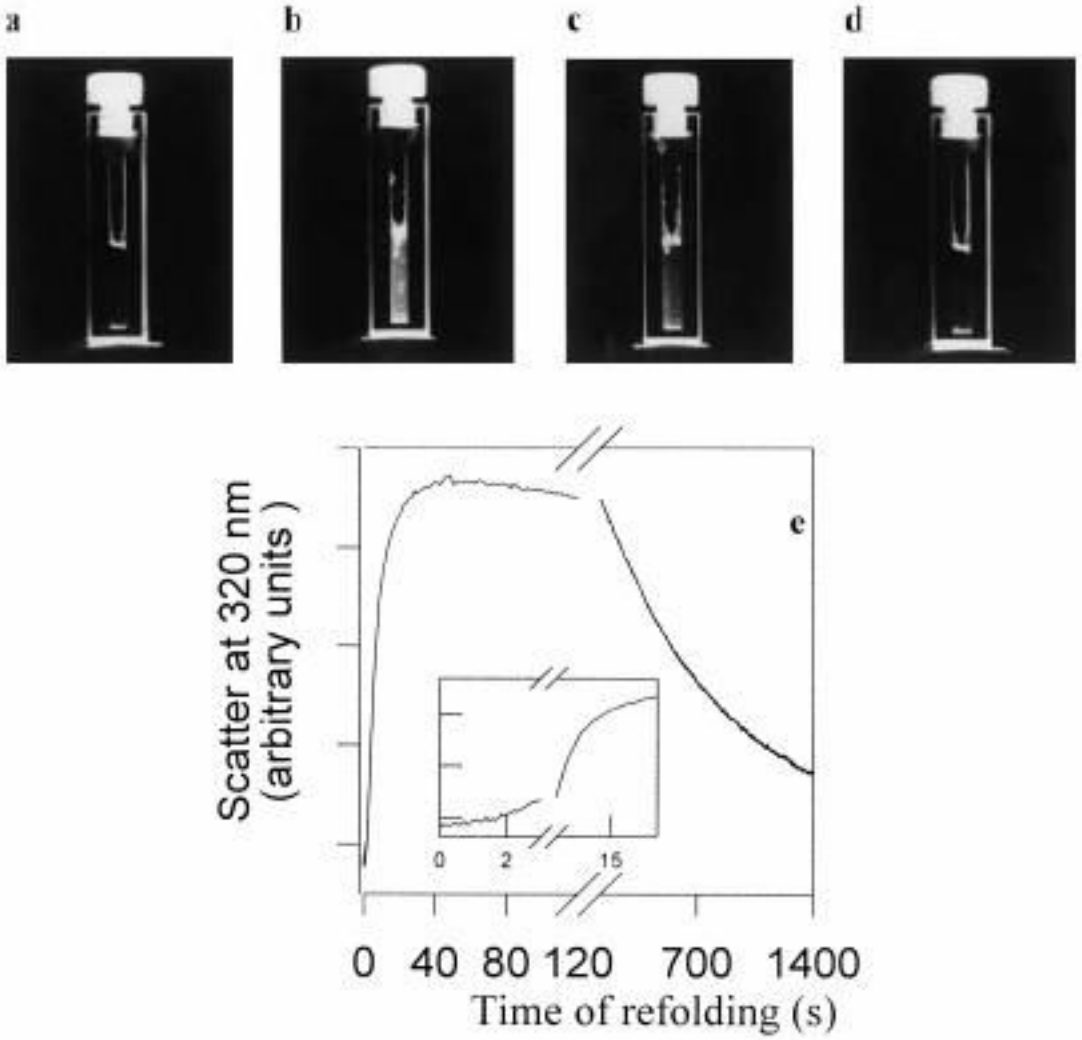

Reversible formation of on-pathway macroscopic aggregates during the folding of maltose binding protein

C. GANESH,[1,4] FAISAL. N. ZAIDI,[2] JAYANT. B. UDGAONKAR,[2] AND RAGHAVAN VARADARAJAN[1,3]

Protein Science (2001), 10:1635–1644.

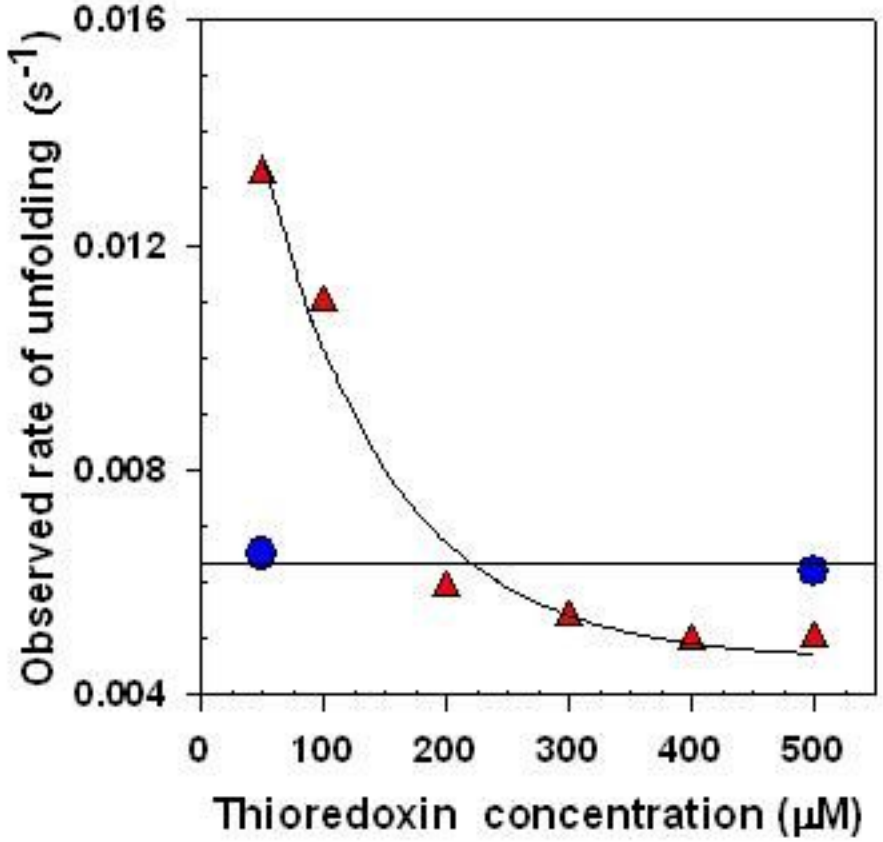

Reversible formation of aggregate during the unfolding of thioredoxin at pH 3 but not at pH 7

Ajazul Wani and Jayant Udgaonkar (2007) Biochemistry

Thioredoxin unfolds via an amyloidogenic intermediate at low pH

Hamid & Udgaonkar (2007) *Biochemistry*

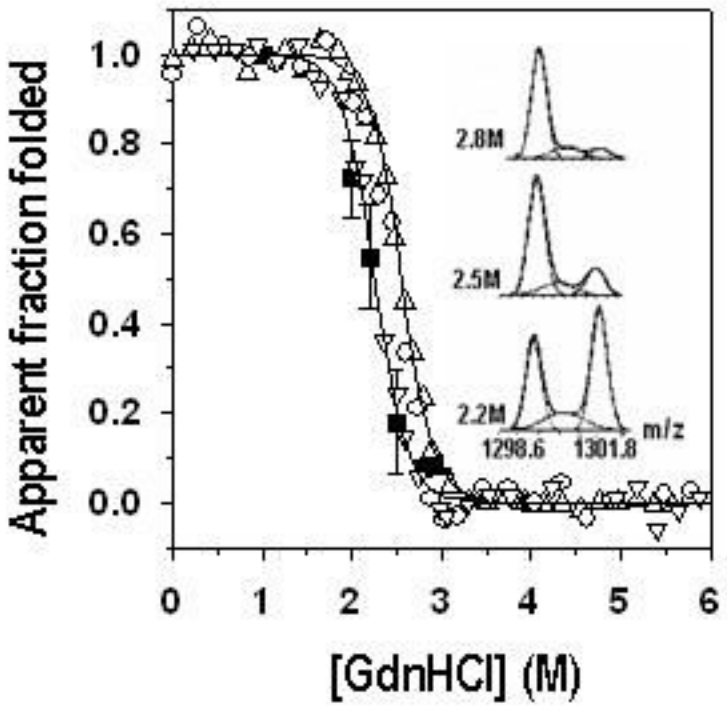

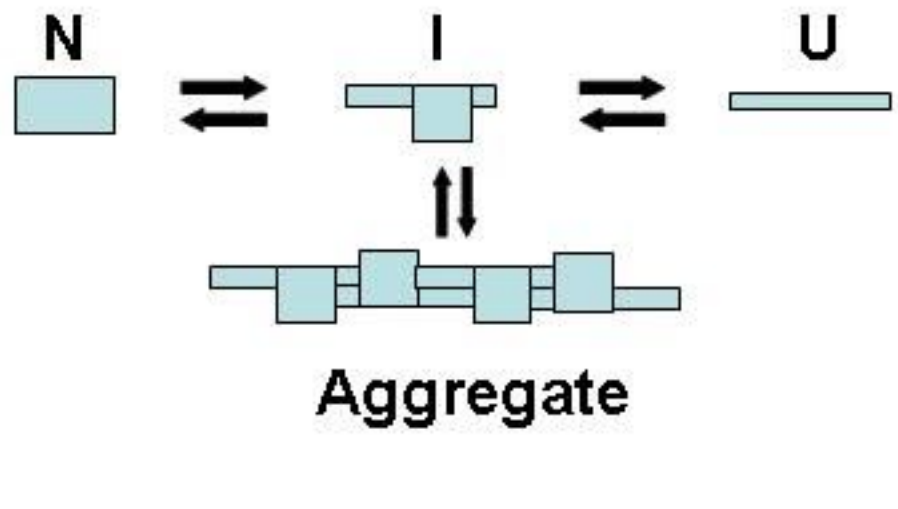

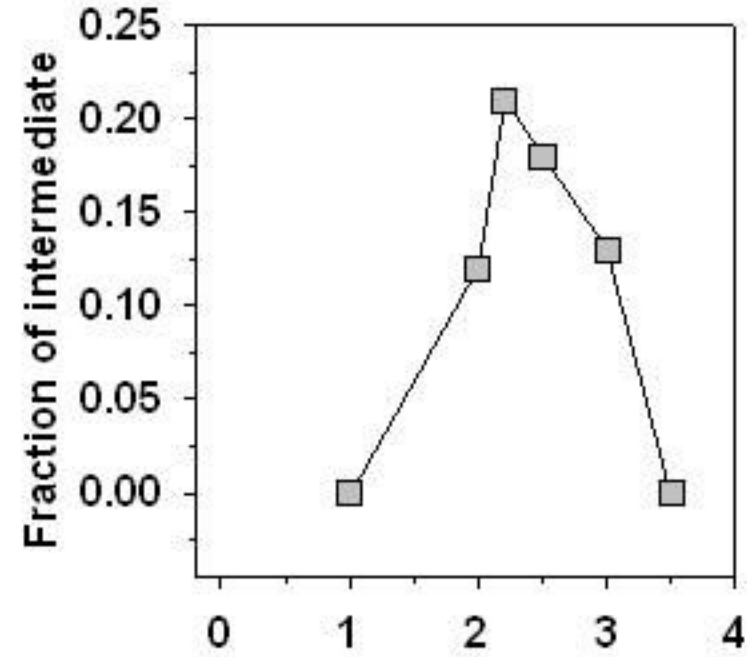

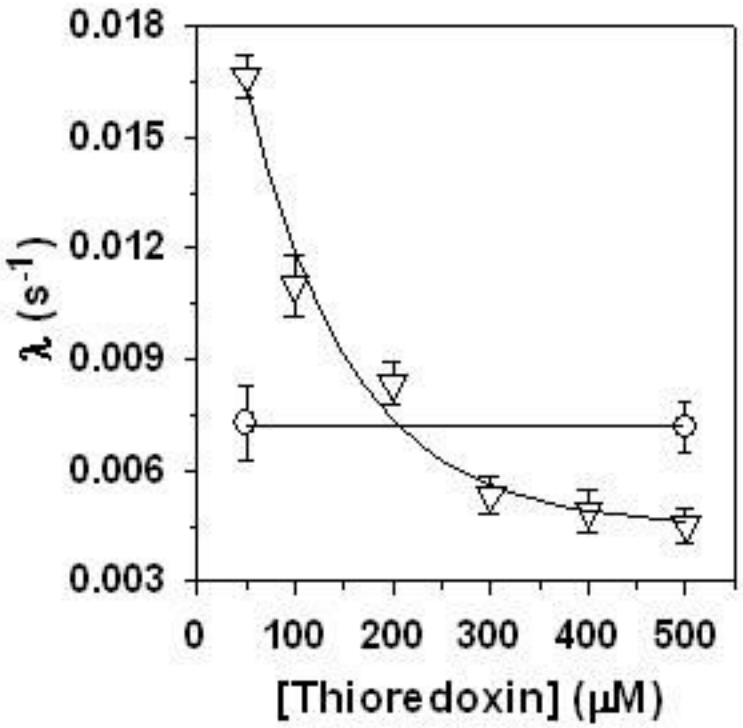

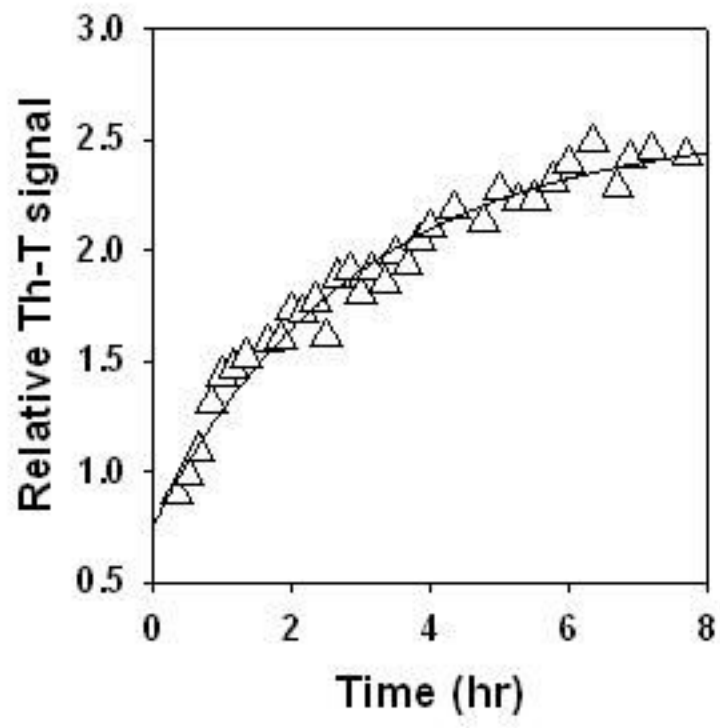

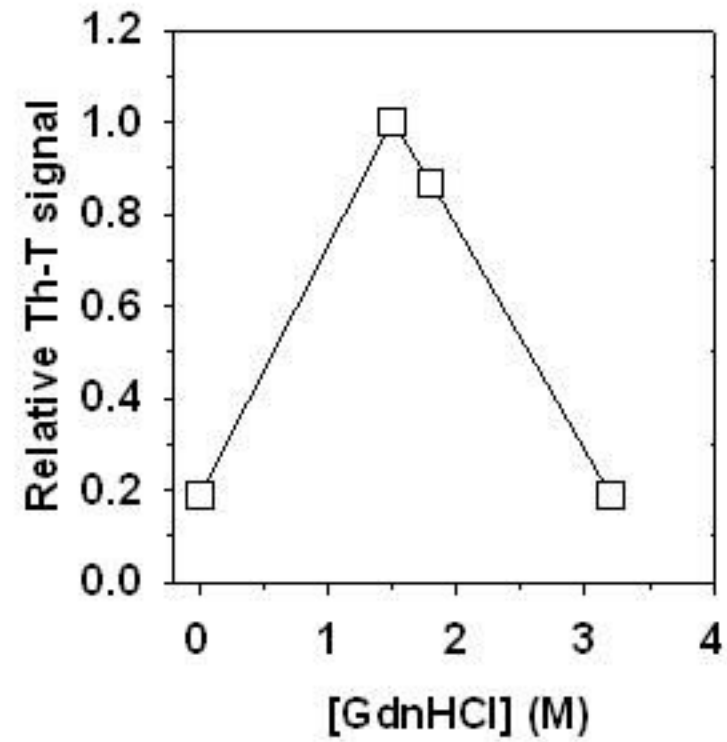

Mechanisms of amyloid fibril formation by proteins

CURRENT SCIENCE, VOL. 98, NO. 5, 10 MARCH 2010

Santosh Kumar and Jayant B. Udgaonkar*

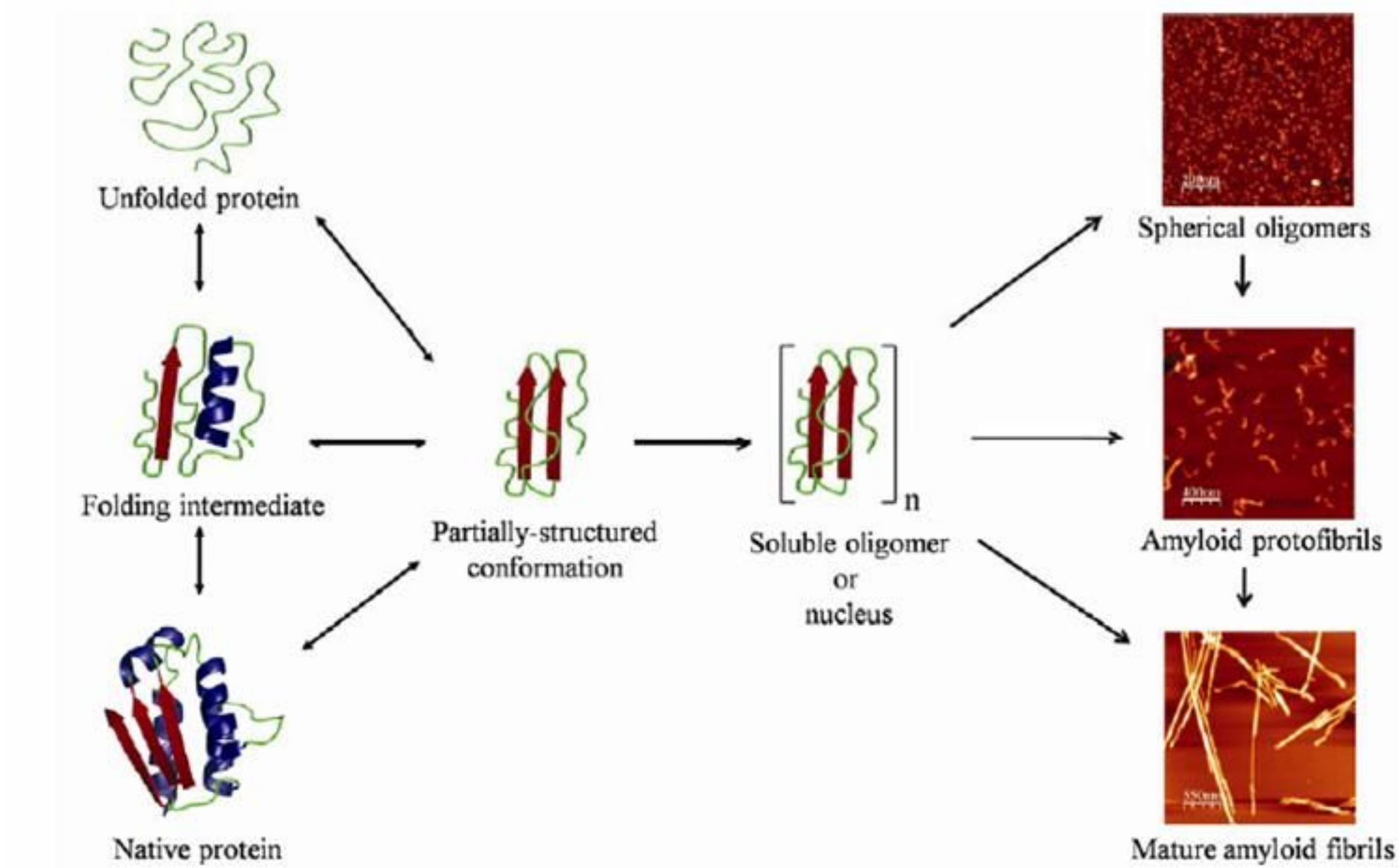

Figure 3. Protein folding and amyloid formation. Amyloid fibril formation commences from partially (un)folded conformers, which can form by partial unfolding of globular proteins, partial folding of natively unfolded proteins, or by conformational change in folding intermediates. These partially (un)folded amyloidogenic conformations self-assemble into amyloid fibrils. During the amyloid fibril formation reactions of many proteins, the conversion of partially (un)folded conformations into fibrils occurs through pre-fibrillar aggregates (spherical oligomers and/or protofibrils). The scale bars in the atomic force microscopy images of spherical oligomers, protofibrils and mature fibrils represent, respectively 200, 400 and 550 nm.

Ordered protein aggregates are associated with several human disorders

Amyloid precursor proteins and their associated diseases.

Precursor protein	Associated diseases
Amyloid β precursor protein	Alzheimer's disease
	Hereditary cerebral hemorrhage with amyloidosis, Dutch type
Apolipoprotein AI	Hereditary renal amyloidosis
	Familial amyloid polyneuropathy, type III
Apolipoprotein AII	Hereditary systemic amyloidosis
Atrial natriuretic protein	Isolated atrial amyloid
BRI precursor protein variants	Familial British dementia
	Familial Danish dementia
Calcitonin	Medullary thyroid carcinoma
Cystatin C	Hereditary cerebral hemorrhage with amyloidosis, Icelandic type
Fibrinogen Aα-chain variants	Hereditary renal amyloidosis
Gelsolin	Familial amyloidosis, Finnish type
Immunoglobulin heavy chain	Primary systemic amyloidosis
	Myeloma-associated amyloidosis
Immunoglobulin light chain	Primary systemic amyloidosis
	Myeloma-associated amyloidosis
Insulin	Insulin-related amyloidosis
Islet amyloid polypeptide (amylin)	Type II diabetes
Kerato-epithelin	Lattice dystrophies of the cornea
Lactoferrin	Familial corneal amyloidosis
Lysozyme	Hereditary systemic amyloidosis
	Hereditary renal amyloidosis
Medin (lactadherin fragment)	Aortic medial amyloidosis
β_2-microglobulin	Hemodialysis-related amyloidosis
Prolactin	Aging pituitary
	Senile hypophyseal prolactinoma
Serum amyloid A	Secondary systemic amyloidosis
	Familial Mediterranean fever
	Muckle–Wells syndrome
Transthyretin	Senile systemic amyloidosis
	Familial amyloid polyneuropathy, types I and II
	Familial amyloid cardiomyopathy
Prion protein	Kuru
	Creutzfeldt–Jakob disease
	Fatal familial insomnia
	Gerstmann-Sträussler-Scheinker disease

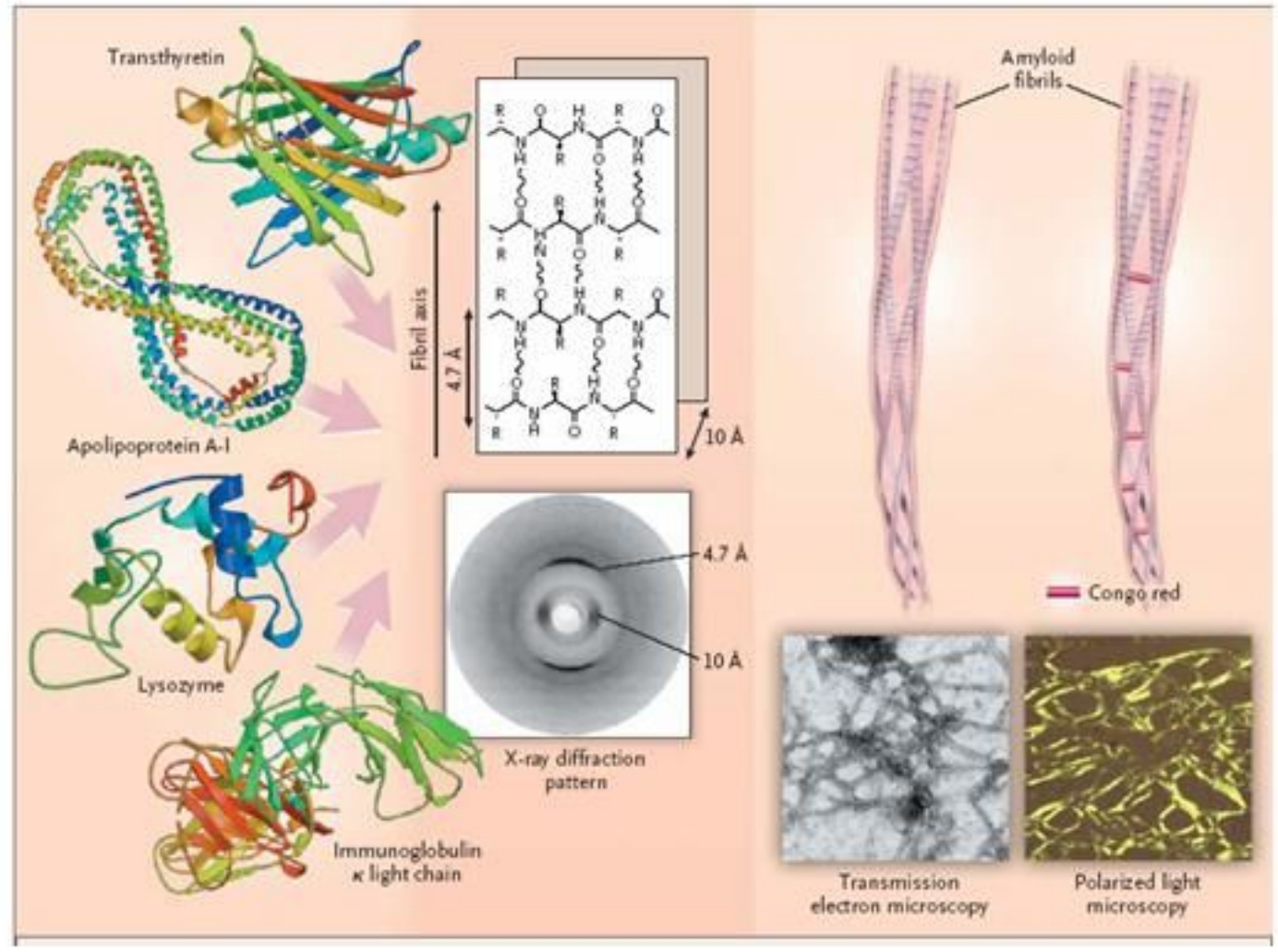

Is there a common mechanism for amyloid fibril formation?

Table 2 Proteins forming naturally nonpathological amyloid-like fibrils with specific functional roles

Protein	Organism	Function of the resulting amyloid-like fibrils	References
Curlin	*Escherichia coli* (bacterium)	To colonize inert surfaces and mediate binding to host proteins	22
Chaplins	*Streptomyces coelicolor* (bacterium)	To lower the water surface tension and allow the development of aerial hyphae	23
Hydrophobin[a] EAS	*Neurospora crassa* (fungus)	To lower the water surface tension and allow the development of aerial hyphae	23a
Proteins of the chorion of the eggshell[b]	*Bombyx mori* (silkworm)	To protect the oocyte and the developing embryo from a wide range of environmental hazards	23b
Spidroin	*Nephila edulis* (spider)	To form the silk fibers of the web	23c
Intralumenal domain of Pmel17	*Homo sapiens*	To form, inside melanosomes, fibrous striations upon which melanin granules form	24
Ure2p (prion)	*Saccharomyces cerevisiae* (yeast)	To promote the uptake of poor nitrogen sources ([URE3])	25
Sup35p (prion)	*Saccharomyces cerevisiae* (yeast)	To confer new phenotypes ([PSI+]) by facilitating the readthrough of stop codons on mRNA	26–28
Rnq1p (prion)	*Saccharomyces cerevisiae* (yeast)	Not well understood ([RNQ+], also known as [PIN+], phenotype)	28a
HET-s (prion)	*Podospora anserina* (fungus)	To trigger a complex programmed cell death phenomenon (heterokaryon incompatibility)	31, 32
Neuron-specific isoform of CPEB (prion)	*Aplisia californica* (marine snail)	To promote long-term maintenance of synaptic changes associated with memory storage	30

Yeast prions are not functionally or structurally related to their mammalian namesakes

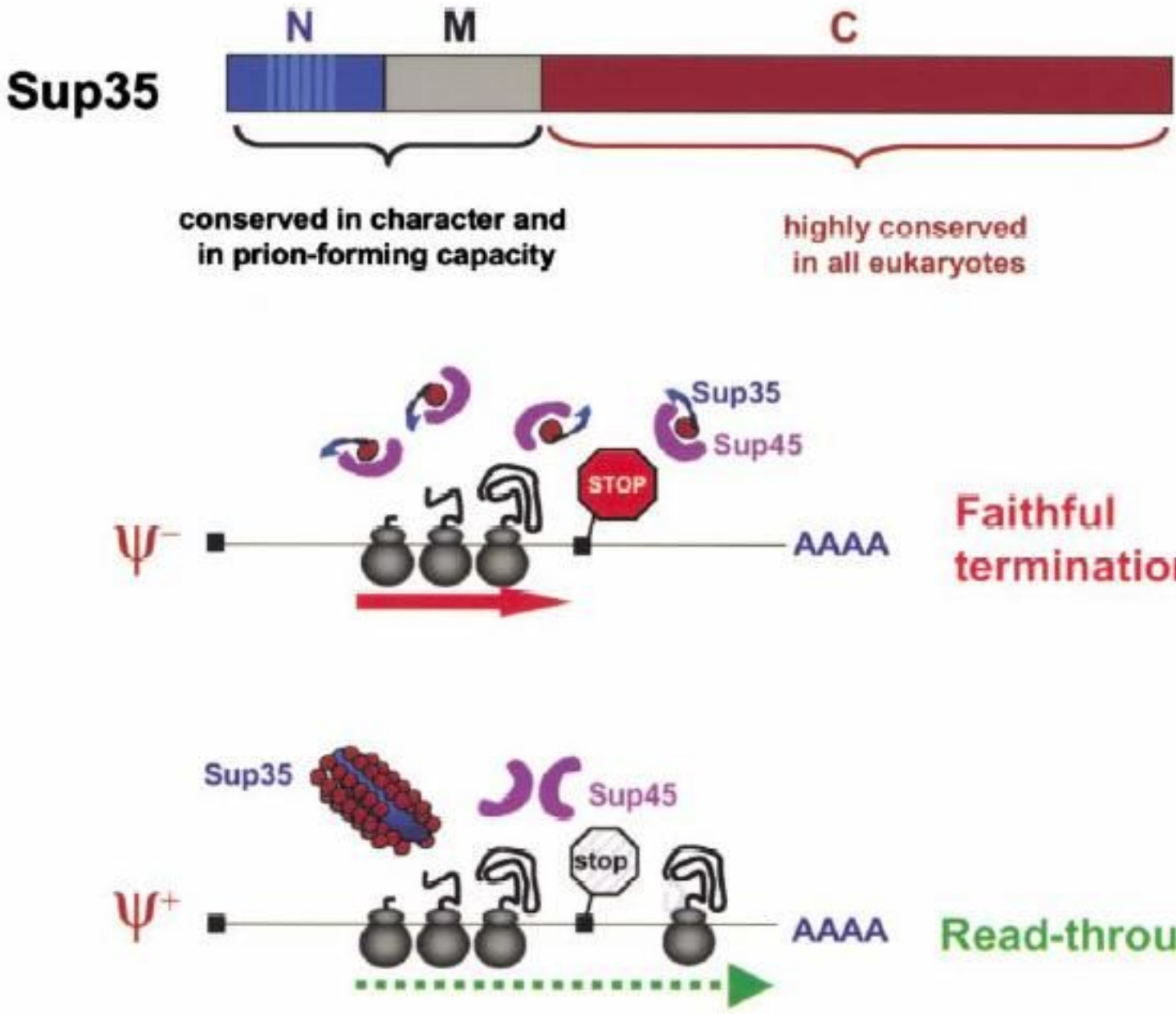

Figure 3. Function of the Yeast Prion, Sup35

(A) Sup35 consists of an amino-terminal glutamine-rich module crucial for conversion into the prion state.

(B) In the ψ^- state, Sup35 is required for reliable termination of translation.

(C) In ψ^+ yeast cells, however, Sup35 is sequestered in ordered fibrillary aggregates. Shortage of functional Sup35 leads to transgressions in stop codon recognition and translation of downstream reading frames (red line). In the off state, such pseudogenes may accumulate otherwise toxic mutations. Acquisition of the on (ψ^+) state may lead to the appearance of new phenotypes, hence increasing the complexity of genetic variability.

Structures of amyloid fibrils

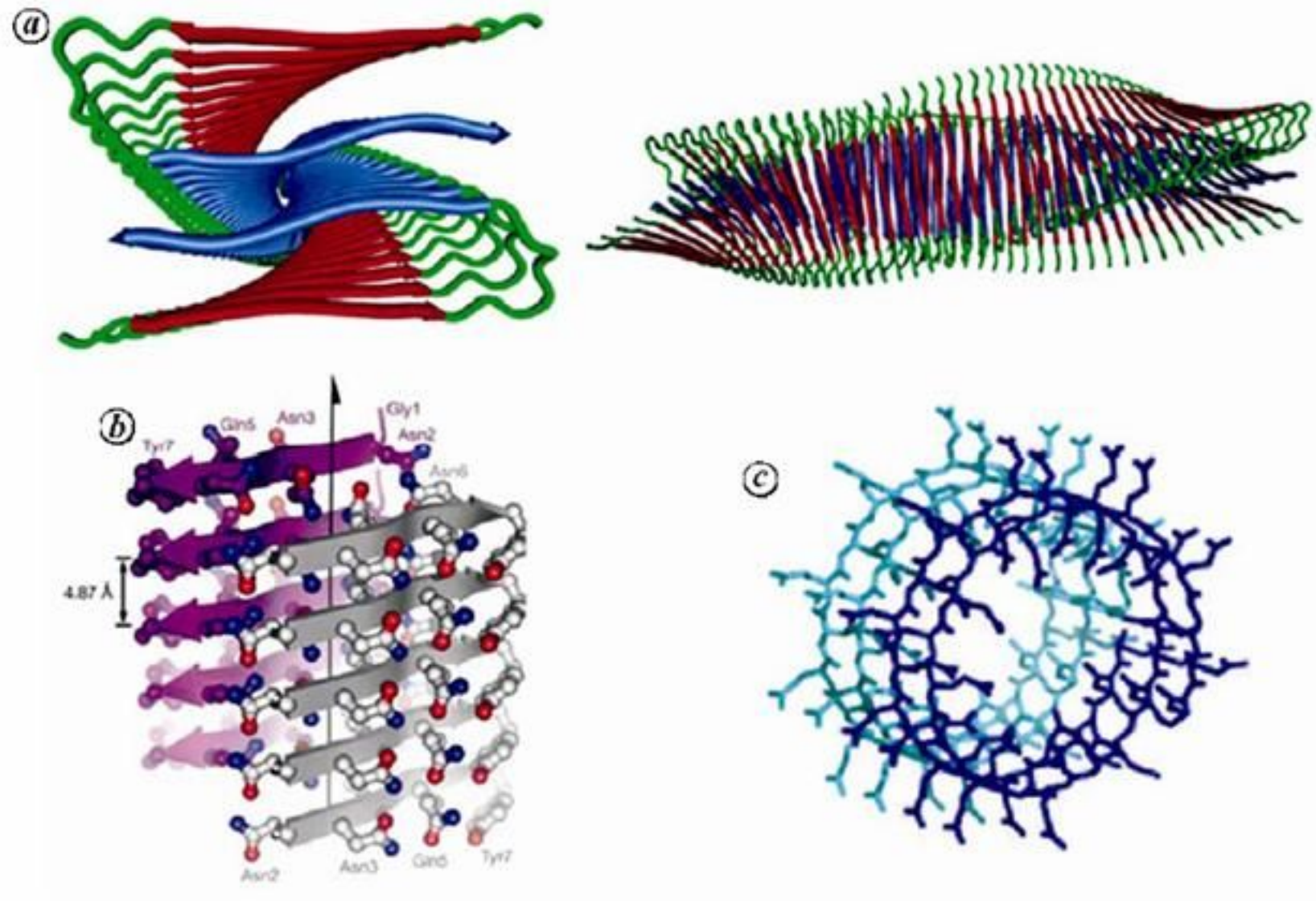

Figure 1. Structural models of amyloid fibrils. *a*, Ribbon diagram of an amyloid-β_{1-40} protofilament, as viewed parallel (left panel) and perpendicular (right panel) to the fibril axis. This structural model is based on solid-state NMR data combined with constraints from electron microscopy data. Each Aβ molecule contributes two β-strands in the parallel β-sheets. Reprinted with permission from Petkova *et al.*[44]. *b*, Steric zipper, the cross-β motif in the fibrils of GNNQQNY. Each arrow represents the backbone of the β-strand. The side chains from the two β-strands intercalate to form a dry interface between them. Reprinted with permission from Nelson *et al.*[47]. *c*, β-helix structure of polyglutamine (PolyQ) fibrils[50]. A stick model of two stacked subunits of Q_{42} is shown. Reprinted from Singer and Dewji[51].

Conformational heterogeneity in amyloid fibrils

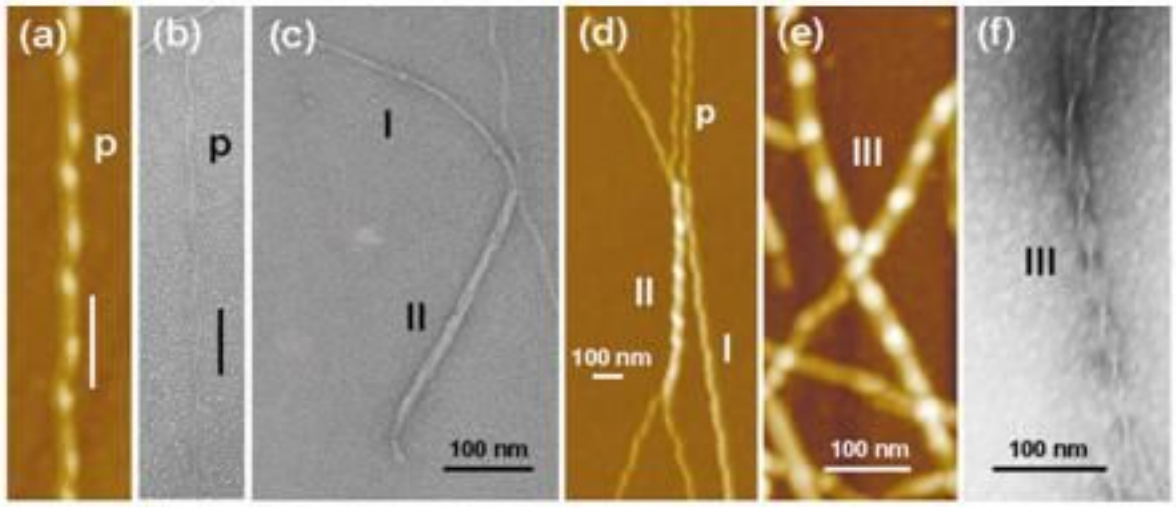

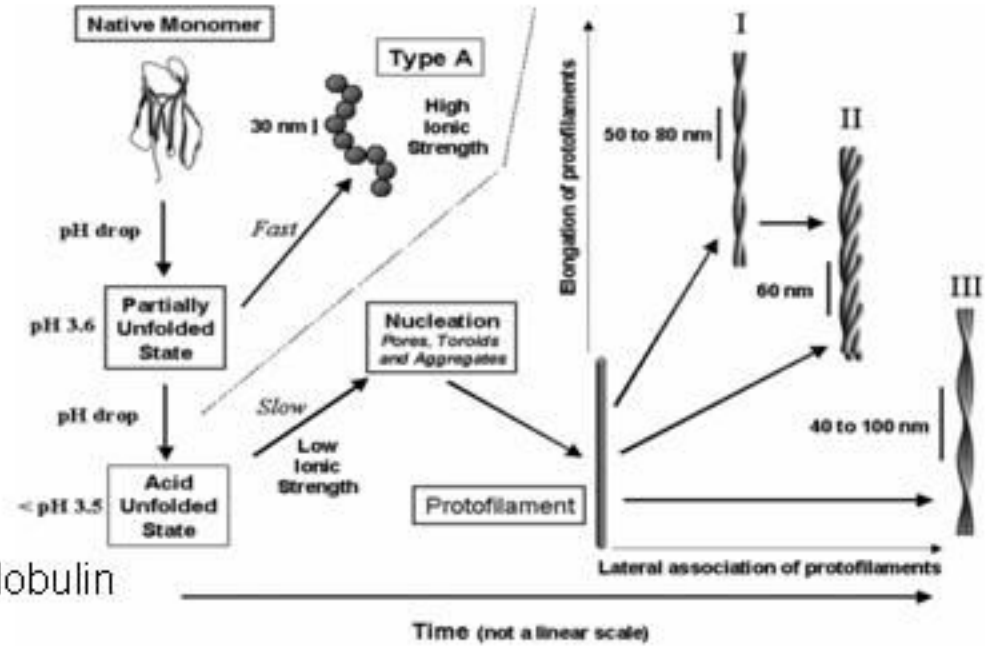

β_2 microglobulin

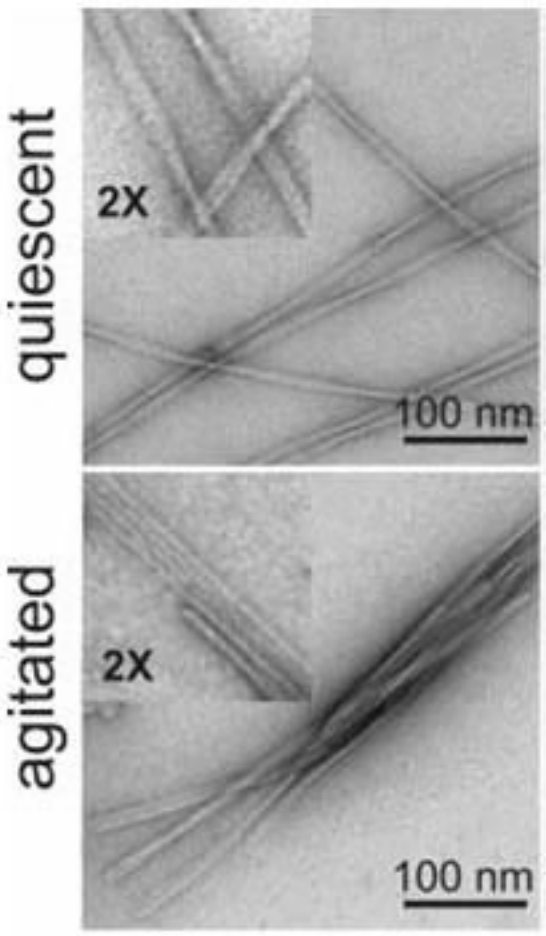

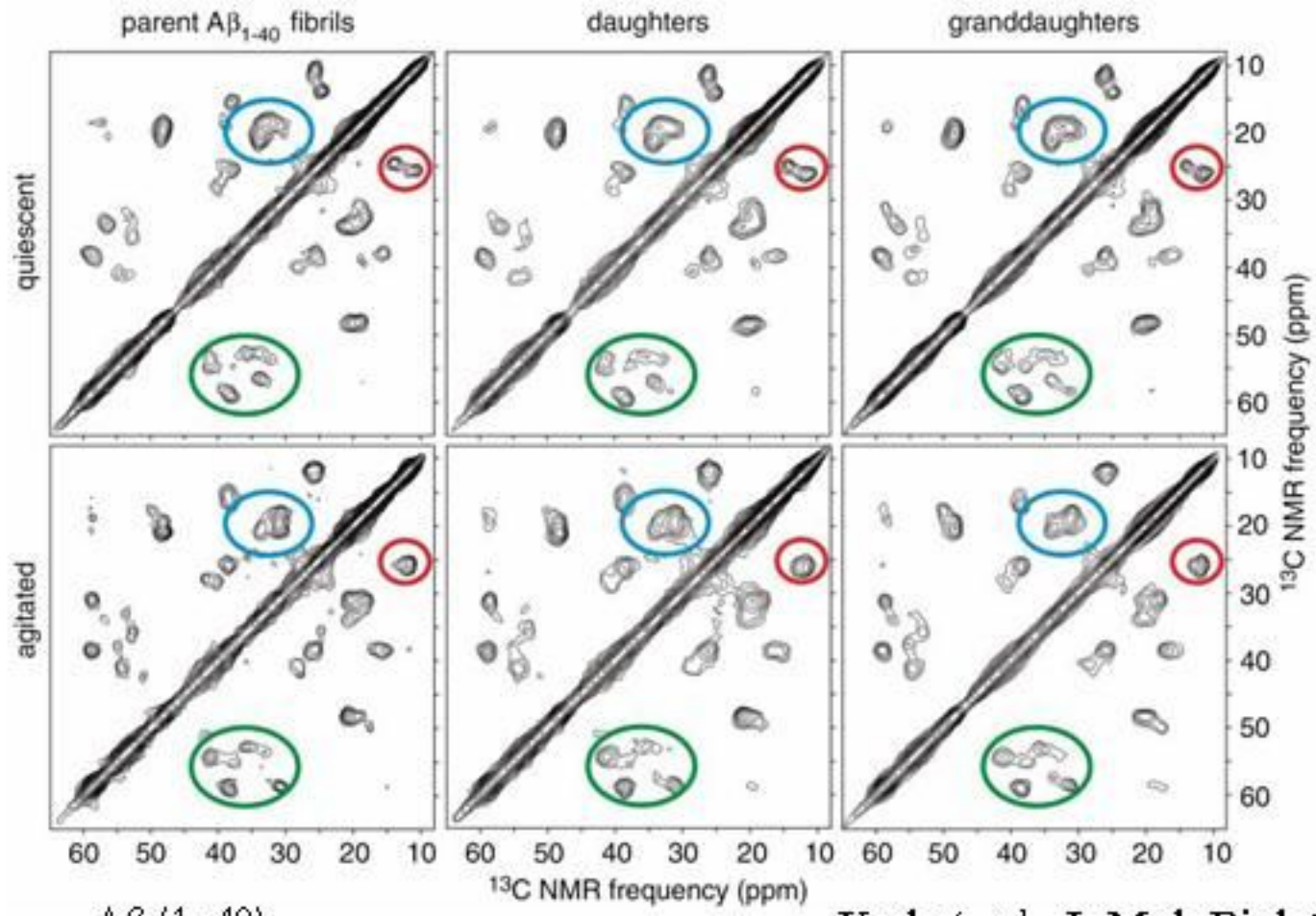

Aβ (1–40)

Kad *et. al.*, J. Mol. Biol. 330, 785–797, 2003
Petkova *et. al.*, Science, 307, 262-265, 2005

Prion strain diversity and fibril conformation

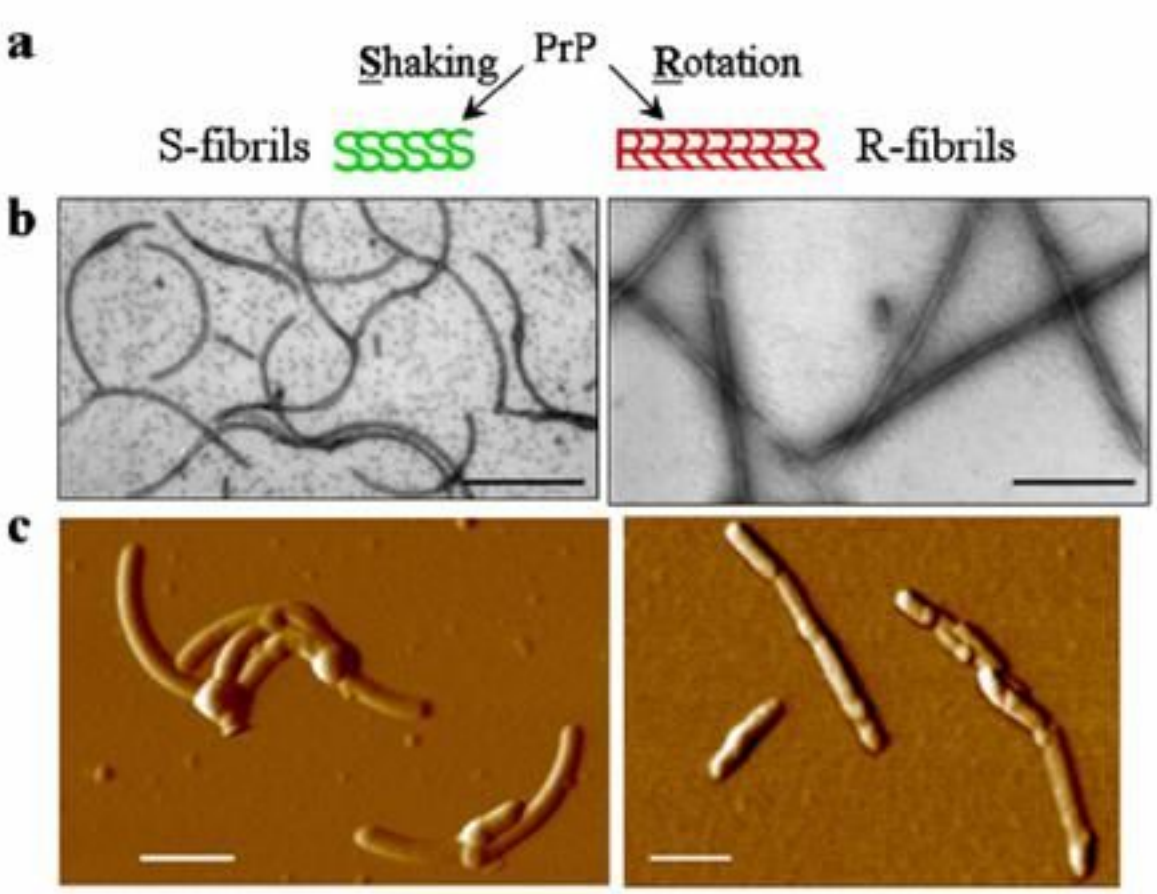

Makarava and Baskakov (2008) J. Biol. Chem

A

```
        55 56  72  80   97 109  112  138 139  143
hu   K-G  G---G---G----S---M----M---  I   I  ----S   D
mo   K-   T---S---S----N---L----V---  M   I  ----N   D
Sha  K-G  T---G---G----N---M----M---  M   M  ----N   D
    23                                              144
```

B

Seed	Protein Monomer					Equivalent to
	hu	mo	Sha	hu138	hu138/139	
[hu]	+	+	-	+	-	
[mo]	+	+	-	+	-	
[Sha]	-	+	+	+	+	
$[mo]_{Sha}$	-	+	+	N/D	N/D	[Sha]; [hu138/139]
[hu138]	+	+	-	+	-	[mo]
[hu138/139]	-	+	+	+	+	[Sha]
$[hu138]_{hu138/139}$	-	+	+	+	+	[hu138/139]; [Sha]
[Sha138/139]	+	N/D	-	N/D	N/D	[hu]

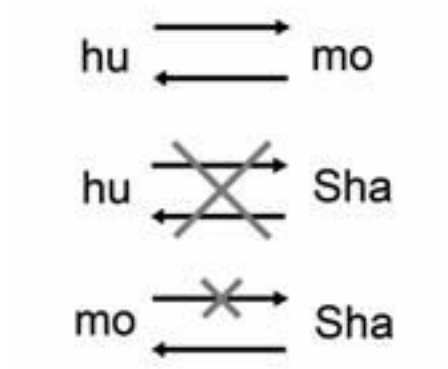

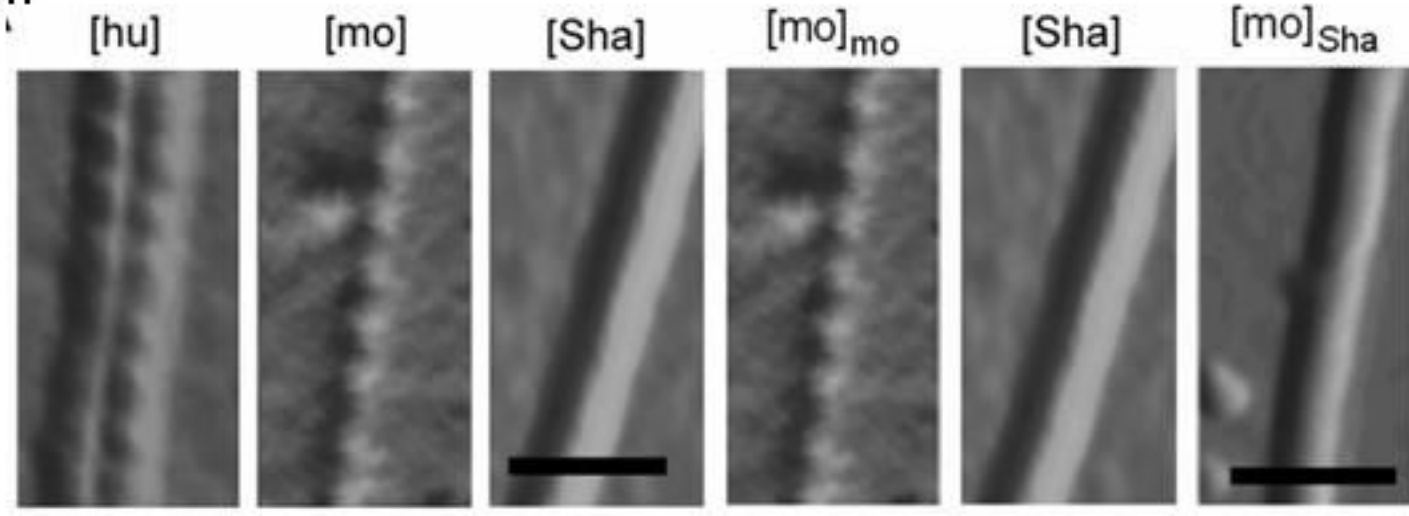

Jones and Surewicz (2005) Cell

Amyloid fibril formation and disease

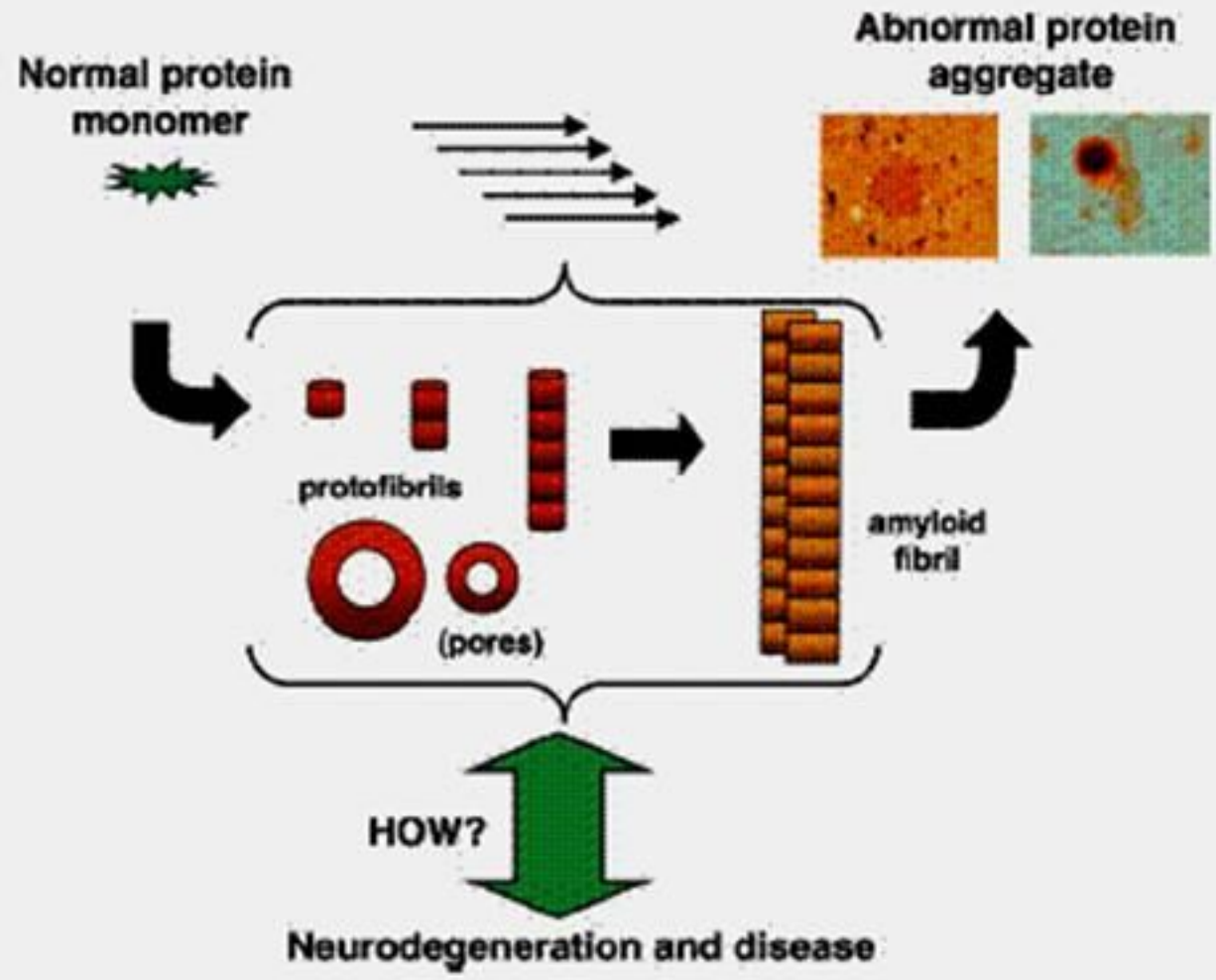

Figure 1 A general mechanistic scheme combining information from studies of ex vivo and in vitro protein aggregation. The conversion of normal proteins, such as α-synuclein and Aβ, into disease-associated deposits, such as amyloid plaques in AD (image at *left*) and Lewy bodies in PD (image at *right*), occurs via a multi-step process involving the intermediacy of oligomeric forms that are less stable but potentially more toxic than the end-product fibril. The mechanism by which these intermediates may cause neuronal dysfunction and death is not clear.

Evidence of fibril-like β-sheet structures in a neurotoxic amyloid intermediate of Alzheimer's β-amyloid

Sandra Chimon, Medhat A Shaibat, Christopher R Jones, Diana C Calero, Buzulagu Aizezi & Yoshitaka Ishii

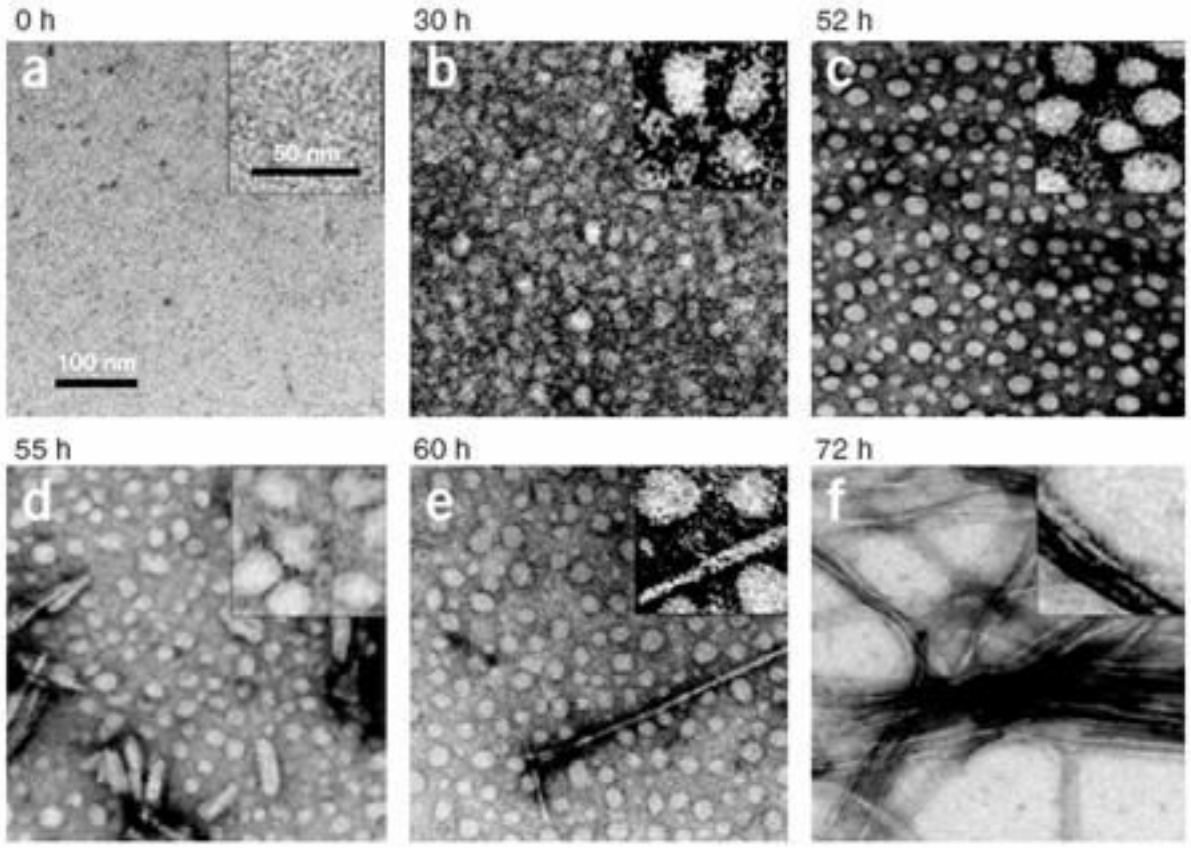

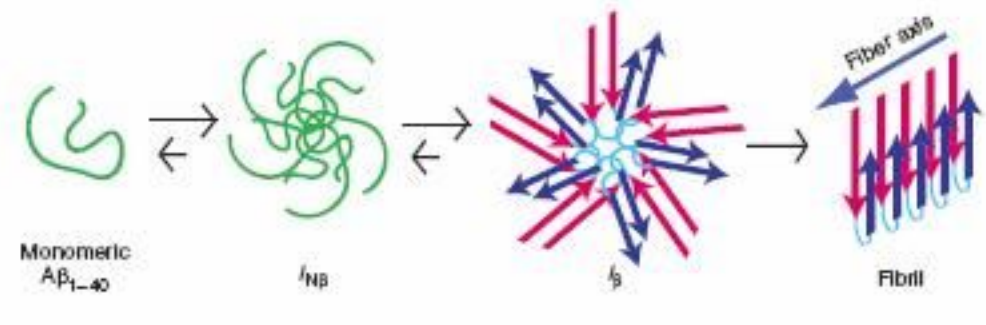

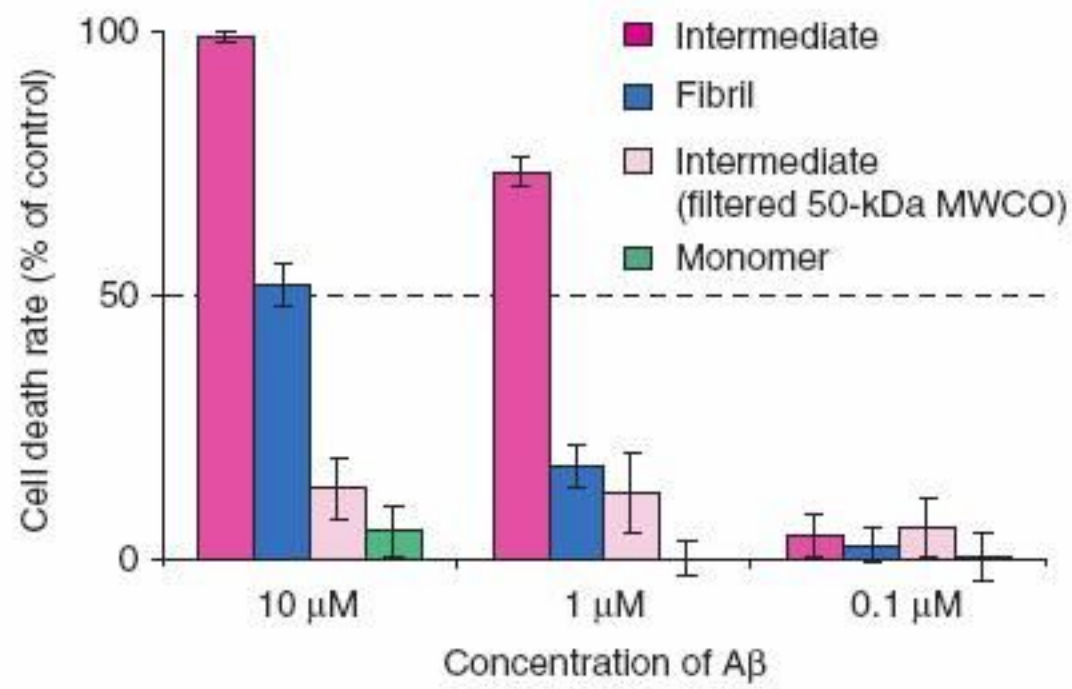

Membrane Permeabilization: A Common Mechanism in Protein-Misfolding Diseases

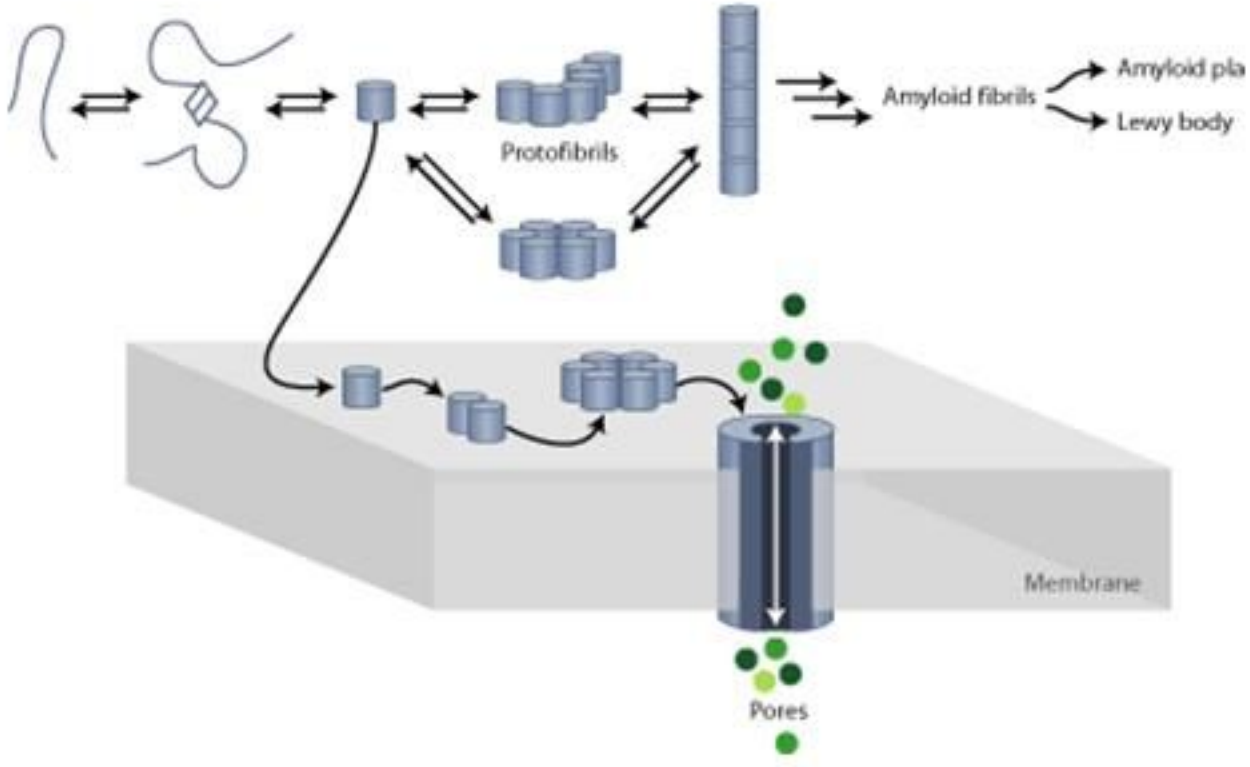

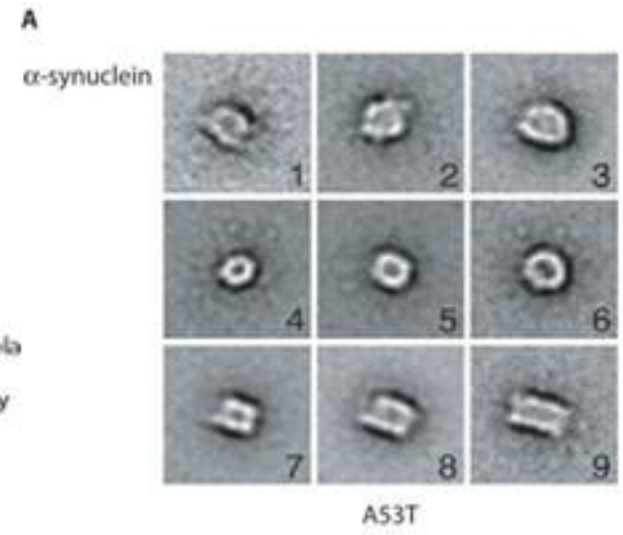

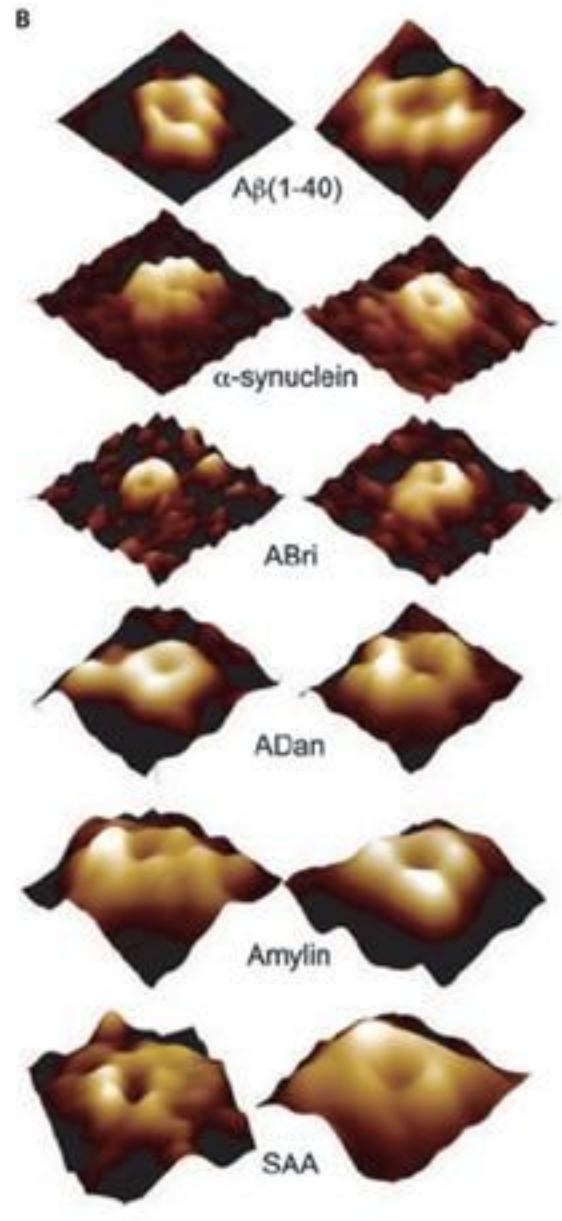

H. A. Lashuel, Sci. Aging Knowl. Environ. 2005, pe28 (2005)

Barstar forms a soluble oligomer (the A form) at low pH

- It exists as a symmetrically arranged aggregate of 16 monomeric subunits
- The aggregate appears to have a rigid core, but with the N-terminal 20 residues of each monomeric subunit in a highly dynamic random coil conformation, which shows transient local ordering of structure.

(Khurana & Udgaonkar, 1994; Khurana et al, 1995; Juneja & Udgaonkar, 2002)

Native state

A form

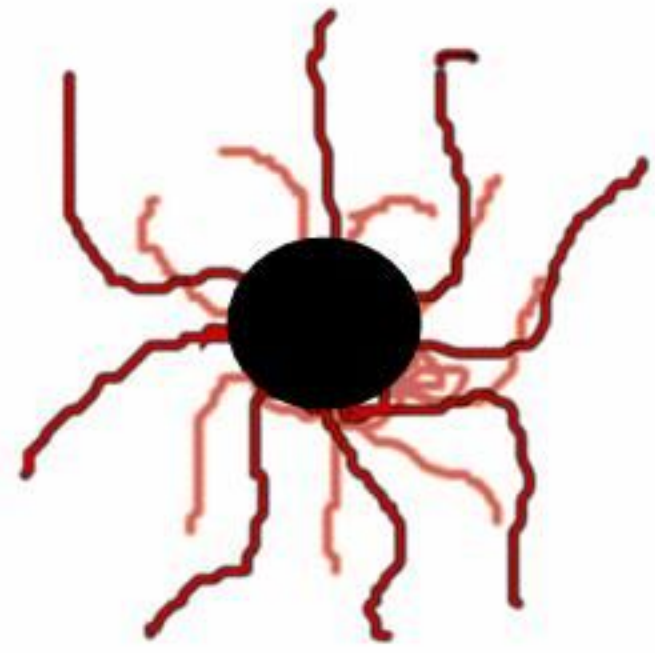

Mechanism of Formation of Amyloid Protofibrils of Barstar from Soluble Oligomers: Evidence for Multiple Steps and Lateral Association Coupled to Conformational Conversion

Santosh Kumar, Subhendu K. Mohanty and Jayant B. Udgaonkar*

J. Mol. Biol. (2007) **367**, 1186–1204

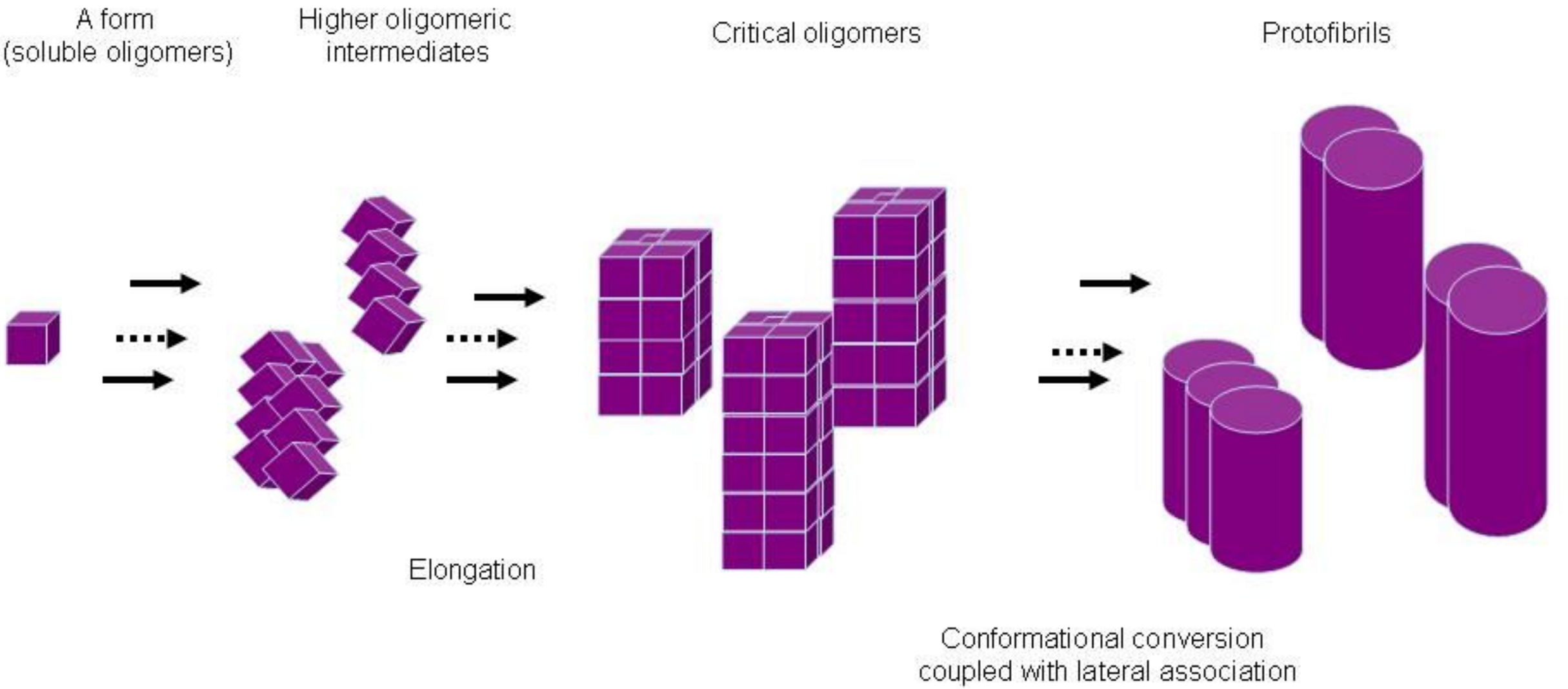

Aggregation is progressive.
Lateral association is coupled to conformational conversion.

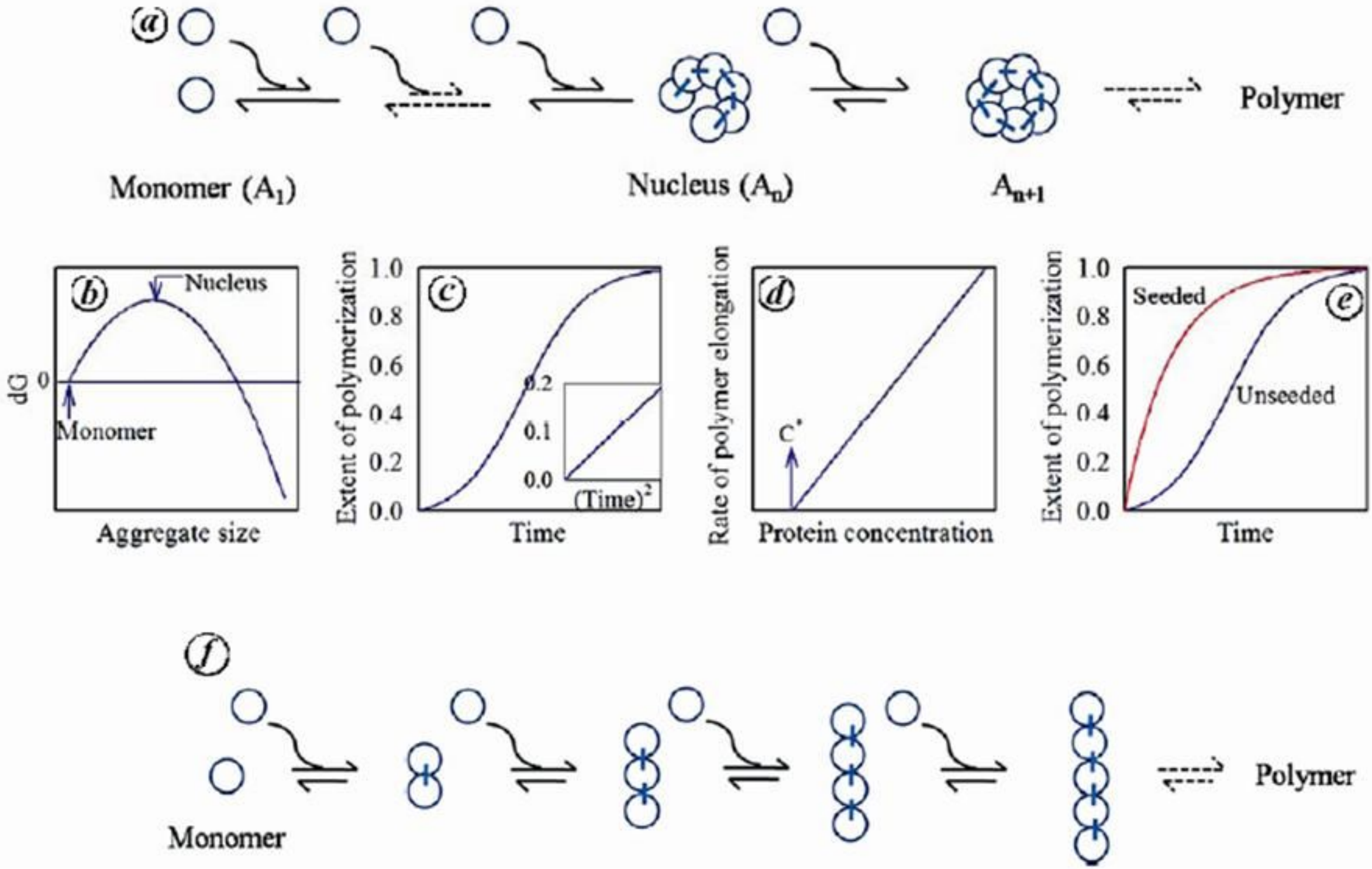

Figure 2. Protein aggregation reactions. *a*, Schematic of an NDP reaction showing nucleation and elongation phases. *b*, Free energy barrier in an NDP reaction. Panels *c*–*e* show the three characteristic kinetic features of an NDP reaction, namely, the presence of a lag phase (*c*); A critical concentration C* (*d*); Removal of the lag phase by seeding (*e*). *f*, Schematic of an isodesmic polymerization reaction.

Nucleation of a phase transition

To form a B-rich phase in a meta-stable solution of components A and B requires that enough B molecules come together to form a nucleus that is so large that further growth of the B-rich phase will be spontaneous

The process of nucleation is the formation of this critical nucleus, which requires that the system reach the top of an energy barrier

The free energy ΔG of forming a spherical droplet that nucleates a phase transition has 2 contributions

$$\Delta G = 4\pi r^2 \gamma - \frac{4}{3}\pi r^3 \varepsilon_0$$

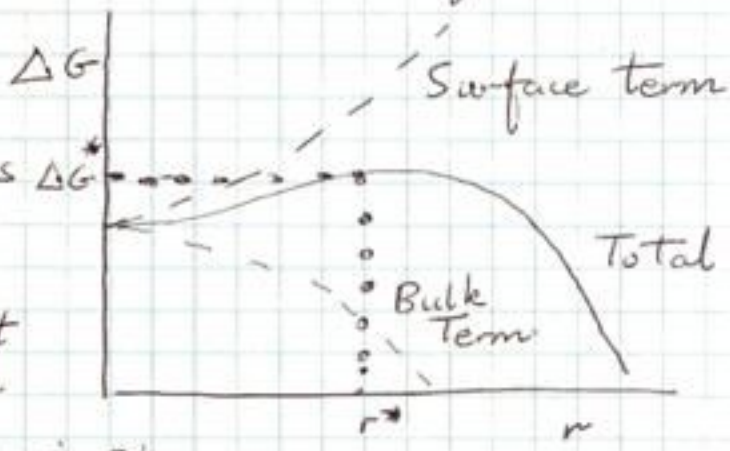

Growth is driven by ε_0 the energy per unit volume for forming BB contacts inside the droplet

Growth is opposed by the surface tension γ between the B rich droplet and the A rich solution

The radius r^* of the critical nucleus is the point at which $\Delta G(r^*) = \Delta G^*_{crit}$ is a maximum

$$\left.\frac{d\Delta G}{dr}\right|_{r^*} = 0 \longrightarrow r^* = \frac{2\gamma}{\varepsilon_0}$$

A large surface tension γ implies that large droplets are required to nucleate the phase transition

$$\Delta G_{crit} = 4\pi (r^*)^2 \left[\gamma - \frac{r^* \varepsilon_0}{3} \right]$$

$$= \frac{16\pi\gamma^2}{3\varepsilon_0^2}$$

Droplet formation is an activated process. The rate of forming a droplet is proportional to $\exp(-\Delta G_{crit}/kT)$.

Passive Polymerization

$$A_n + A_1 \underset{k_{off}}{\overset{k_{on}}{\rightleftharpoons}} \frac{[A_n][A_1]}{[A_{n+1}]} = K = \frac{k_{off}}{k_{on}} \quad n \geq 1$$

A_1 is the monomer, A_n denotes the n-mer

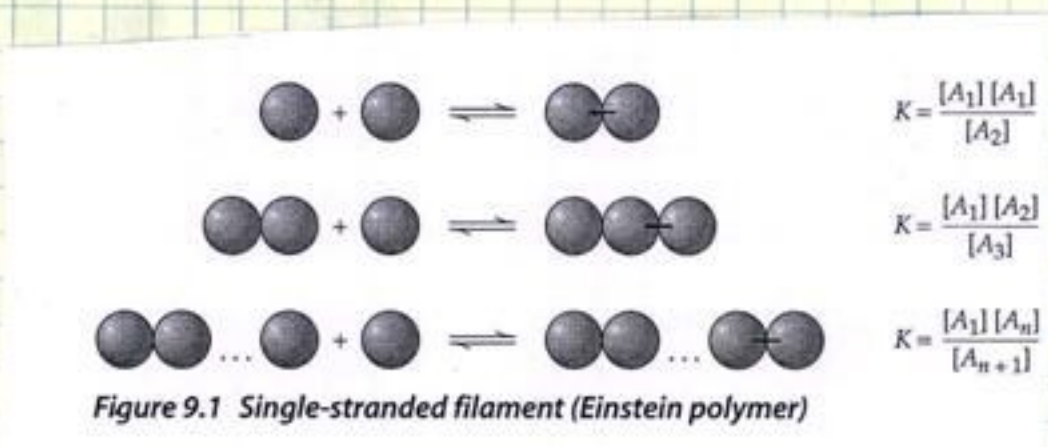

Figure 9.1 Single-stranded filament (Einstein polymer)

In reality K is expected to depend on the length of the polymer.

When a monomer binds to a long polymer, it loses more translational and rotational entropy than when it binds to another monomer, because a dimer moves and rotates more freely than a long polymer.

Thus the association between two monomers will be stonger than between a monomer and a long polymer

K is about 10 times smaller for the monomer-monomer reaction compared to the monomer-long polymer reaction

Once a polymer is more than about 10 subunits long, it can be considered to be a long polymer ⇒ K for a 10-mer is within a factor of 2 of that of an infinitely long polymer

Thus, we can think of this entropic effect as influencing nucleation but not growth.

Mechanics of motor proteins and the cytoskeleton

J. Howard

Single stranded filaments

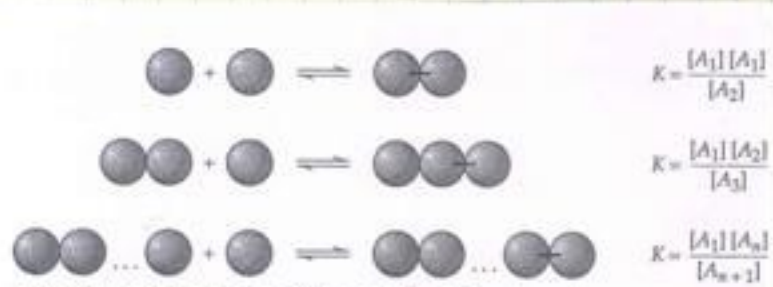

Figure 9.1 Single-stranded filament (Einstein polymer)

$$K = \frac{[A_n][A_1]}{[A_{n+1}]}$$

$$\frac{[A_n]}{K} = a_n = \frac{[A_{n+1}]}{[A_1]}$$

$$a_n = a_1^n = \exp\left(-\frac{n}{n_0}\right) \qquad n_0 = -\frac{1}{\ln a_1}$$

$\Rightarrow$ There is an exponential distribution of polymer lengths

$$[A_n] = K \exp\left(-n/n_0\right).$$

The average length of the polymers (not counting monomers) is

$$n_{av} = \sum_2^\infty n p_n = \sum_2^\infty n \frac{a_n}{\sum_2^\infty a_n} = 1 + \frac{1}{1-a_1} \qquad \left(\sum_{k=0}^\infty a q^k = \frac{a}{1-q}\right)$$

The total number of subunits is

$$a_t = \sum_1^\infty n a_n = \frac{a_1}{(1-a_1)^2} \qquad \left(\sum_{k=0}^\infty k q^k = \frac{q}{(1-q)^2}\right)$$

The concentration of monomers therefore depends on the total conc of subunits according to

$$a_1 = 1 + \frac{1}{2a_t} - \sqrt{\frac{1}{a_t} + \frac{1}{4a_t^2}}$$

When $a_t >> 1$, $a_1 \cong 1 - \frac{1}{\sqrt{a_t}}$ $\qquad n_0 \cong \sqrt{a_t}$ $\qquad n_{av} \cong 1 + \sqrt{a_t}$

$$n_{av} \cong \sqrt{\frac{A_t}{K}}$$

Thus, even when the total subunit concentration is 100-times greater than K, the average polymer would contain only about 10 subunits

Single stranded filaments are short!

Multi-stranded filaments

Two-stranded filaments have 2 different classes of bonds- one within the strands and one between the strands.

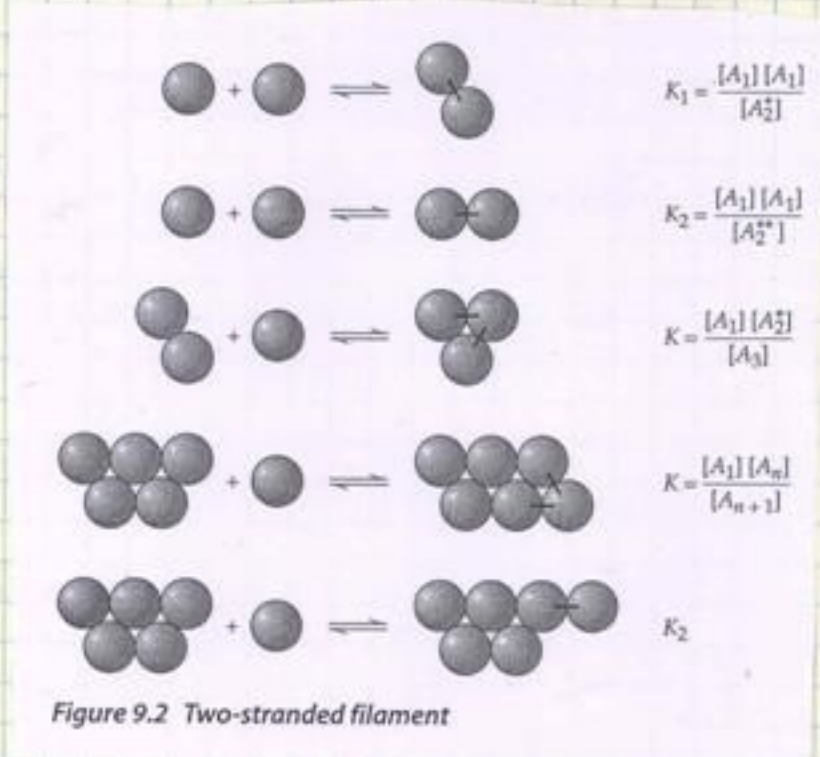

Figure 9.2 Two-stranded filament

There are 2 different nuclei A_2^* and A_2^{**} and 3 different dissociation constants K, K_1 and K_2.

$$a_n = \frac{K}{K_1} a_1^n = \frac{K}{K_1} \exp\left(-\frac{n}{n_0}\right)$$

$$a_2^* = \frac{K}{K_1} a_1^2 \qquad a_2^* = \frac{K}{K_2} a_1^2$$

The total no of subunits is

$$a_t = a_1 + \frac{K}{K_2} a_1^2 + \frac{K}{K_1} \frac{a_1^2 (2 - a_1)}{(1 - a_1)^2}$$

The average length of the polymers (not counting monomers or the nuclei a_2^* and a_2^{**} is

$$n_{av} = 2 + \frac{1}{1 - a_1} \cong \sqrt{\frac{K_1}{K}} \sqrt{a_t} \qquad \left[\text{the approximation holds when } a_t >> 1\right]$$

When $a_t >> 1$, $a_1 \cong 1$ and $a_n \cong \frac{K}{K_1}$ provided $n < n_0$

Thus, the lengths of the polymer are exponentially distributed

$$n_{av} \cong \sqrt{\frac{K_1}{K}} \sqrt{\frac{[A_t]}{K}}$$

When $K \approx 1 \mu M$ and $K_1 = K_2 = 0.1\ M$ and $[A_t] = 10 \mu M$

then $n_{av} \cong 1000$!

The ends of a two-stranded filament are energetically unfavorable so that there will be only a low concentration of them at equilibrium.

Lengthening and shortening of multi-stranded filaments

The rate of elongation of multi-stranded filaments, in subunits per second, is given by

$$\frac{dn}{dt} = k_{on}[A_1] - k_{off}$$

Considering the annealing reactions that lead to an increase in length of an n-mer

$$\frac{dn}{dt} = k_{on}[A_1] + 2k_{on,2}[A_2] + \cdots + m k_{on,m}[A_m] +$$

($k_{on}[A_1]$: addition of monomer; $2k_{on,2}[A_2]$: addition of dimer)

If $k_{on,m} = k_{on}$, $\frac{dn}{dt} = k_{on}\sum_{m=1}^{\infty} m[A_m] = k_{on}[A_t]$

Thus elongation is not necessarily an end property because in general $[A_t] > [A_1]$

But when m is large, the translational and rotational diffusion of n-mers becomes very slow

$D \sim \ln m/m$ translation
$\sim 1/m$ axial rotation
$\sim \frac{\ln m}{m^3}$ rotation around axes $\perp$ to filament axes

Hence, $k_{on,m} \ll k_{on}$ for large m

Thus only monomers and short polymers will contribute significantly to the growth rate. Since the concentration of short polymers is much less than that of monomers ($\frac{A_n}{A_1} = \frac{K}{K_1} \cong 10^{-5}$), the total contribution of annealing to growth will be minor.

In other words, growth is by monomer addition

Annealing and Breakage

Consider the annealing/breakage reaction

$$A_n + A_m \underset{k_{off,m}}{\overset{k_{on,m}}{\rightleftharpoons}} A_{n+m}.$$

$$\frac{[A_n][A_m]}{[A_{n+m}]} = \frac{K^2}{K_1} = \frac{k_{off,m}}{k_{on,m}}.$$

Since $k_{on,m} < k_{on}$ (because the polymer will diffuse more slowly than the monomer)

$$k_{off,m} = \frac{K^2}{K_1} k_{on,m} \leq \frac{K^2}{K_1} k_{on} = \frac{K}{K_1} k_{off}.$$

Breakage of a multi-stranded filament

The change in length due to breakage is

$$\frac{dl_n}{dt} = -k_{off} - 2\,k_{off,2} + \cdots - m\,k_{off,m}.$$

where $k_{off,m}$ is the rate constant for breaking off of an m-mer

∴ the dissociation constant for annealing / breakage of an m-mer is independent of m (ie independent of fragment length) and because long fragments do not anneal, the breakage into long fragments also does not occur.

At the molecular level, long polymer fragments diffuse away from each other so slowly that they have a high chance of reannealing before they escape.

Thus only the dissociation of monomers and the breaking off of small oligomers will contribute significantly to shortening

However, the total contribution from small oligomers is small because breaking a two-stranded filament requires severing 3 bonds, whereas removing a subunit from the end requires severing only 2 bonds

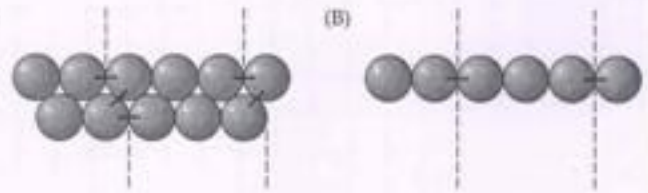

Figure 9.3 Breaking a two-stranded filament is difficult
Dissociation of the terminal subunit from a two-stranded filament (A) is more likely to occur than breakage in the middle because it involves breaking only two bonds rather than three. By contrast, breakage of and dissociation from a one-stranded filament involves breaking only one bond (B).

As a consequence $k_{off,m} / k_{off} \leq \frac{K}{K_1} \cong 10^{-5}$ for $m > 1$

Thus, shrinkage is by monomer subtraction

In contrast, single stranded filaments shorten primarily by breakage because the breakage and dissociation both require only one bond to be severed.

Other properties of multi-stranded filaments

1. There exists a critical concentration, K_c.

   When $[A_t] < K_c$ there are hardly any polymers

   $[A_t] > K_c$ almost all excess subunits go into filaments

The critical concentration is the monomer concentration at which the elongation rate is zero

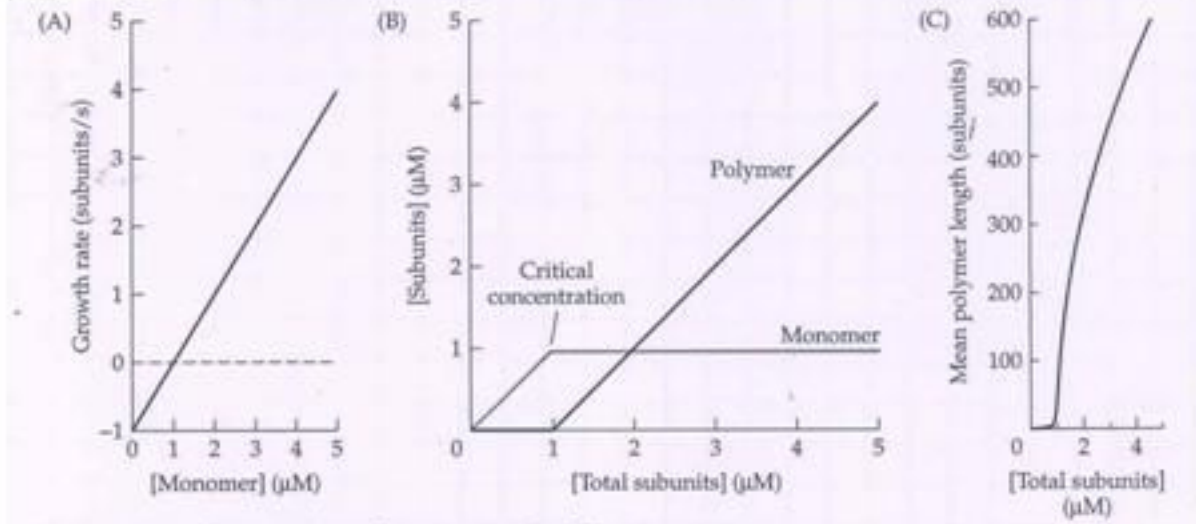

Figure 9.4 Polymerization of a two-stranded filament
(A) Growth rate for a multistranded filament according to Equation 9.6. (B) The concentration of subunits in their monomeric and polymeric forms as a function of the total subunit concentration. Note the sharp transition in polymer concentration about the critical concentration. (C) Mean length as a function of the total subunit concentration. In these examples, the off-rate constant is 1 s^{-1}, the on-rate constant is 1 $\mu M^{-1}s^{-1}$, and the dissociation constant (equal to the critical concentration) is 1 μM.

When the total subunit conc is greatly in excess of the critical concentration, the monomer conc approaches the critical conc.

2. The concentrations of the nuclei A^* and A^{**} are very small, equal to $\sim \frac{K^2}{K_1}$ and $\frac{K_1^2}{K_2}$, respectively.

   (When $K = 1\,\mu M$, $K_1 = K_2 = 0.1\,M$, $[A^*] = [A^{**}] \sim 0.1\,nM$

3. The ends of filaments will be predominantly blunt, rather than having long protofilaments grow from them.

4. The mean lengths of filaments increase very steeply above the the critical concentration

Aggregation and micellization processes

Surfactant molecules can aggregate into clusters called micelles. A typical spherical micelle may contain 60 surfactant molecules.

$n\,A_1 \overset{K}{\rightleftharpoons} A_n$

$A_1 \equiv$ monomer
$A_n \equiv$ micelle (assume each micelle has exactly n surfactant molecules)

$$K = \frac{[A_n]}{[A_1]^n}$$

The number of molecules per object is

$$\nu = \frac{[A_1] + n[A_n]}{[A_1] + [A_n]}$$

Let $x = [A_1]$

$$\nu(x) = \frac{1 + nKx^{n-1}}{1 + Kx^{n-1}}$$

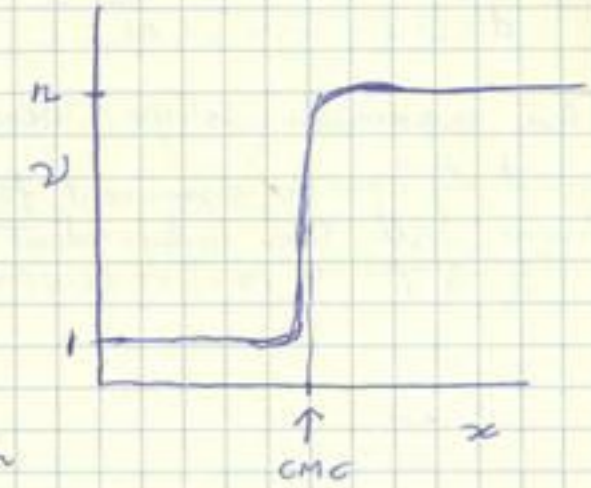

The model predicts a sharp transition at the critical micellar concentration (CMC), the concentration at which $x^{n-1} \approx 1/K$.

At small x, $x^{n-1} \ll 1/K \Rightarrow \nu = 1$ | the solution contains mostly monomers

At low concentrations, the high cost in translational entropy of recruiting the molecules and assembling them into a cluster outweighs the energetic advantage of sequestering their hydrocarbon tails from water

At concentrations of x above the CMC, $x^{n-1} \gg 1/K$

and $\nu = n \Rightarrow$ the solution contains mostly micelles

At high concentrations, there is less translational entropy to overcome, because the average distance between surfactant molecules in solution is small. Then the sticking energy dominates and the molecules form micelles.

The sharpness of the transition increases with n.

Nucleation

Polymerization into larger structures involves a set of necessary but unfavorable steps in the reaction that bottleneck the formation of large aggregates. These steps are viewed as constituting formation of a critical nucleus

Thermodynamic viewpoint: the nucleus represents a turning point in the balance between lost translational and rotational entropy and intermolecular bond energy

⇒ An aggregate is post-nuclear if, for a given concentration of monomers, the addition of a monomer adds to its stability rather than increasing its instability.

Kinetic viewpoint: the rate of monomer addition to the aggregate exceeds the rate of monomer loss, after the nucleus size is surpassed but not before.

The nucleus may be the result of a singular steric step, such as closure of a ring, or a tube, or the completion of the first turn of a helix.

But nucleation theories do not require such a special structure for the turning point in stability.

see Bishop & Ferrone (1984) Biophys J. 46, 631-644.

$$\begin{aligned} A + A_n &\rightleftarrows A_{n+1} \qquad n < n^* \\ A + A_n &\rightleftarrows A_{n+1} \qquad n > n^* \end{aligned} \tag{3}$$

The equilibrium probability of finding a given species A_n can be related to a Gibbs free energy (relative to some standard state) as

$$[A_n] = [A_{standard}] \exp[-\Delta G(n)/RT] \tag{4}$$

in which R is the gas constant, T the temperature in Kelvins, and $[A_{standard}]$ is the standard state concentration. One logical choice for this "standard state" is the initial monomer concentration. Then the energy of each aggregate is measured relative to the initial concentration, although differences between curves as the initial concentration is varied would then be masked. Another common choice is some arbitrary concentration, say, 1 mM. Then the free energies are measured relative to a fixed concentration. Such fixed standard states can produce a paradoxical result on occasion, namely that the aggregate may be favored relative to the standard state. This simply means that the arbitrarily chosen standard is too high. In any case, the decrease in probability in finding A_n relative to $[A_{standard}]$ corresponds to an increase in energy. When a sequence of steps involves the increase in energy, the steps in the reaction can be viewed as climbing an energetic barrier that must be overcome for the aggregation process to proceed (Fig. 1). At equilibrium,

$$k_n^+ c[A_n] = k_{n+1}^-[A_{n+1}] \tag{5}$$

from which it follows that $[A_{n+1}]/[A_n] = ck_n^+/k_{n+1}^-$. However, it is also clear that

$$\begin{aligned} \frac{[A_{n+1}]}{[A_n]} &= \exp\left\{-\left[\frac{\Delta G(n+1) - \Delta G(n)}{(n+1) - n}\right] \Big/ RT\right\} \\ &= \exp\left(-\left\{\frac{d\Delta G}{dn}\right\} \Big/ RT\right) \end{aligned} \tag{6}$$

In other words, the slope of the free energy plot, $d\Delta G/dn$, is related to the ratio of the rate constants into and out of a state for a given monomer concentration c. The changeover in rates is therefore related to the change in slope of the free energy barrier, and a barrier that is linear with size gives a constant rate ratio. When the turning point is sufficiently sharp, the implication is that there is one state with a particularly small population that will represent the rate-limiting step for the reaction. This bottleneck is a thermodynamic nucleus, a necessary but very scarce species in the reaction path. This is quite distinct from a structural nucleus, in which a

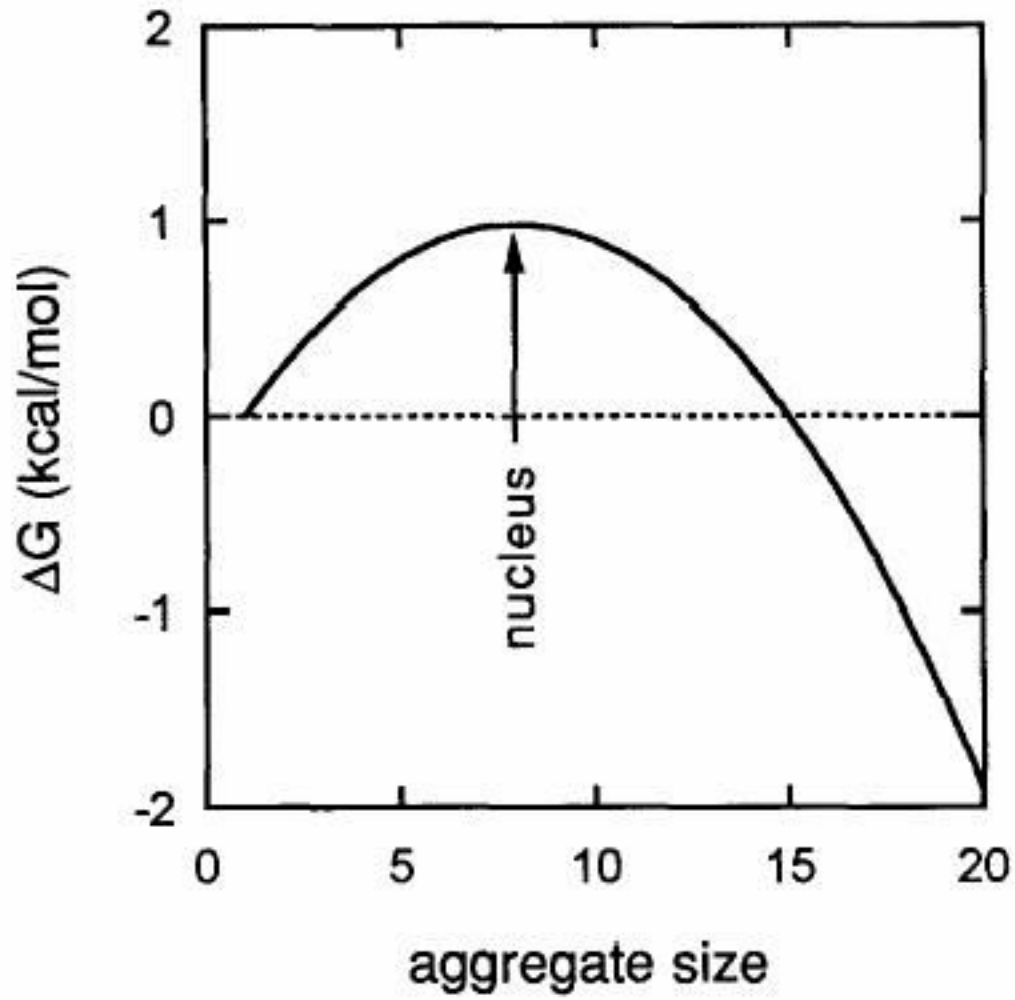

/pical free energy barrier. Free energy of the aggregate ΔG (relative to the shown on the vertical axis, whereas size of the aggregate is shown on the is. The nucleus is the species whose size corresponds to the peak of the energy is for which the population is smallest. Polymerization requires that the aggregate ugh this maximum, which equates the reaction to a barrier crossing. The slope it any size n is controlled by the concentration times the ratio of rate constants, assume that the rate constants are independent of n on either side of the nucleus that the slope is the same for different sizes n, in turn implying that the free ar with n in that range. At large values of n, this assumption is reasonable.

Ferrone

Oosawa model

The nucleus is in a very unfavorable thermodynamic equilibrium with the monomeric protein

Fibril mass is proportional to t^2 at the beginning of the reaction, with essentially no lag phase.
The concentration dependence of the effective rate constant is given by $c^{(n+1)/2}$
where c is the initial concentration, and n is the size of the nucleus

Nucleation:
Linear assembly with the formation of a polymerization nucleus

$$P_1 + P_1 <> P_2$$
$$P_2 + P_1 <> P_3$$
$$. \quad .$$
$$P_{n-1} + P_1 <> P_n$$

$$K_n = \frac{[P_i]}{[P_{i-1}][P_1]}$$

n is the number of monomers in the nucleus. The addition of consecutive monomers involves the formation of only one inter-subunit contact. The value of K_n is the same for all steps, and small.

Growth:

$$P_n + P_1 <> P_{n+1}$$
$$P_{n+j} + P_1 <> P_{n+j+1}$$
$$. \quad .$$

$$K_g = \frac{[P_{n+j+1}]}{[P_{n+j}][P_1]}$$

Each monomer is added in a cooperative manner: its addition involves the formation of contacts with two or more monomers in the already assembled structure . The value of K_g is the same for all growth steps, and large.

$K_g >> K_n$: a necessary condition for self assembly to belong to the NP class.

The critical concentration, C_r is a unique concentration value below which all protein exists as monomers.

$$C_r = K_g^{-1}$$

Homogeneous nucleation

Classical equilibrium nucleation theory: all polymerization processes are suffuently slow to allow an equilibrium to be established between nuclei and monomers.

$\Delta(t)$ = concentration of polymerized monomers.
$c(t)$ = free monomer concentration
c_0 = total monomer concentration

$\Delta(t) = c_0 - c(t)$ | changes by addn or loss of monomers at polymer ends

$c_p(t)$ = concentration of polymers | any aggregate larger than a nucleus

Assume: ① pre-nuclear aggregates are in equilibrium with monomers.
② conc. of prenuclear aggregates $\ll \Delta(t), c(t)$.
③ rates of addition and loss of monomers at polymer ends are independent of length for sufficiently long polymers

Then $\frac{d\Delta}{dt} = (k_+ c - k_-) c_p$

[Convenient to relate k_- to a solubility c_s: $k_- = k_+ c_s$
Then the reaction naturally ceases when $c(t) = c_s$]

If any species of size $i+1$ or larger is defined as a polymer then the rate of homogeneously formed polymers is

$$\frac{dc_p}{dt} = k_+ c c_i - k_-^* c_{i+1}$$

[k_- : asymptotic limit of the dissociation rate for infinitely long polymers.
k_-^* : first dissociation rate const to decrease $\bar{c}$ aggregate size]

$\therefore k_+ c \gg k_-$, especially in the initial phase of the reaction
and $c_i = K_i c^i$ | eqb nucleation theory $i c \rightleftarrows c_i$

$$\frac{dc_p}{dt} = k_+ c c_i = k_+ K_i c^{i+1}$$

Augmenting the formation of polymers

1. Fragmentation.

Assume that polymers break at a rate proportional to their length

For a linear polymer, length $\propto (c_0 - c)$.

$$\therefore \frac{dc_f}{dt} = k_+ K_i c^{i+1} + k_f (c_0 - c)$$

k_f = rate constant of polymer fragmentation

2. Heterogeneous nucleation

Nucleation of additional polymers at the surfaces of existing polymers.

The concentration of sites to which heterogenous nuclei attach and grow scales as the concentration of monomers already incoporated into polymers; ie as $(c_0 - c)$

If ϕ = probability that a given polymer site can support heterogenous nucleation

$$\frac{dc_p}{dt} = k_+ K_i c^{i+1} + k_+ \phi K_j c^{j+1} (c_0 - c)$$

K_j = equilibrium const for forming nuclei of size j and attaching them to surface sites

3. Lateral growth

A special case of heterogenous nucleation

Each growth step is favorable and there is no nucleus to act as a limiter of the reaction rate

If k_+' = rate constant of lateral association

$$\frac{dc_p}{dt} = k_+ K_i c^{i+1} + \phi k_+' c(c_0 - c)$$

General form of augmented nucleated mechanisms

$$\frac{dc_p}{dt} = k_+ K_i c^{i+1} + Q\ (c_0 - c).$$

Secondary Processes.

Type	Example	Q
Fragmentation	Actin	k_f
Heterogeneous nucleation	Sickle hemoglobin	$k_+ \phi K_j c^{j+1}$
Lateral Growth	Collagen.	$\phi k'_+ c$

Perturbation method

$$\frac{dc_p}{dt} = a_0 + a_1 \Delta_1 \qquad \frac{d\Delta_1}{dt} = c_p^{(1)} b_0$$

where $a_0 = k_+ K_i c_0^{i+1}$

$a_1 = k_+ [Q_0 - (i+1) K_i c_0^i]$

$b_0 = k_+ (c_0 - c)$

Solution $c_p^{(1)} = \frac{a_0}{\sqrt{a_1 b_0}} \sinh \sqrt{a_1 b_0}\, t$

$$\Delta_1 = \frac{a_0}{a_1} (\cosh \sqrt{a_1 b_0}\, t - 1) \equiv A (\cosh Bt - 1)$$

where $A = \frac{a_0}{a_1}$ $\qquad B = \sqrt{a_1 b_0}$

1. For $Bt << 1$

$$\Delta_1 = \tfrac{1}{2} B^2 A t^2 \quad \Big| \quad B^2 A = k_+^2 (c_0 - c_s) K_i c_0^{i+1}$$ independent of Q_0

In this limit, homogenous nucleation dominates over the secondary process.

2. For $Bt >> 1$

$$\Delta_1 = \tfrac{1}{2} A e^{Bt}$$

In this limit, the secondary process dominates over the homogenous process to produce this exponential autocatalytic behavior

The kinetic behavior of insulin fibrillation is determined by heterogeneous nucleation pathways

FABIO LIBRIZZI[1,2] AND CHRISTIAN RISCHEL[3,4]

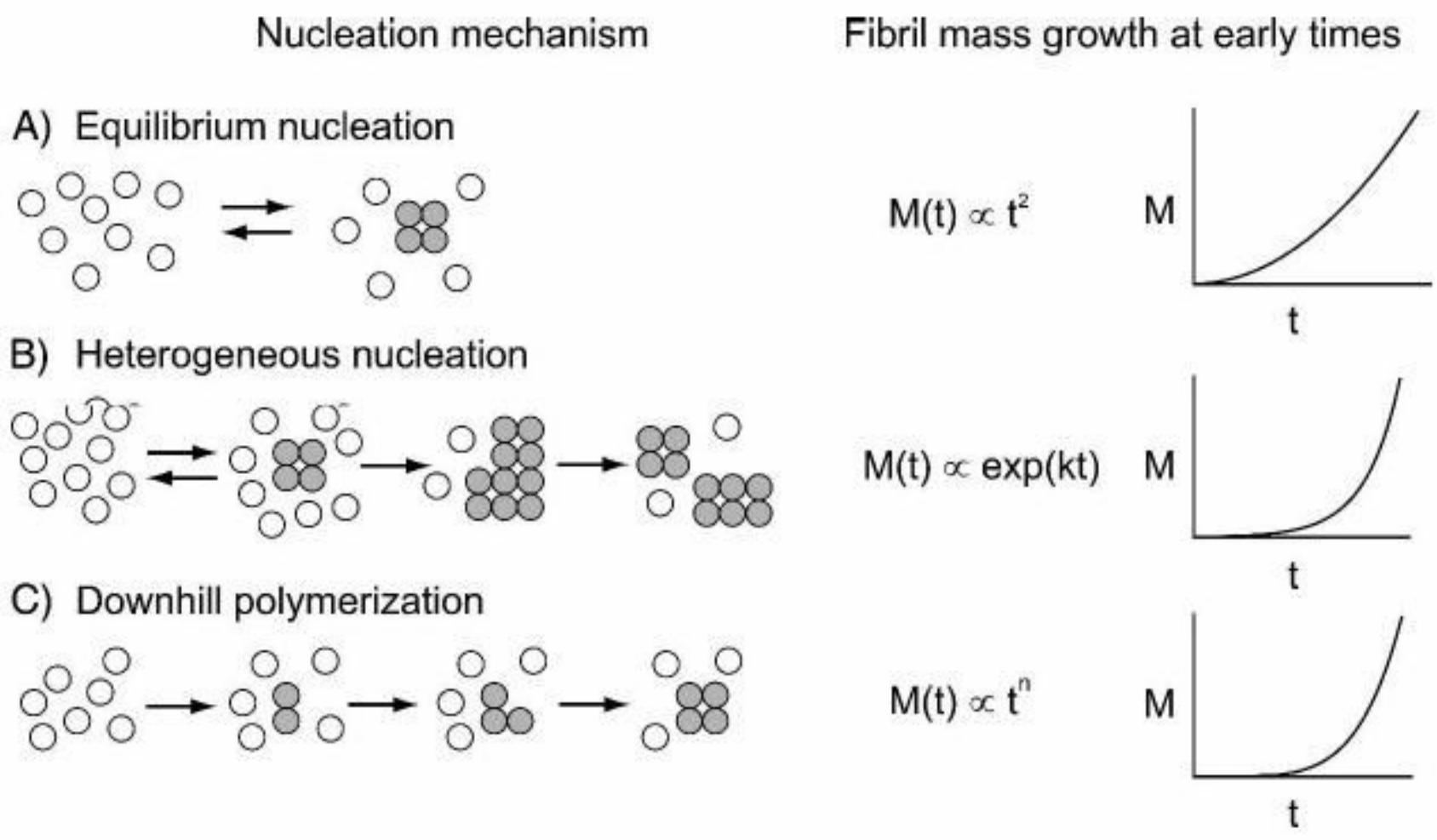

Figure 1. Possible mechanisms in a nucleation–elongation fibrillation. (*A*) Equilibrium nucleation (Oosawa's model; Oosawa and Asakura 1975). (*B*) Heterogeneous nucleation (sickle cell hemoglobin; Ferrone et al. 1980, 1985). (*C*) Forward nucleation (the figure shows t^5; Flyvbjerg et al. 1996).

Criteria for nucleated polymerization (NP)

1. Critical concentration for the start of the polymerization reaction
2. The observation of a lag phase
3. Seeding with fibrils abolishes the lag phase

The most outstanding feature is the concentration dependence of the nucleation rate:

$k_{nucl} \sim c^{n/2} \sim 1/t_{lag}$

n = number of monomers building up the nucleus
t_{lag} is a measure for the duration of the lag phase

For the NP mechanism, n is strictly > 2

The nucleus is the least stable species on the NP pathway, which is stabilized by addition of further monomers.

Downhill polymerization

Nucleus is formed by successive addition of monomers or smaller aggregates.

The initial kinetics is described by a power law growth, in which the exponent is determined by the number of slow steps necessary for the formation of the nucleus. Exponent minus 1 is the number of slow steps Necessary for nucleus formation

A pronounced lag phase is observed when the exponent in the power law is high enough.

The concentration dependence can be as low as linear.

Polymerization of tubulin.

Secondary nucleation

Nucleation is catalyzed by existing aggregates or fibrils. Initially, nuclei must be formed by monomers, but after the creation of a certain amount of aggregates, the secondary pathway takes control of growth.

There are at least three simple mechanisms by which a fibril can catalyze the formation of other fibrils:

- Fragmentation
- Branching
- Nucleation on the fibril surface

All three mechanisms lead to an exponential growth of the total mass of fibril with time. A pronounced lag phase and very fast subsequent aggregation is possible, depending on the actual rate constants.

The concentration dependence is determined by the mechanism of creation of the first fibrils, and the nature of the secondary pathway.

If this concentration dependence is weak, it could be because:

1. The monomer is the reactive species, and non-productive oligomer formation can blunt the concentration dependence.
2. The nucleation rate in the secondary pathway is almost independent of monomer concentration.

Aggregation of sickle cell hemoglobin

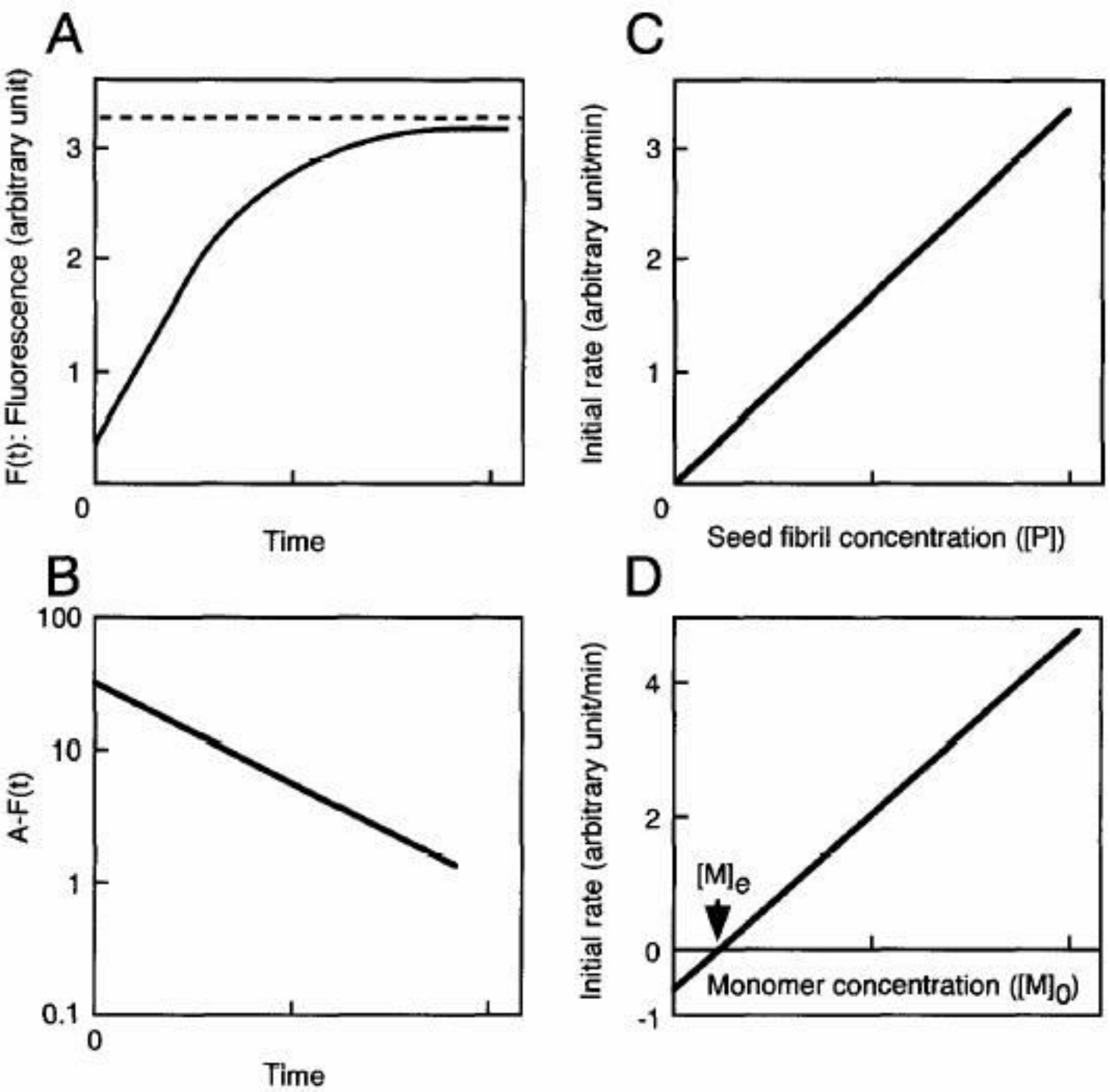

FIG. 1. Kinetics of amyloid fibril extension *in vitro*. (A) Time course of fluorescence after the initiation of the polymerization reaction. $F(t)$ represents fluorescence as a function of time. The reaction mixture contains both amyloid fibrils and their monomeric constituents. (B) The semilogarithmic plot of the difference: $F(\infty) - F(t)$ versus incubation time. A is tentatively determined as $F(\infty)$ and is shown as a broken line in A. (C) Effect of the seed fibril concentration on the initial rate of amyloid fibril extension. The initial concentration of the monomeric constituents in the reaction mixture ($[M]_0$) is constant. (D) Effect of the monomer concentration on the initial rate of amyloid fibril extension. The seed fibril concentration in the reaction mixture ([P]) is constant. Note that at $[M]_0 = 0$, the negative initial rate, i.e., the depolymerization of amyloid fibrils, is observed. Note also that at $[M]_0 = [M]_e$, the net rate of extension is 0.

$$\log[A - F(t)] = a - bt$$

Differentiating Eq. (1) by t yields

$$\frac{1}{\ln 10} \times \frac{-F'(t)}{A - F(t)} = -b$$

Rearranging Eq. (2) yields

$$F'(t) = B - CF(t)$$

where $B = bA \ln 10$, $C = b \ln 10$,

$F'(t)$ represent the rate of fluorescence increase at a given time.

[20] Kinetic Analysis of Amyloid Fibril Formation

By HIRONOBU NAIKI and FUMITAKE GEJYO

We now assume that the kinetic properties of amyloid fibril extension can be described as

$$[\mathrm{P}] + [\mathrm{M}] \underset{k_{-1}}{\overset{k_2}{\rightleftharpoons}} [\mathrm{P}] \tag{4}$$

where [P] is the number concentration of amyloid fibrils, [M] is the concentration of the monomeric constituents, and k_2 and k_{-1} are the apparent rate constants for polymerization and depolymerization, respectively. [P] is constant throughout the reaction.

If t is the reaction time, $f(t)$ is the concentration of the monomeric constituents that have newly polymerized into amyloid fibrils during the reaction, and $[\mathrm{M}]_0$ is the initial monomer concentration, then Eq. (4) can be written as

$$f'(t) = k_2[\mathrm{P}][\mathrm{M}] - k_{-1}[\mathrm{P}] \tag{5}$$

$$[\mathrm{M}] = [\mathrm{M}]_0 - f(t) \tag{6}$$

where $f'(t)$ represents the rate of amyloid fibril extension at a given time and $k_2[\mathrm{P}][\mathrm{M}]$, and $-k_{-1}[\mathrm{P}]$ denote the rate of polymerization and depolymerization, respectively.

The insertion of Eq. (6) into Eq. (5) and subsequent rearrangement yields the following differential equation:

$$f'(t) = D - Ef(t) \tag{7}$$

where $D = (k_2[\mathrm{M}]_0 - k_{-1})[\mathrm{P}]$ and $E = k_2[\mathrm{P}]$.

Equation (7) is the same as Eq. (3). Therefore, Fig. 1B shows that the kinetics of amyloid fibril extension follows a first-order kinetic model as described by Eq. (4).

We now obtain the equilibrium monomer concentration (critical concentration) $[M]_e$ by setting $f'(t)$ in Eq. (5) equal to zero to obtain

$$[M]_e = \frac{k_{-1}}{k_2} = \frac{1}{K} \tag{8}$$

where K is the equilibrium association constant.

Measurement of Initial Rate of Amyloid Fibril Extension

In the initial phase of amyloid fibril extension, a linear increase is observed (see Fig. 1A). Therefore, a fluorescence increase within the linear phase, $F(t_1) - F(0)$, can be taken as the initial rate of extension.

If $t = 0$, then $f(0) = 0$. Therefore, from Eqs. (5) and (6)

$$f'(0) = k_2[P][M]_0 - k_{-1}[P] \tag{9}$$

Equation (9) explains the following results. First, when $[M]_0$ is constant, the initial rate of extension is proportional to the number concentration of amyloid fibrils ([P]) (Fig. 1C). Second, when [P] is constant, the initial rate of polymerization is found to be proportional to the initial concentration of monomeric constituents ($[M]_0$) (Fig. 1D). Finally, at each monomer concentration, the net rate of extension is the sum of the rates of polymerization and depolymerization (Fig. 1D).

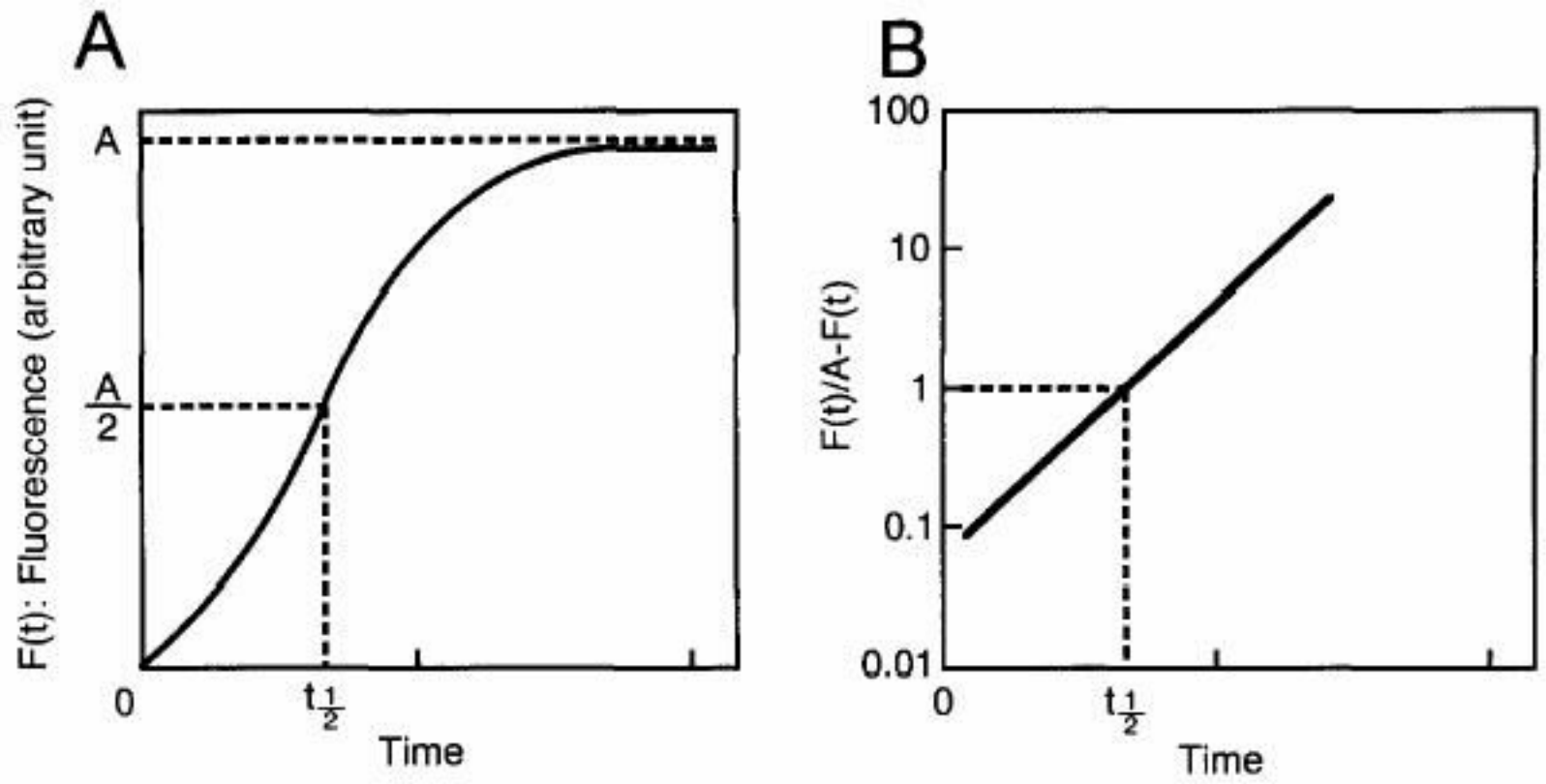

FIG. 2. Kinetics of fAβ formation from fresh Aβ. (A) Time course of fluorescence after the initiation of the reaction. $F(t)$ represents fluorescence as a function of time. (B) The semilogarithmic plots of the value: $F(t)/A - F(t)$ versus incubation time. A is tentatively determined as $F(\infty)$ and is shown as a broken line in A. Note that at $t = t_{1/2}$, $F(t) = A/2$ and $F'(t)$ reaches its maximum, $\ln 10 \cdot a \cdot A/4$.

Interpretation of this plot yields the following equation:

$$\log\left[\frac{F(t)}{A - F(t)}\right] = at + b \tag{10}$$

where t is the reaction time, $F(t)$ is the fluorescence as a function of time, A is tentatively determined as $F(\infty)$, a and b are the slope and the y intercept of the straight line, respectively. Differentiating Eq. (10) by t and subsequent rearrangement yields the following differential equation:

$$F'(t) = BF(t)[A - F(t)] \tag{11}$$

where $B = \ln 10\,(a)/A$, and $F'(t)$ represents the rate of fluorescence increase at a given time.

Scheme 2: Model for M-TTR Amyloidogenesis[a]

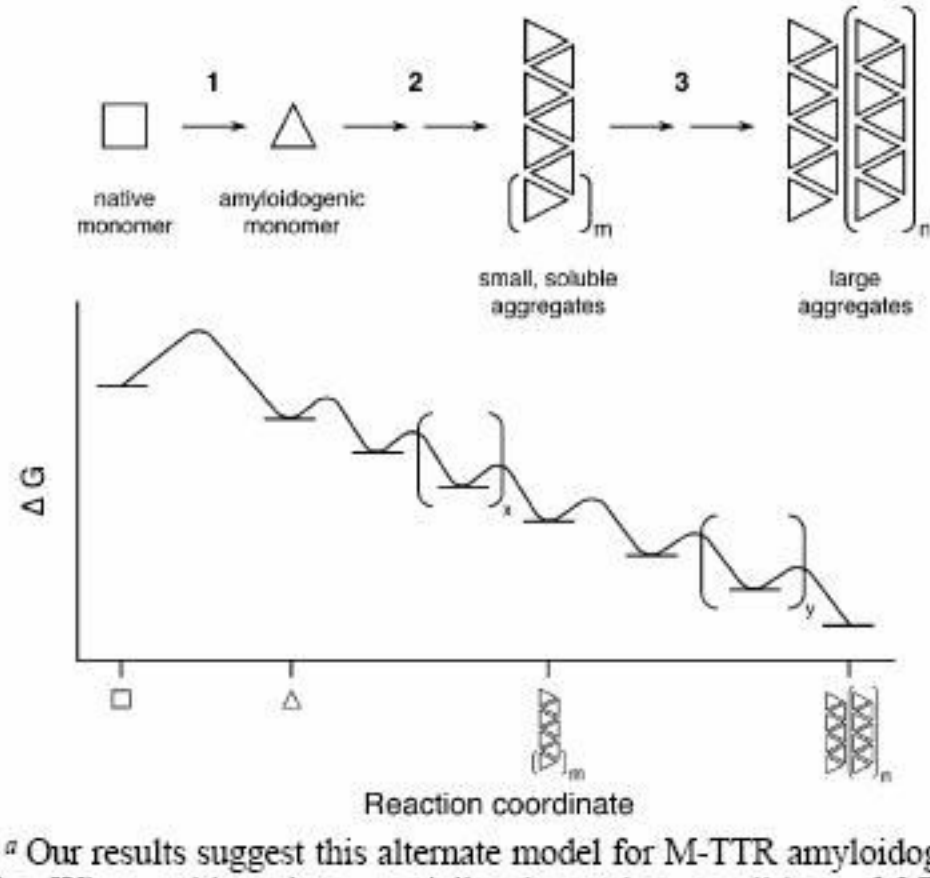

[a] Our results suggest this alternate model for M-TTR amyloidogenesis. When subjected to partially denaturing conditions, M-TTR misfolds into the amyloidogenic monomer (step **1**) and subsequently aggregates. Under these conditions, all of the steps along the pathway are energetically favorable, as illustrated by the free-energy diagram, and essentially irreversible. Nevertheless, M-TTR aggregation is characterized by at least two types of reactions. Initially, aggregation by the addition of monomers to other monomers or to oligomers predominates, leading to the accumulation of small aggregates (step **2**) that grow by monomeric increments, *m*. This phase of the reaction can be monitored by gel filtration (disappearance of monomer and increase in "soluble" aggregates) and by TfT fluorescence; the ability of these early aggregates to bind TfT suggests an amyloid or amyloid-like structure. As the reaction progresses, larger aggregates form primarily by secondary processes, such as the end-to-end or lateral assembly of existing aggregates (step **3**), rather than by monomer addition. Aggregate size increases dramatically in this phase, as evidenced by the rapid increase in turbidity. Only small increases in TfT binding are observed, however, because the total amount of polymerized M-TTR is not changed by these secondary processes. The number of individual steps in each phase of the aggregation reaction is not specified in our model, as indicated by the repeating units *x* and *y*.

On the nucleation and growth of amyloid β-protein fibrils: Detection of nuclei and quantitation of rate constants

(Alzheimer disease/fibrillogenesis/light scattering)

ALEKSEY LOMAKIN[†‡§], DOO SOO CHUNG[†¶], GEORGE B. BENEDEK[†‖], DANIEL A. KIRSCHNER[‡,††,‡‡], AND DAVID B. TEPLOW[‡§‖]

Proc. Natl. Acad. Sci. USA
Vol. 93, pp. 1125–1129, February 1996

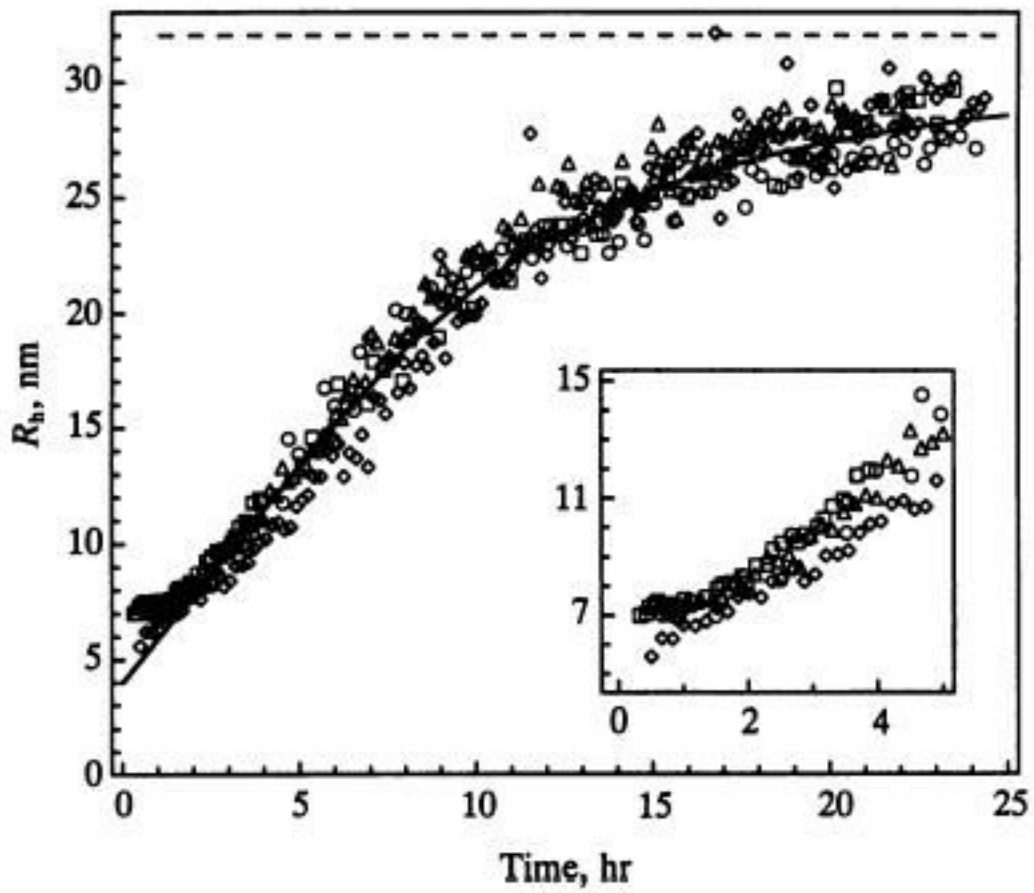

FIG. 2. Temporal evolution of the hydrodynamic radius (R_h) of Aβ fibrils in the concentration domain $C_0 > c^*$. ◇, C_0 = 0.17 mM; △, C_0 = 0.28 mM; ○, C_0 = 0.47 mM; □, C_0 = 1.7 mM. The dashed line indicates the universal asymptotic size of the fibrils. (*Inset*) The initial time domain is expanded to illustrate the 7-nm structures (micelles) observed upon dissolution of Aβ at high concentration.

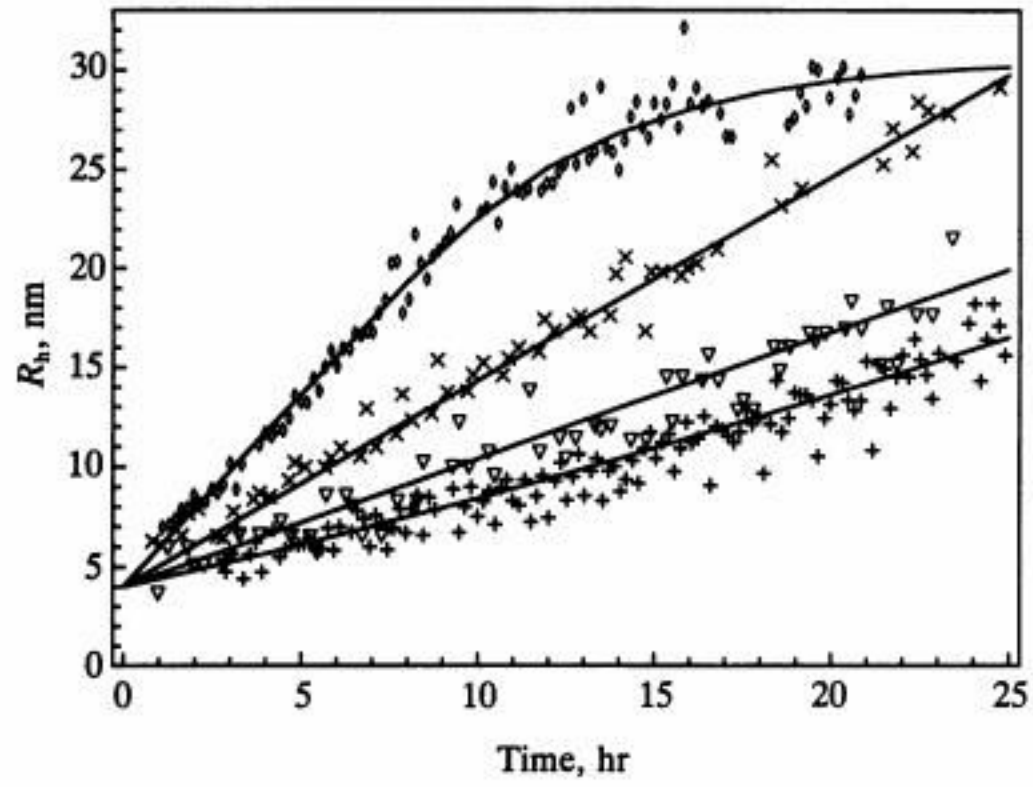

FIG. 3. Temporal evolution of the hydrodynamic radius (R_h) of Aβ fibrils in the concentration domain $C_0 \leq c^*$. ◇, C_0 = 0.11 mM; ×, C_0 = 0.058 mM; ▽, C_0 = 0.028 mM; +, C_0 = 0.025 mM.

Micelles correspond to particles of R_h = 7 nm detected prior to significant fibril growth

The 4 nm hydrodynamic radius obtained by extrapolation to t= 0 corresponds to that of the fibril nucleus.

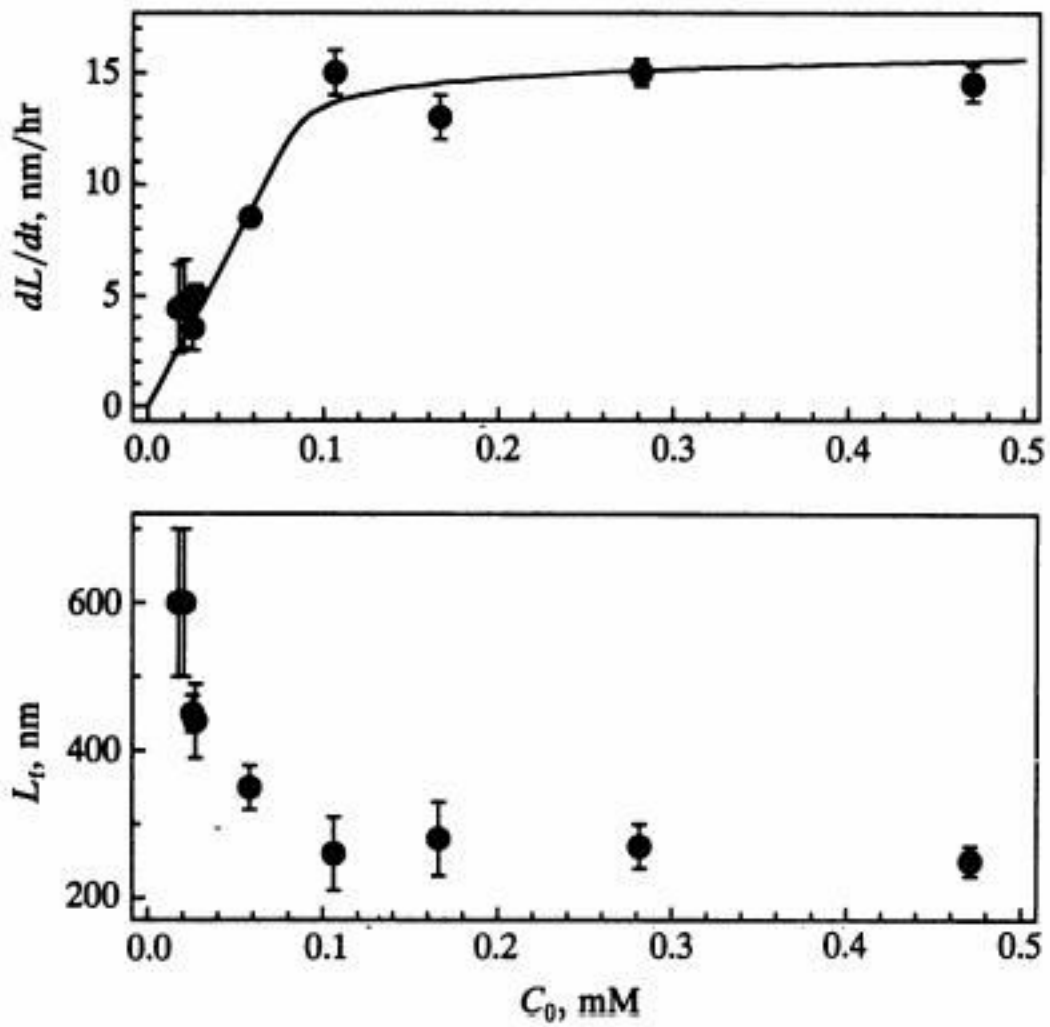

FIG. 4. Concentration dependence of fibril growth. (*Upper*) The initial rate of elongation of fibrils, dL/dt, determined in the time domain where growth was linear, as a function of C_0. The solid line represents the concentration dependence of the theoretical initial elongation rate K_eC/λ for $c^* = 0.1$ mM, $m = 25$, and $K_e = 65$ $M^{-1}\cdot sec^{-1}$. (*Lower*) The final length of fibrils, L_f, as a function of C_0.

The size distribution of fibrils in solution was determined by a constrained regularization method (33) adapted to the analysis of the homodyne correlation function. The observed distribution of diffusion coefficients was relatively narrow; therefore, we present here the average hydrodynamic radii (R_h) of scattering particles. We have used the following interpolation, appropriate for a cylinder of length L and diameter d (34), to relate the experimentally measured R_h values to the fibril length:

$$R_h = \frac{L}{2}\cdot\left(\sqrt{1 - x^2}\Big/\ln\frac{1 + \sqrt{1 - x^2}}{x}\right),$$

where

$$x = \frac{d}{L}\left[1 + \frac{0.37(L - d)}{L}\right].$$

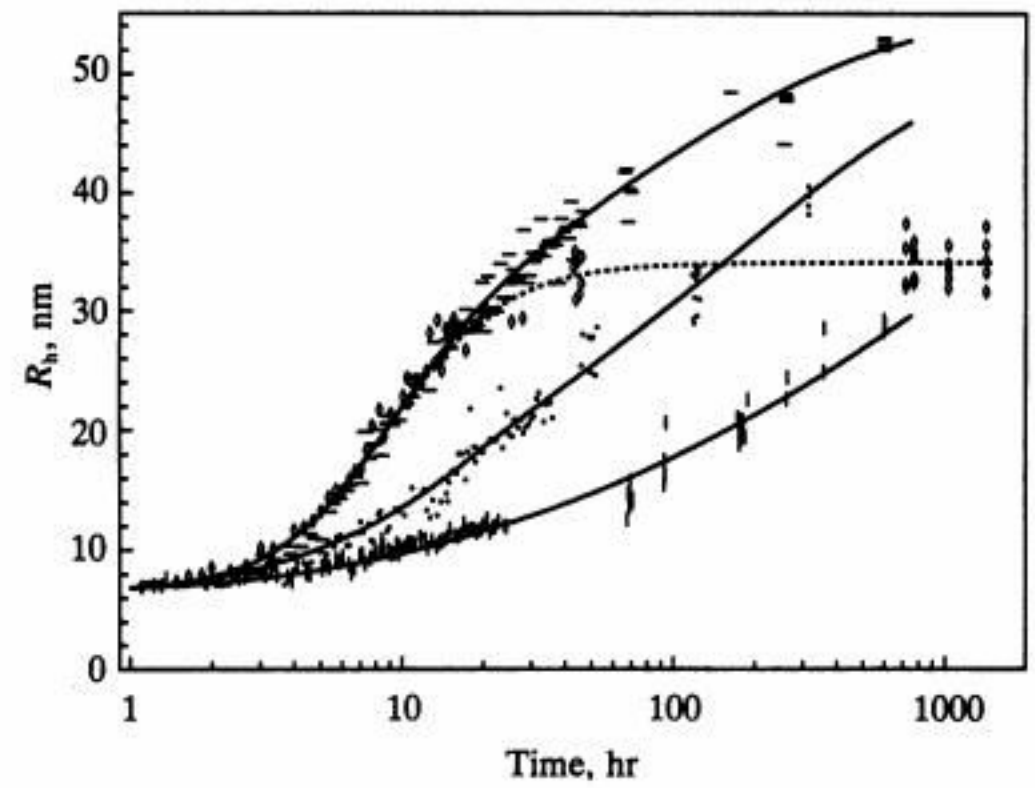

FIG. 5. Temporal evolution of the hydrodynamic radius (R_h) of Aβ fibrils in the presence of the surfactant $C_{12}E_6$. Aβ was dissolved at a concentration of ~0.11 mM in 0.1 M HCl containing the following concentrations of $C_{12}E_6$: ◇, 0.00 mM; – (top curve), 0.044 mM; ●, 0.11 mM; and | (bottom curve), 2.2 mM. The dashed curve highlights the behavior of the sample without $C_{12}E_6$.

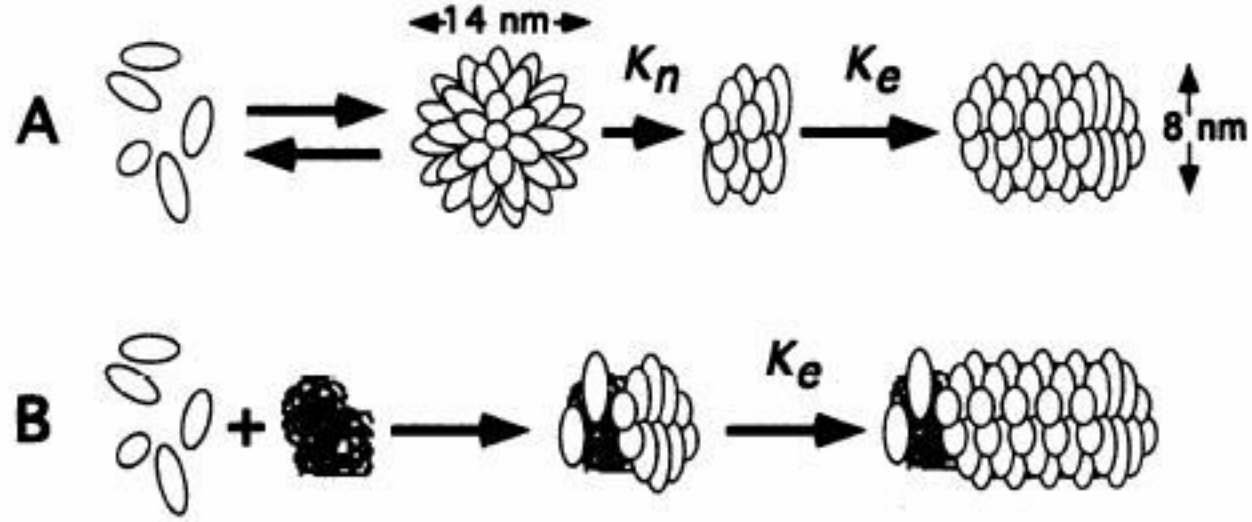

FIG. 6. Aβ fibrillogenesis at low pH. (*A*) Homogeneous nucleation and growth of Aβ fibrils for $C_0 > c^*$. Aβ monomers (ovoids) self-associate to form micelles (R_h = 7 nm, d = 14 nm), from which fibril nuclei (R_h = 4 nm, d = 8 nm) emerge at rate K_n. Aβ monomers add to the ends of these nuclei at rate K_e, producing fibrils of diameter 8 nm. (*B*) Heterogeneous nucleation and growth of Aβ fibrils for $C_0 < c^*$. In this concentration domain, nucleation occurs predominantly on non-Aβ seeds. The resulting fibrils are indistinguishable from those nucleated through micelles.

Solution monomer concentration = C
Rate constant of fiber elongation = k_e
Each fibril grows at a rate of k_eC monomers/s

When $C_0 < C^*$, the initial concentration of monomers = total concentration of dissolved peptide, and the number of growing fibers = number of heteregeneous nuclei initially present

C decreases exponentially with a time constant of $(k_e N_f)^{-1}$, where N_f is the number of growing fibrils per unit volume, resulting in gradual slowing of fibril growth

When $C_0 > C^*$, micelles are formed. The monomer concentration remains slightly above C*. The initial rate of of growth of fibrils Is thus also constant, ~ $k_e C^*$, and is independent of the initial concentration C_0.

At time T, all micelles have been depleted, and the growth rate decreases

If L_f = final length of the fibril, and λ= number of monomers/unit length, then $\lambda L_f = k_e C^* T$. On the other hand, when fibrillogenesis is complete $\lambda L_f = C_0/N_f$. Thus the micelle pool is depleted in time $T= C_0/k_e C^* N_f$

N_f is determined by the number of nuclei formed from micelles during T, and is ~ $k_n T C_0/m$ Where m is the number of monomers per micelle. C_0/m is therefore the initial concentratio of micelles

Thus $T = (k_e k_n/m)^{-1/2}$, which is independent of initial concentration C_0.

Thus the final length of fibrils is given by $\lambda L_f = (k_e C^*/k_n)^{1/2}$, and is concentration independent.

The total number of fibrils is given by $N_f = C_0(k_n/mk_e C^*)^{1/2}$

When nucleation is fast and elongation is slow, numerous short fibrils are formed.

When nucleation is slow and growth is fast, there is a small number of long fibrils.

Nucleated Conformational Conversion and the Replication of Conformational Information by a Prion Determinant

Tricia R. Serio,[1*] Anil G. Cashikar,[2*] Anthony S. Kowal,[2] George J. Sawicki,[2] Jahan J. Moslehi,[2] Louise Serpell,[4] Morton F. Arnsdorf,[3] Susan L. Lindquist[1,2†]

Prion proteins can serve as genetic elements by adopting distinct physical and functional states that are self-perpetuating and heritable. The critical region of one prion protein, Sup35, is initially unstructured in solution and then forms self-seeded amyloid fibers. We examined in vitro the mechanism by which this state is attained and replicated. Structurally fluid oligomeric complexes appear to be crucial intermediates in de novo amyloid nucleus formation. Rapid assembly ensues when these complexes conformationally convert upon association with nuclei. This model for replicating protein-based genetic information, nucleated conformational conversion, may be applicable to other protein assembly processes.

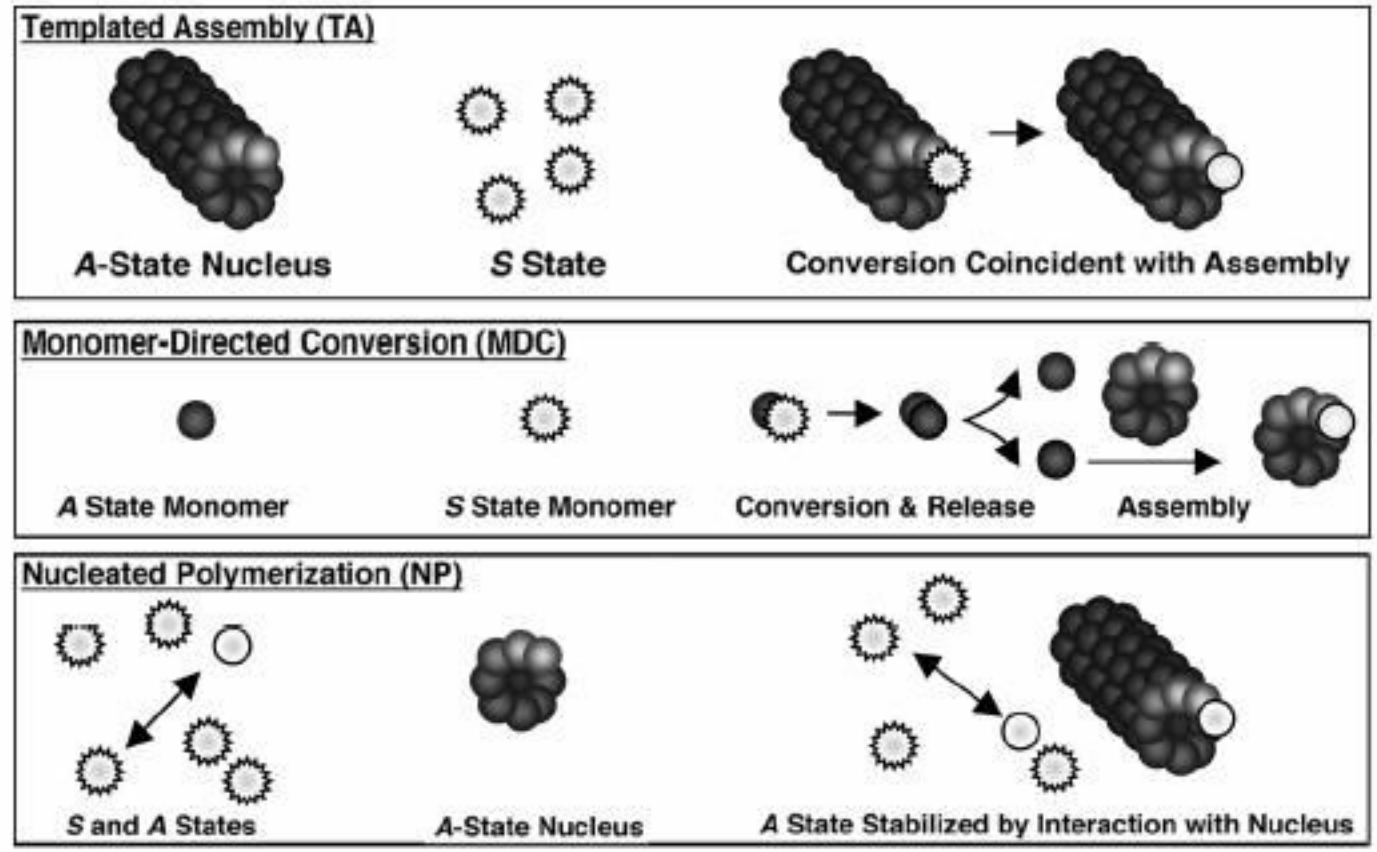

Fig. 1. Models for conversion and assembly. Smooth circles, A-state protein; jagged circles, S-state protein; and open jagged circles denote possible conformational differences between soluble monomers and oligomers. See text for explanations of the models.

Dependence of the rate constants of amyloid protofibril formation on the positions of mutations

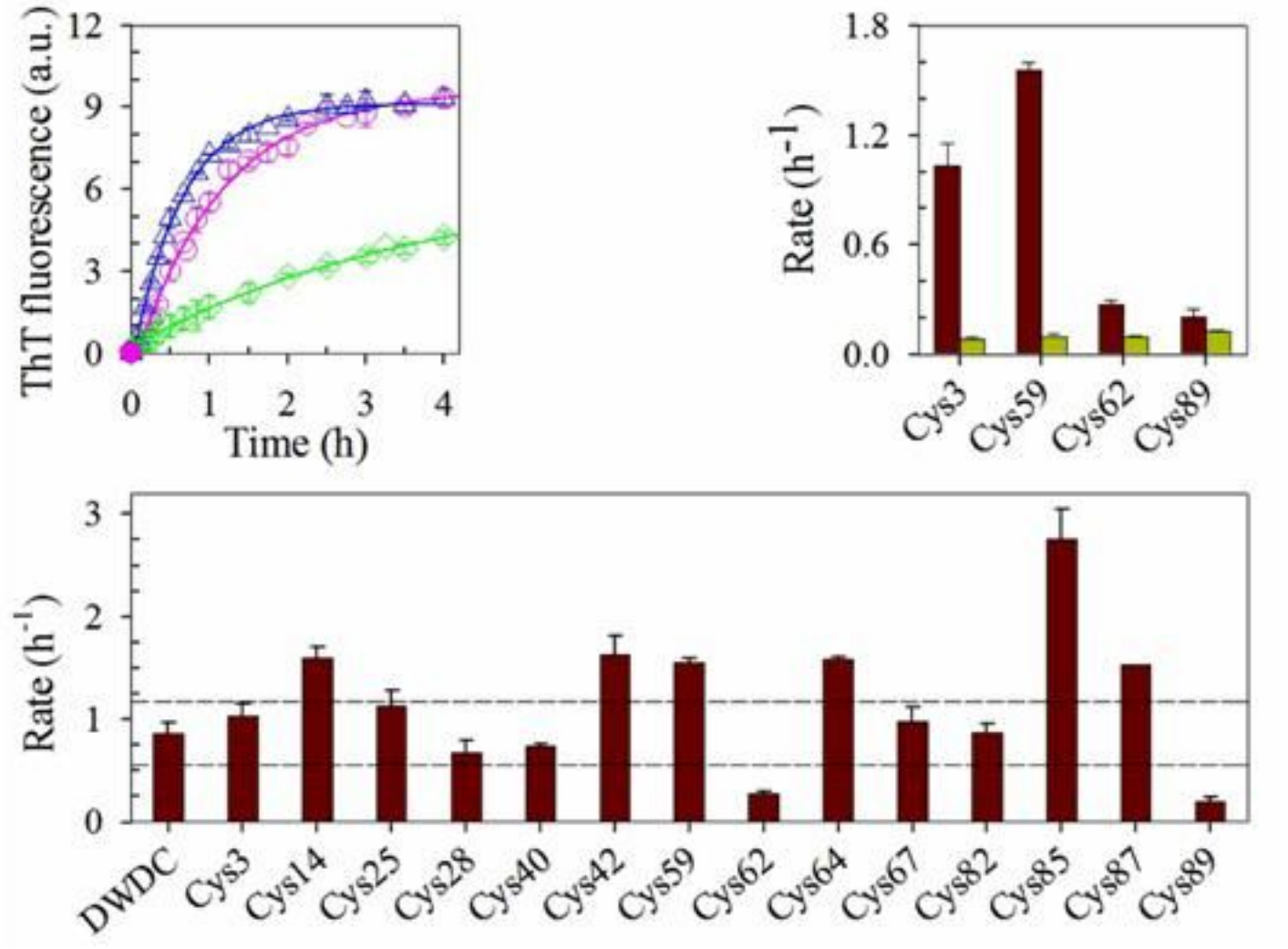

Probe-dependences of the rate constants of amyloid protofibril formation

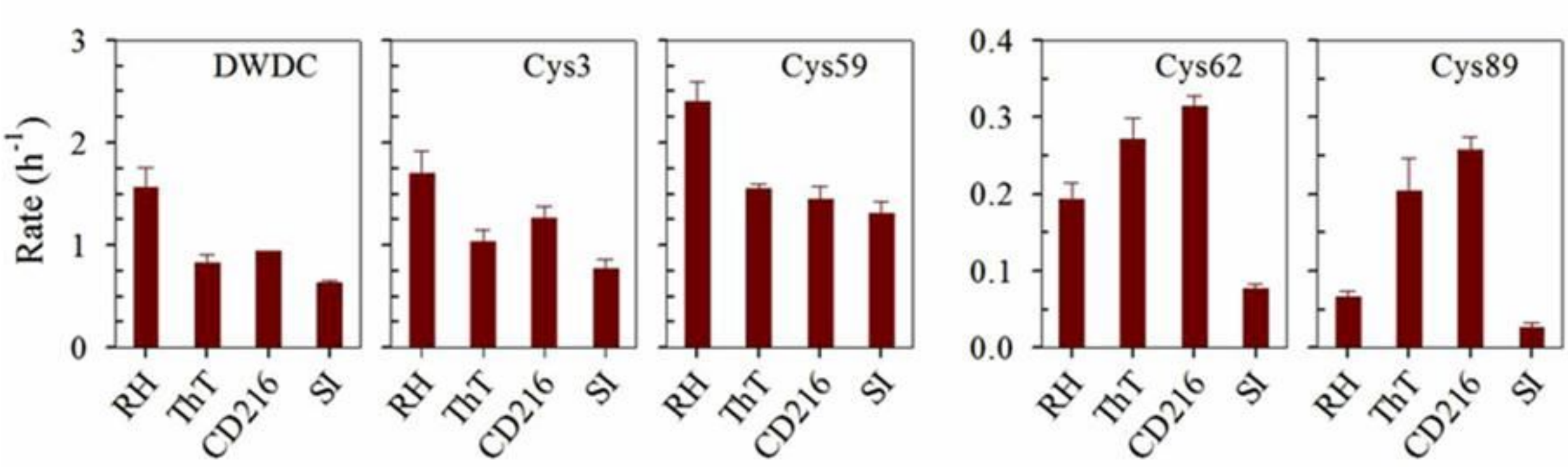

Characterization of the aggregates formed after completion of conformational conversion

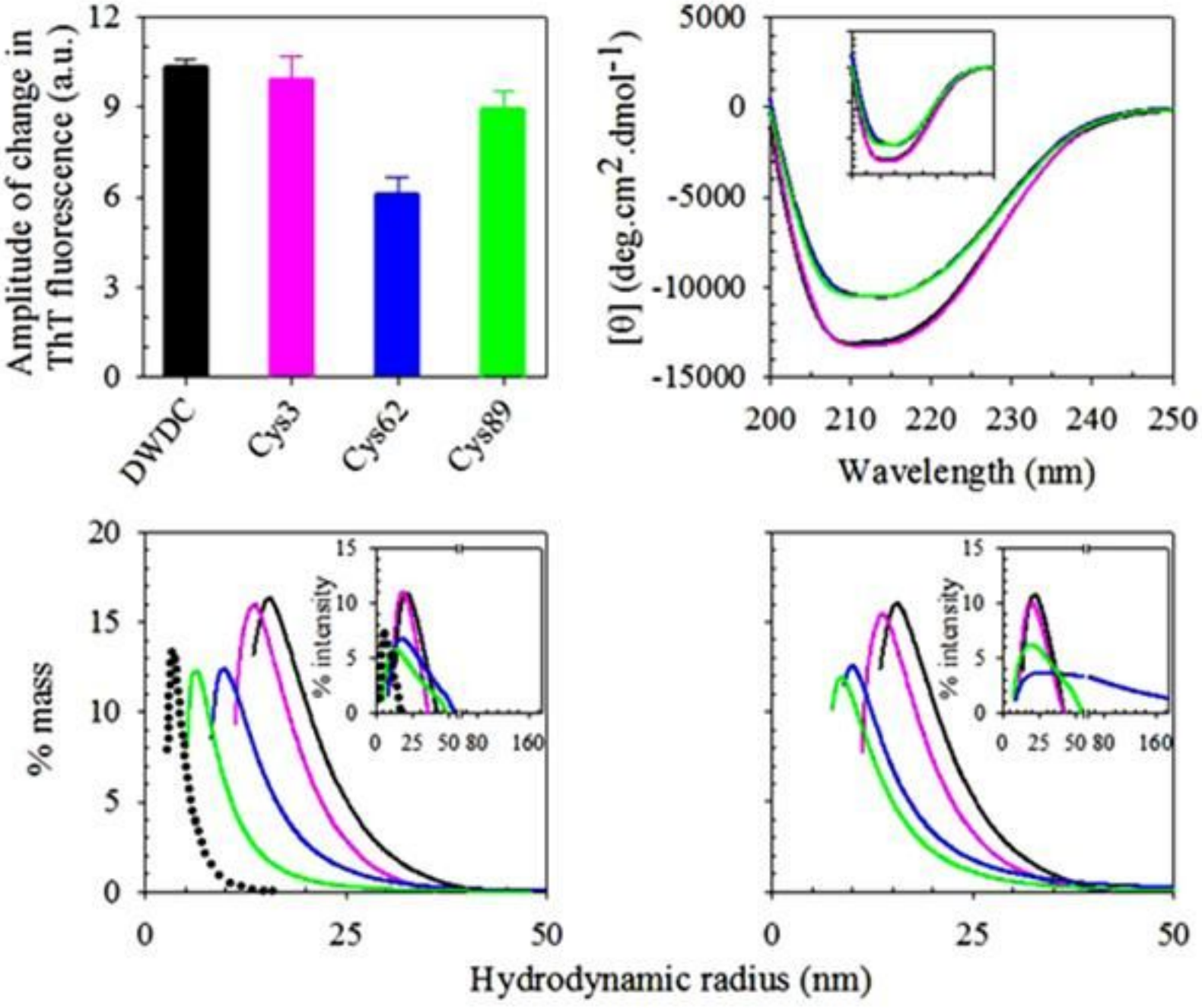

Distributions of the diameters of protofibrils

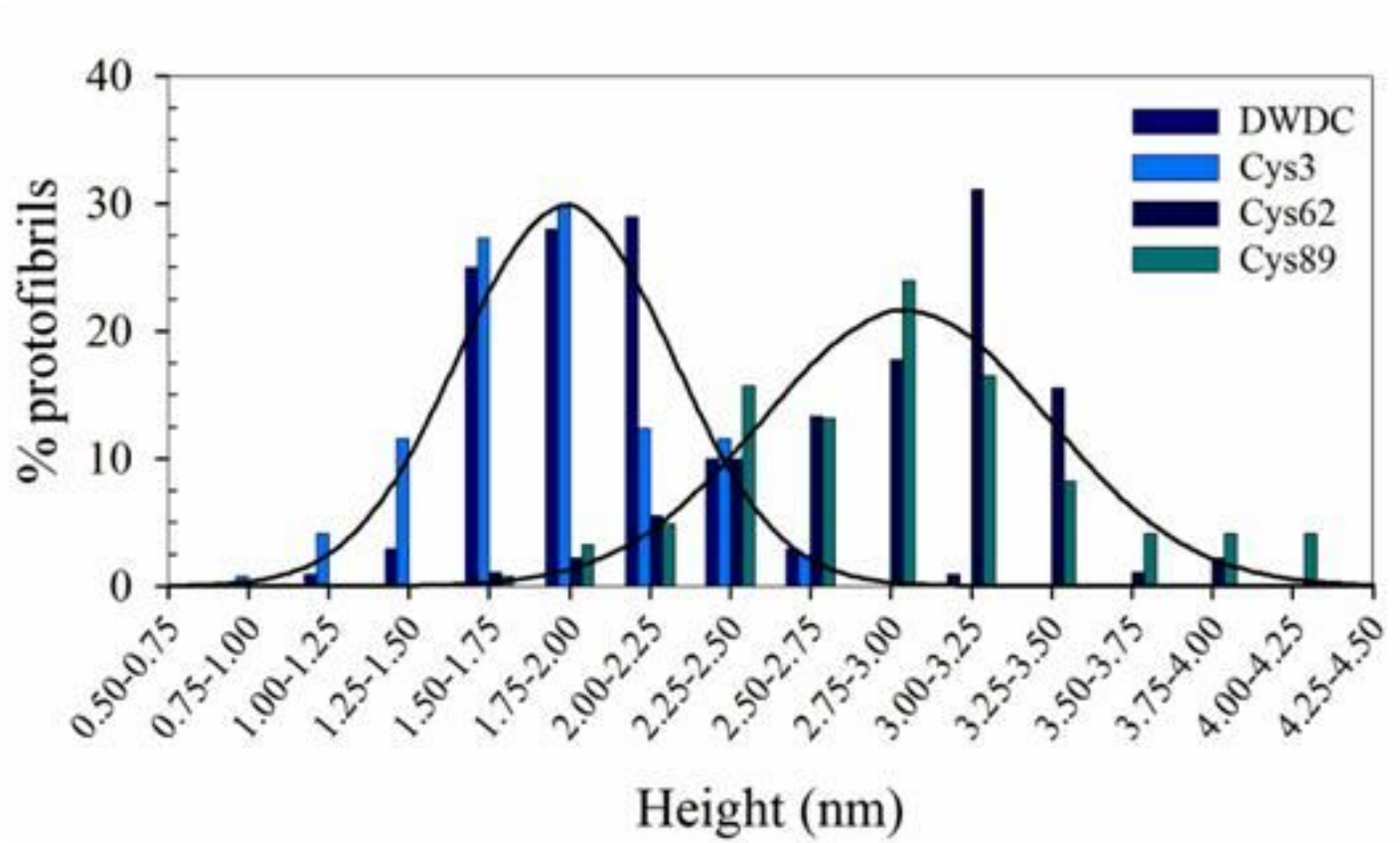

Conformational Conversion May Precede or Follow Aggregate Elongation on Alternative Pathways of Amyloid Protofibril Formation

Santosh Kumar and Jayant B. Udgaonkar*

J. Mol. Biol. (2009) **385**, 1266–1276

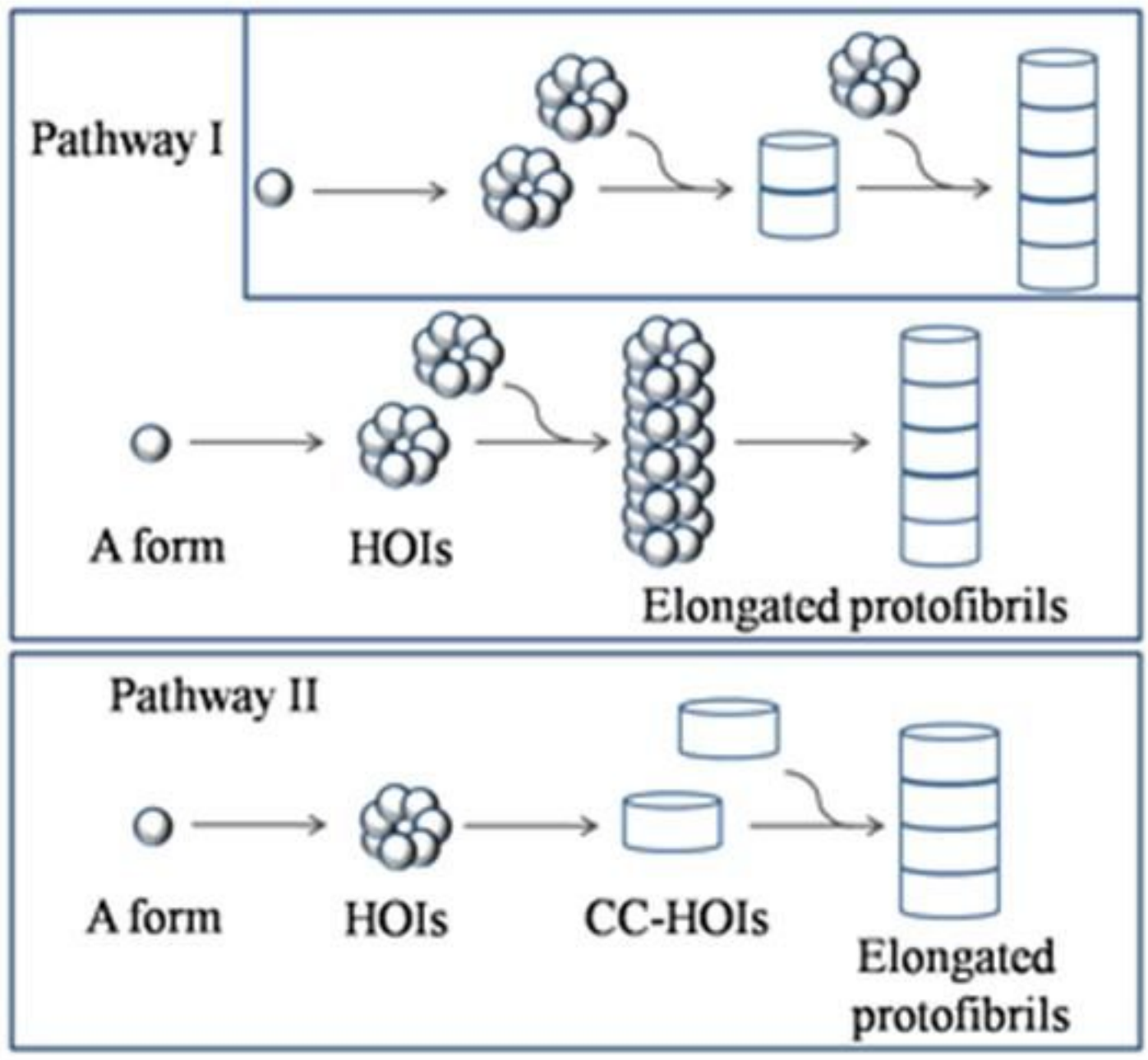

A comparison of TFE-induced protofibrils with thermally-induced protofibrils

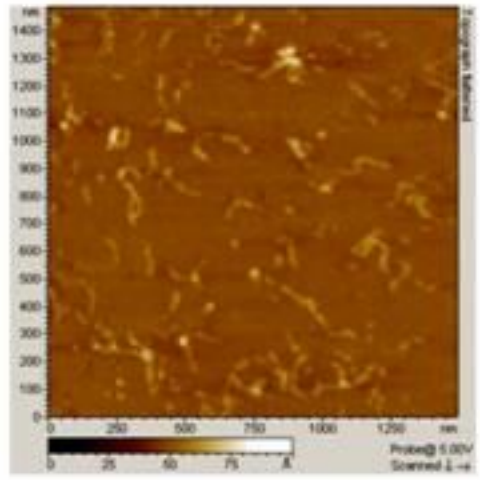

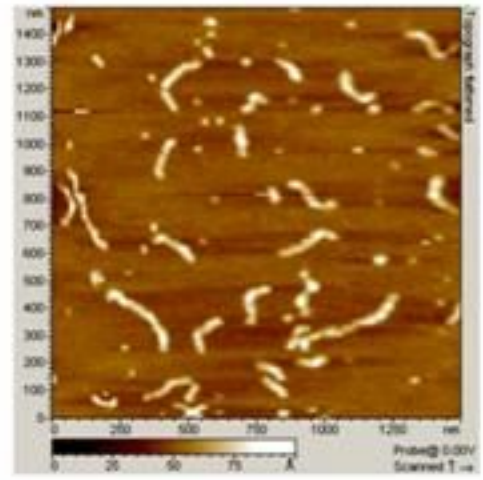

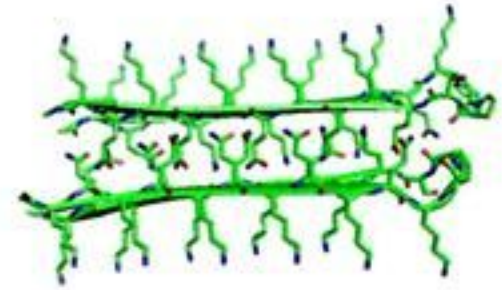

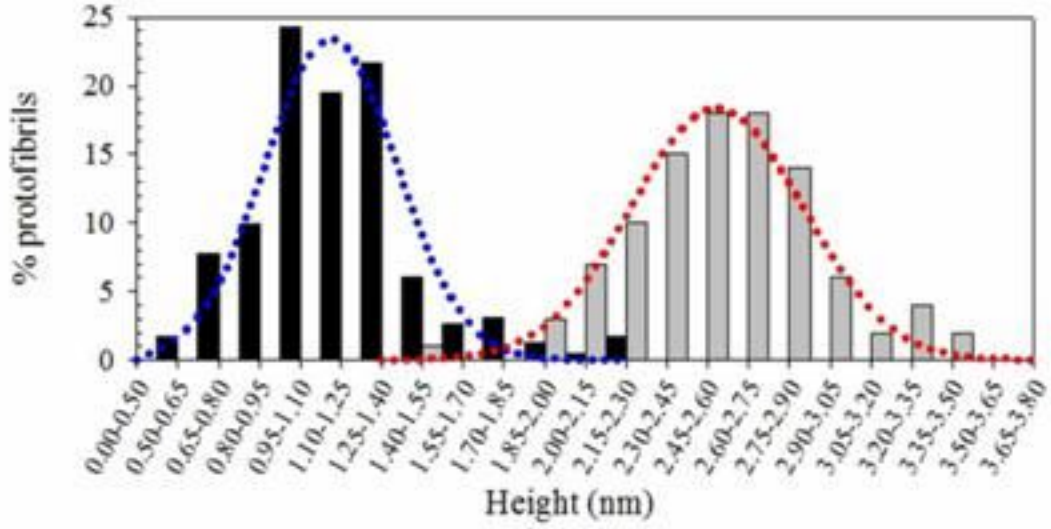

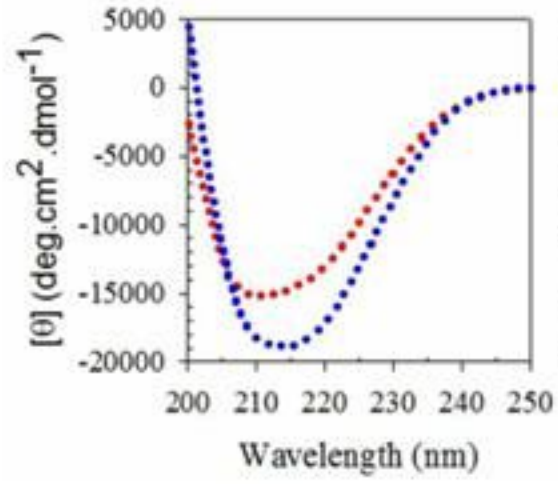

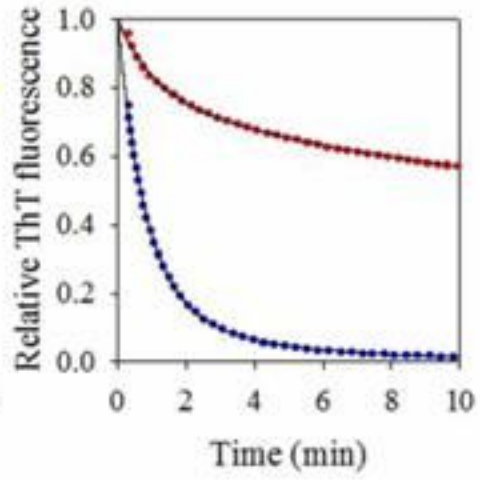

Santosh Kumar and Jayant B. Udgaonkar (2009)

Kinetics of TFE-induced amyloid protofibril formation

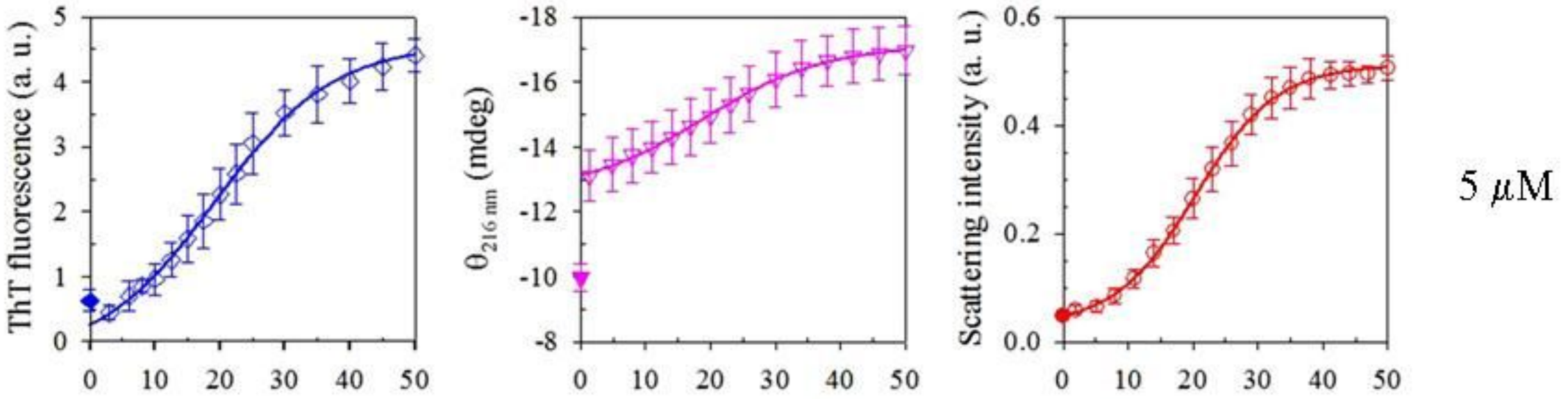

Santosh Kumar and Jayant B. Udgaonkar (2009)

Probe dependence of the observed rate constants

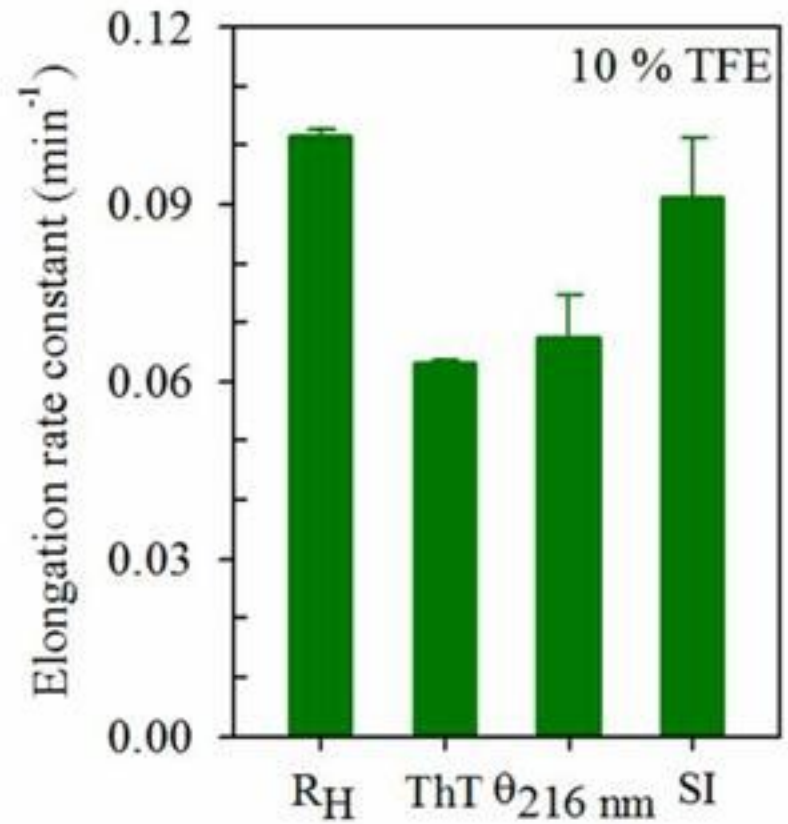

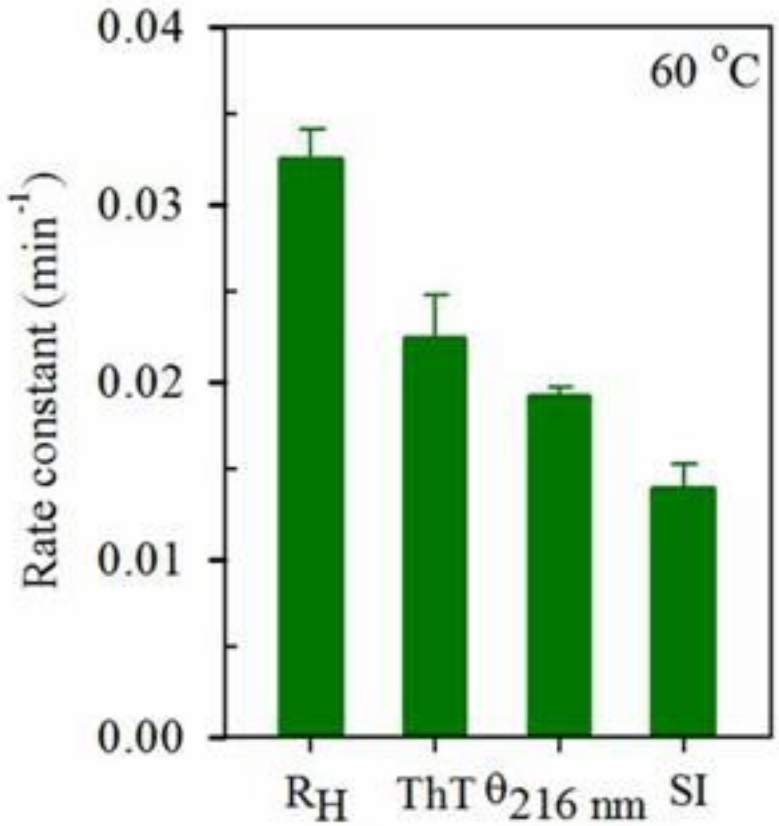

Protein concentration-dependence of the kinetics of TFE-induced amyloid protofibril formation

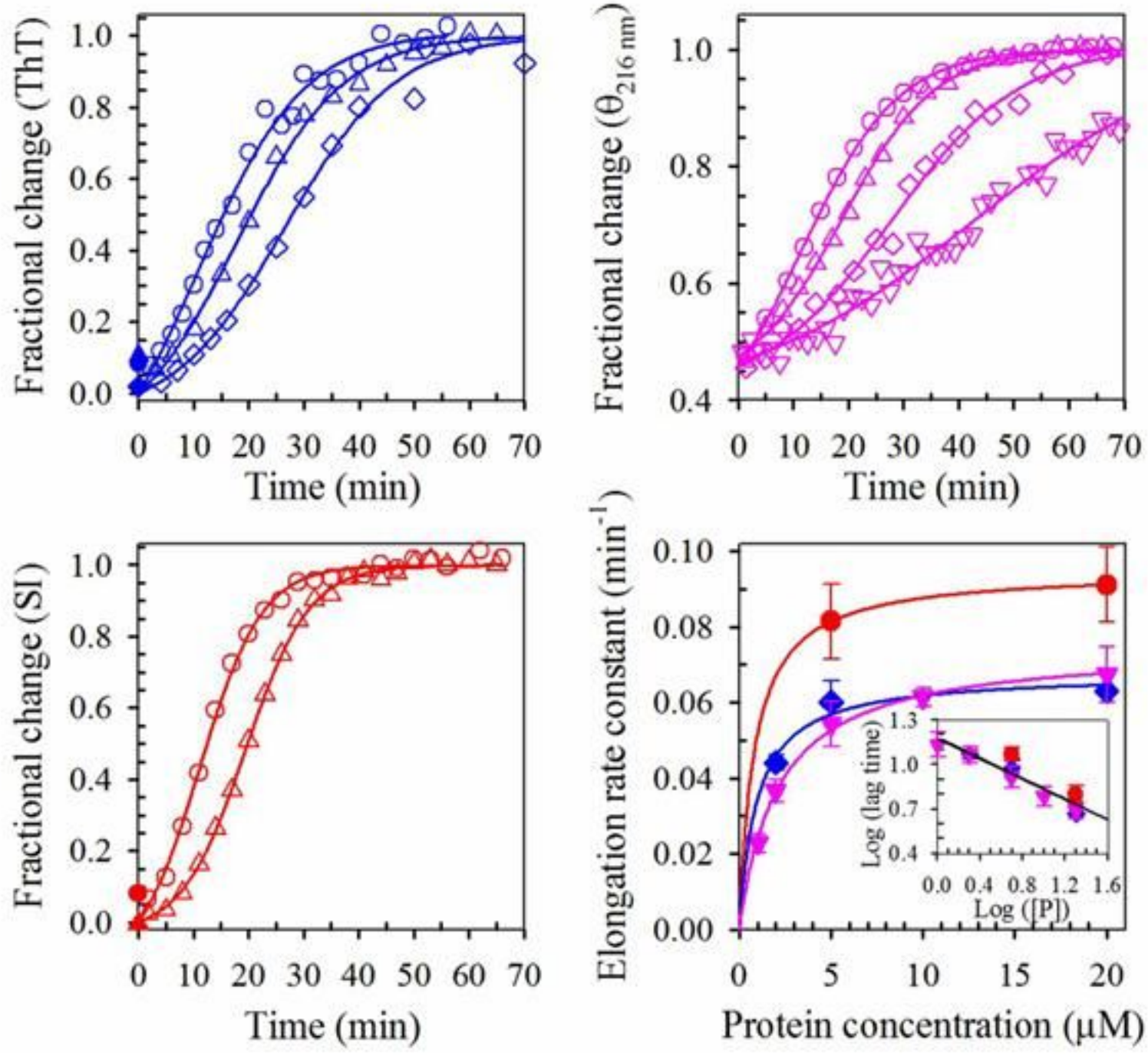

Mechanistic origin of conformational polymorphism

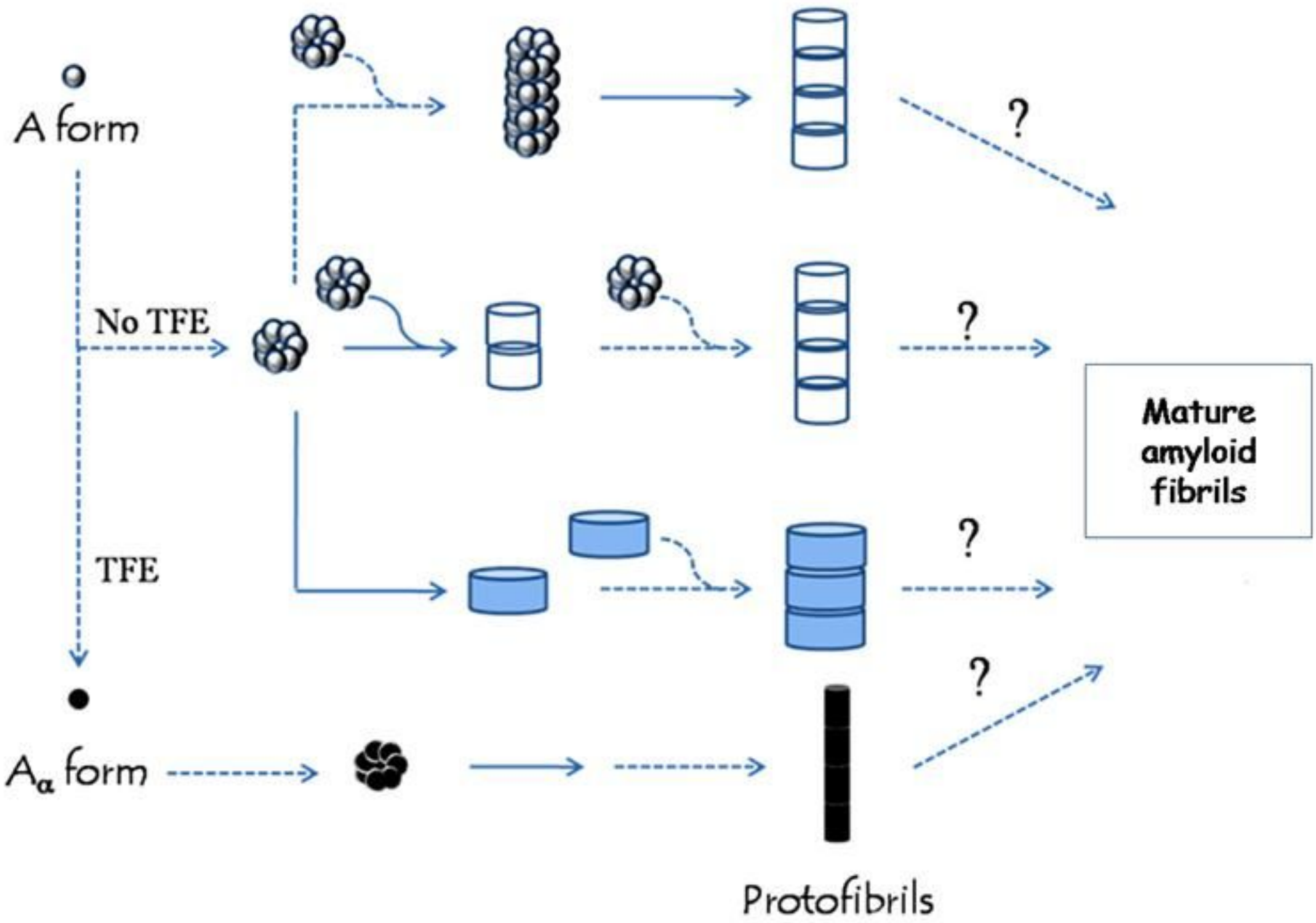

Santosh Kumar and Jayant B. Udgaonkar (2009)

Prion protein

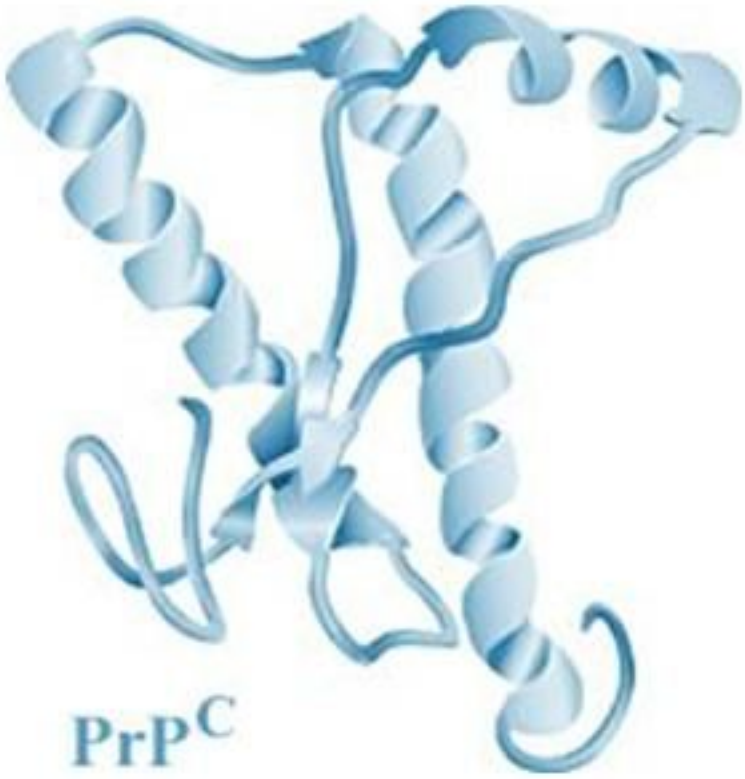

NMR Structure of C-terminal piece

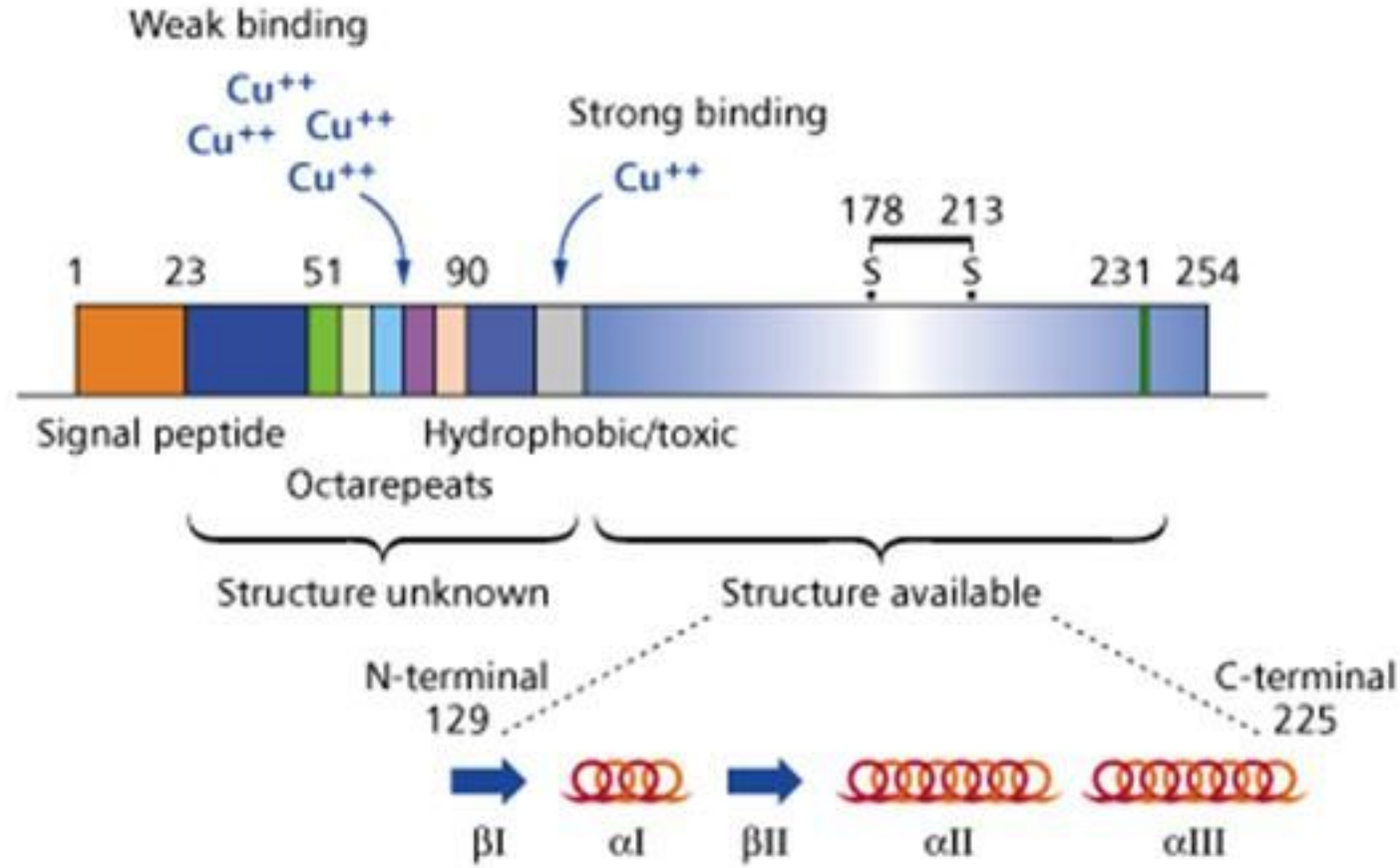

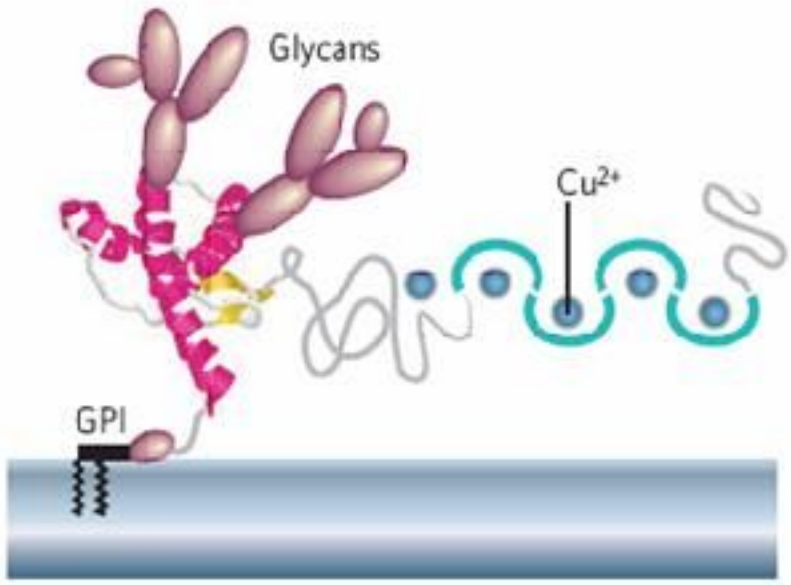

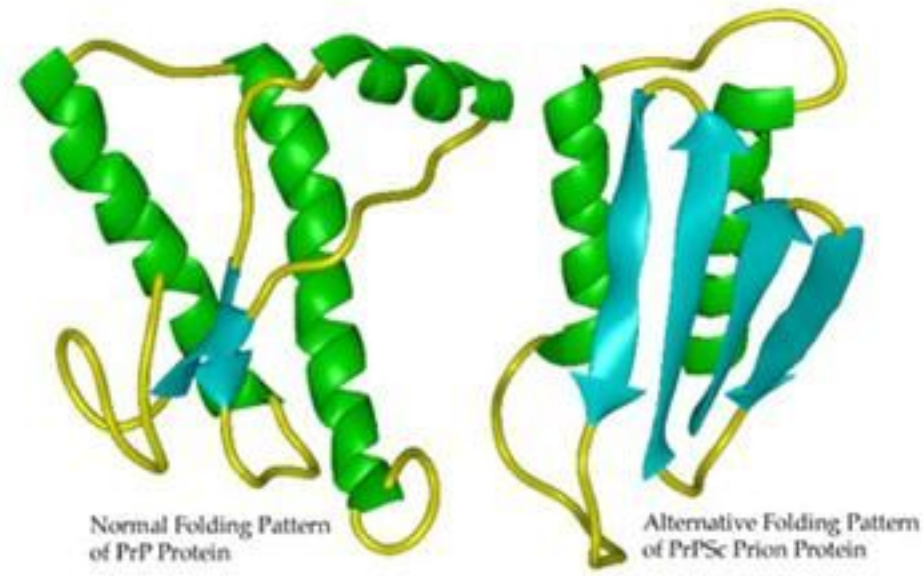

Fibril formation in the Prion protein

Nucleation dependent mechanism

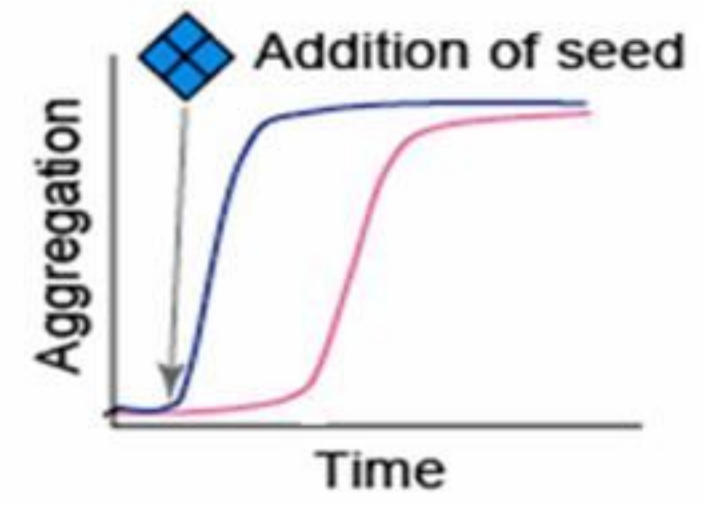

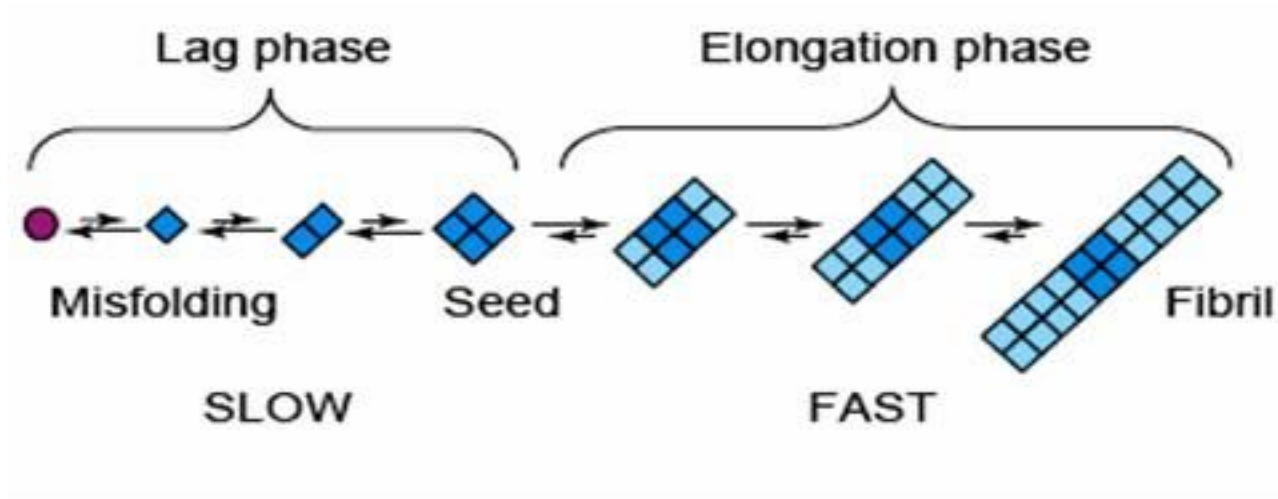

Prion protein propagates through autocatalytic misfolding

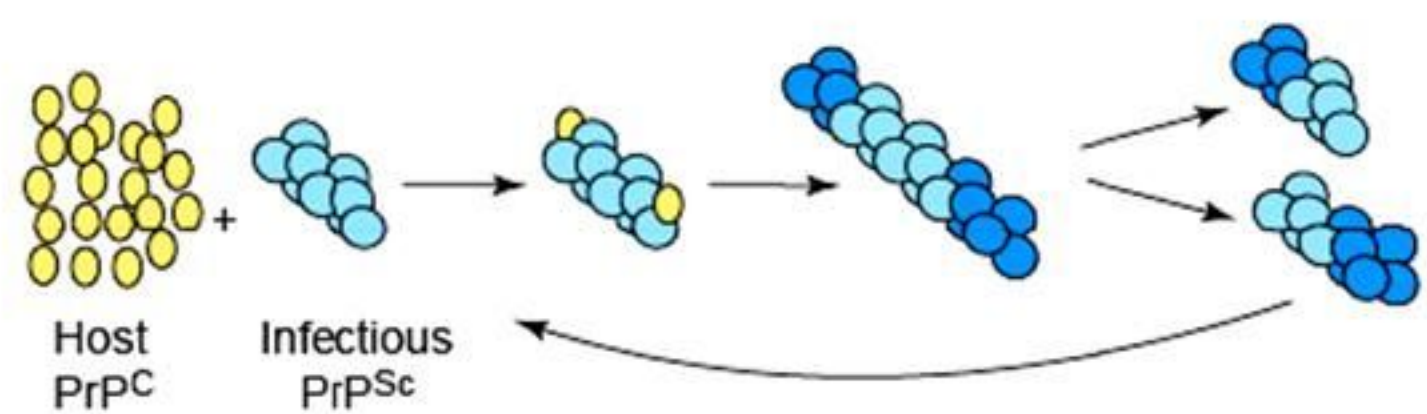

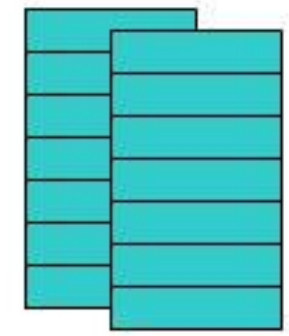

Amyloid fibrils

TIBS (2006), 31, 150-155

Formation of amyloid protofibrils by mouse prion protein

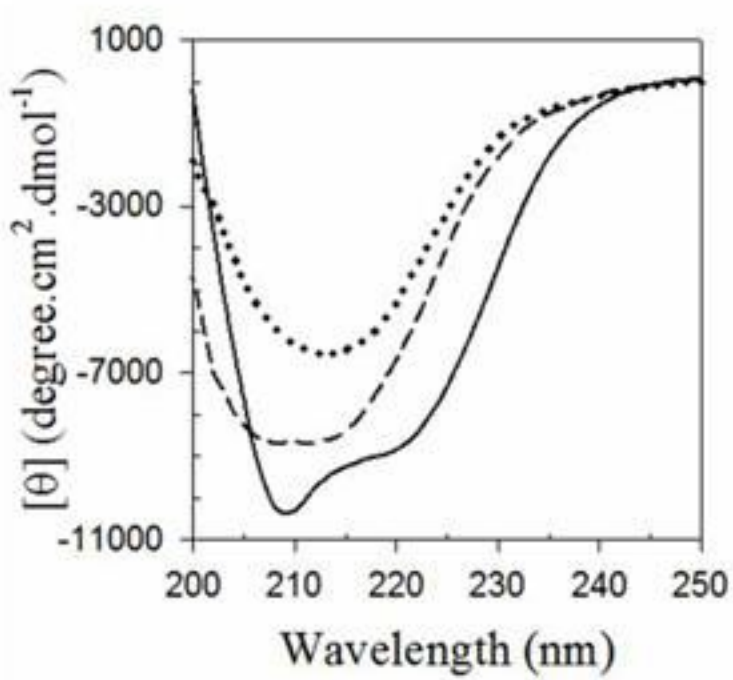

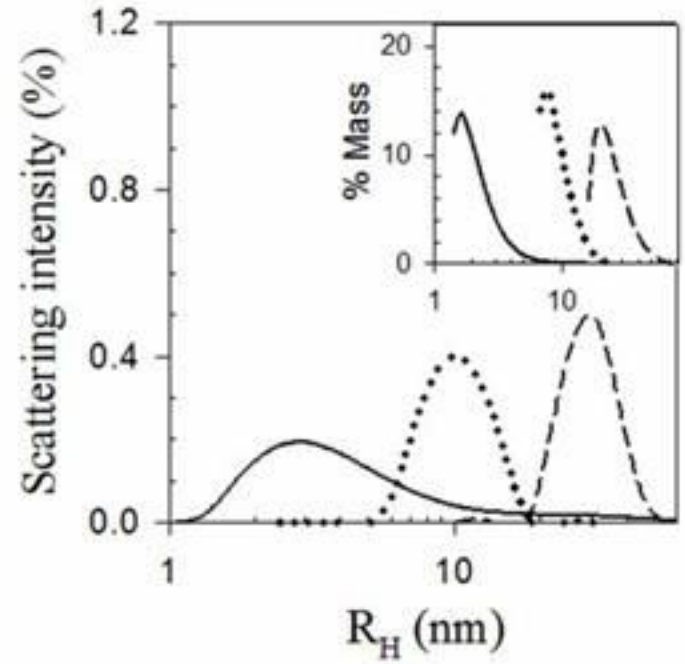

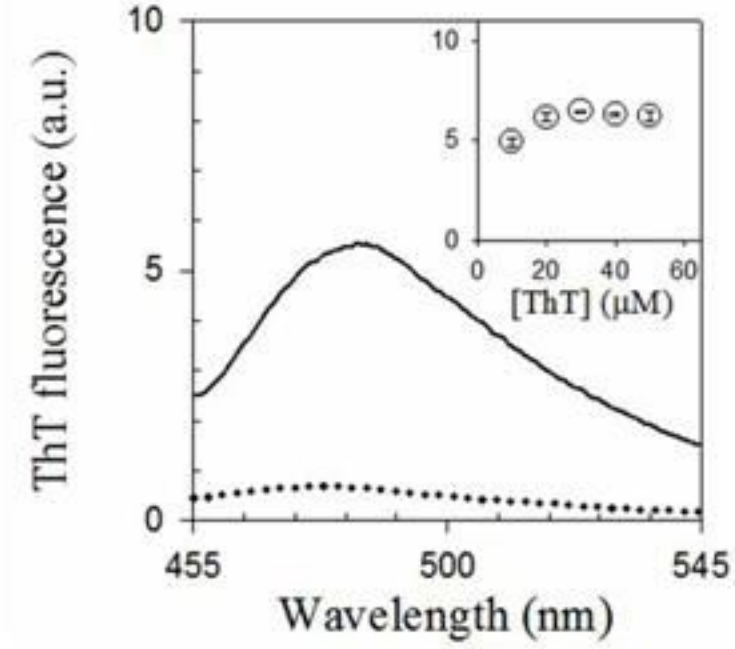

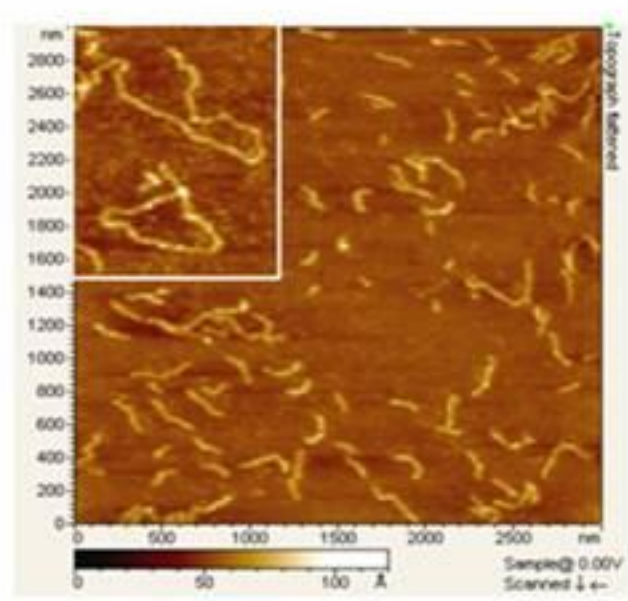

PrP^C
(Cellular form of prion protein)

pH 2, salt

β-rich soluble oligomers

Heat

Worm-like amyloid fibrils

β-rich oligomers exist in equilibrium with a-rich monomers

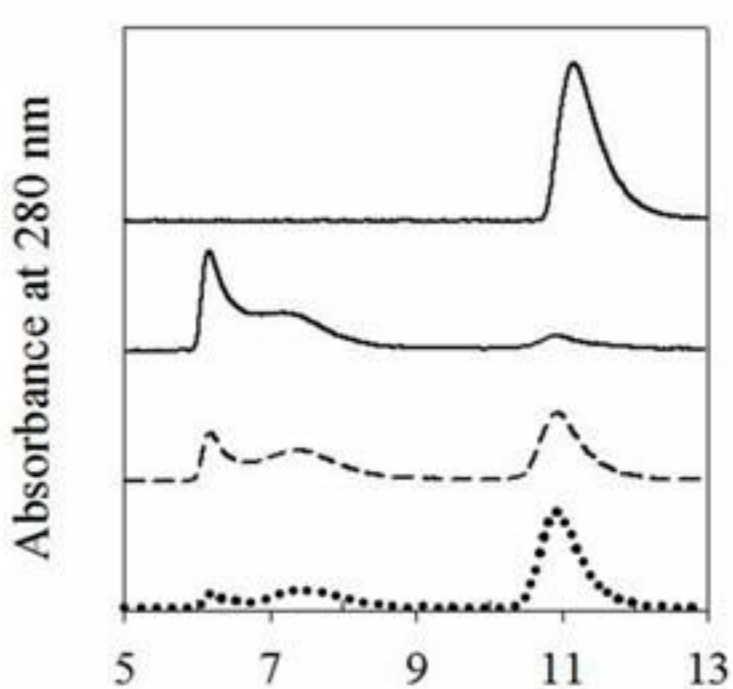

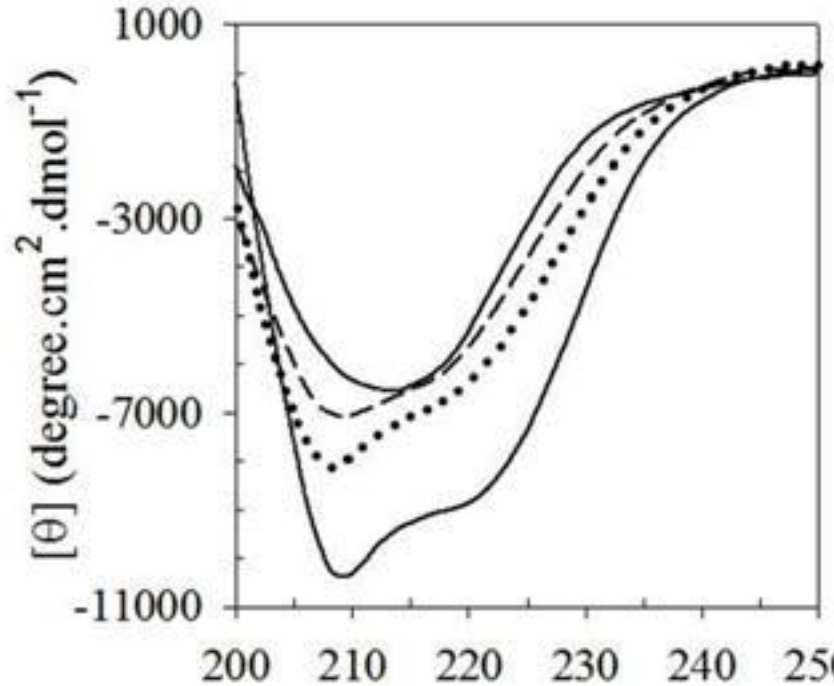

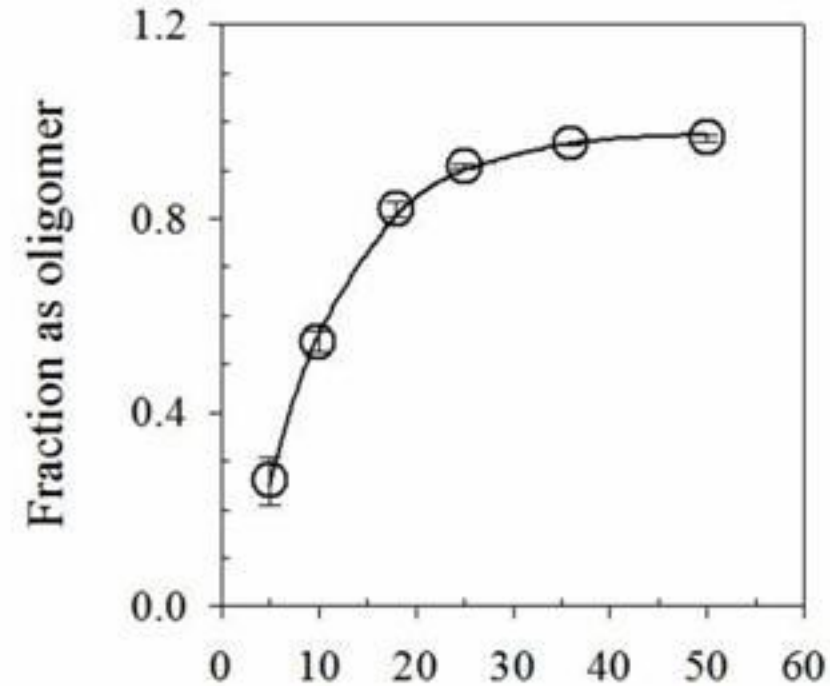

Native PrP
5 μM
10 μM
25 μM

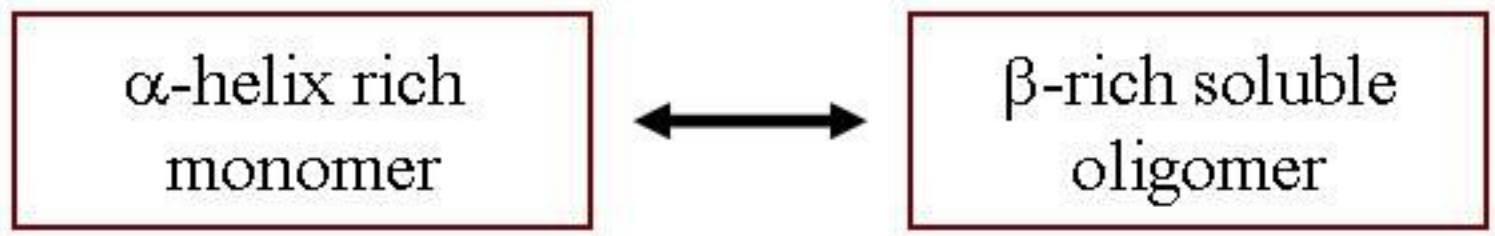

β-rich oligomer and not the α-rich monomer converts into worm-like amyloid fibrils.

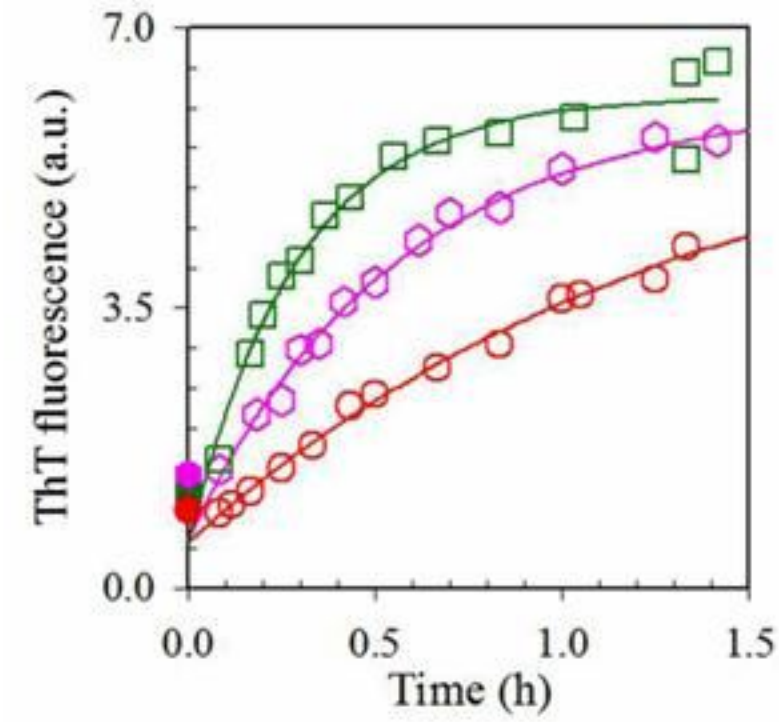

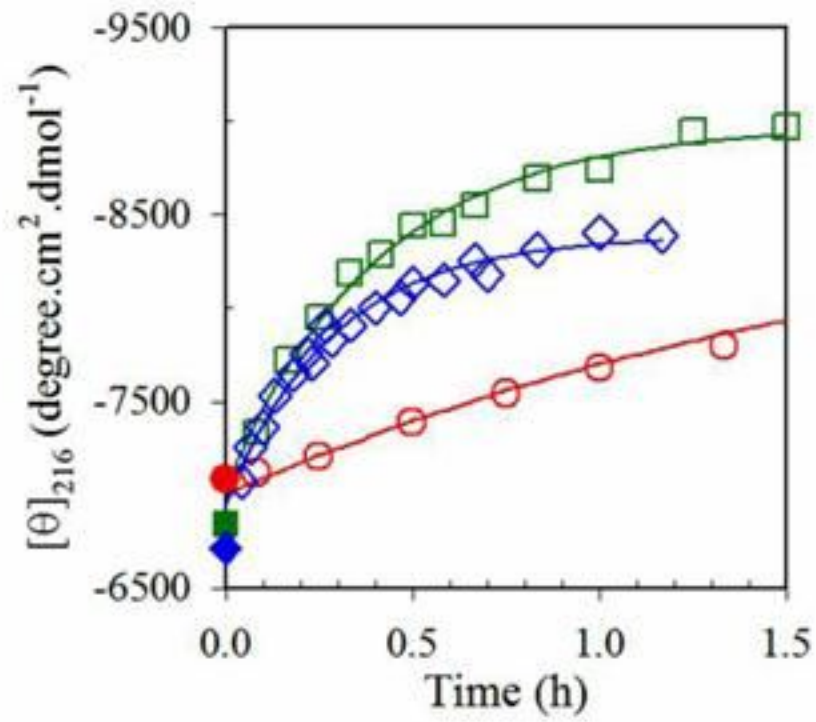

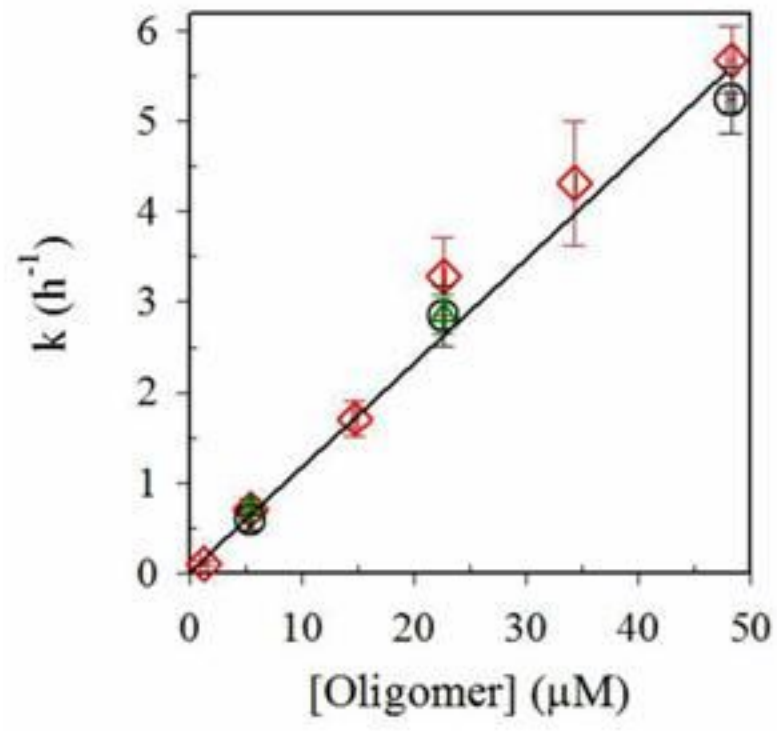

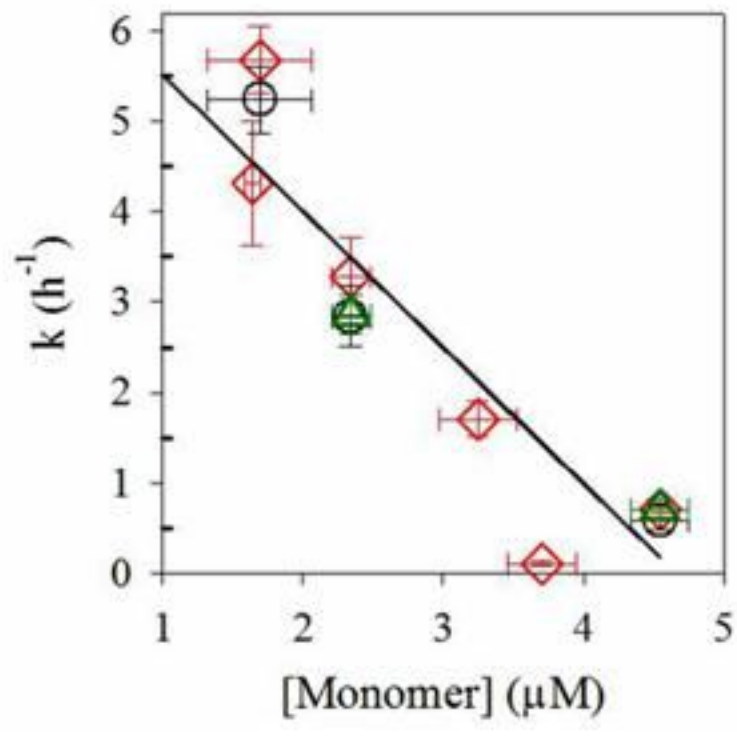

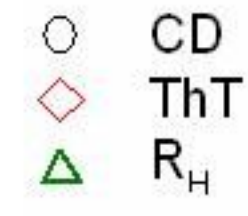

β-rich oligomer converts step-wise into worm-like amyloid fibrils

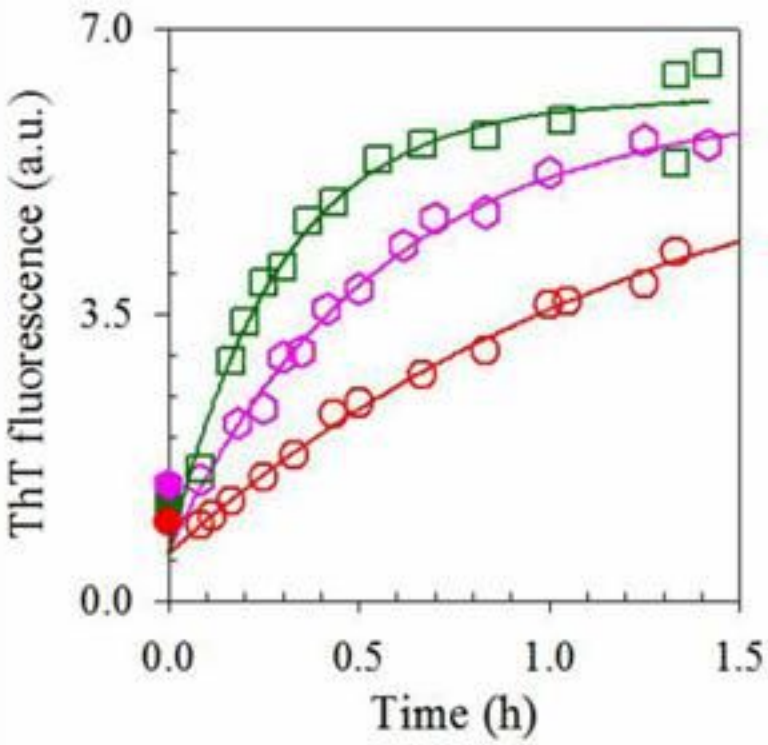

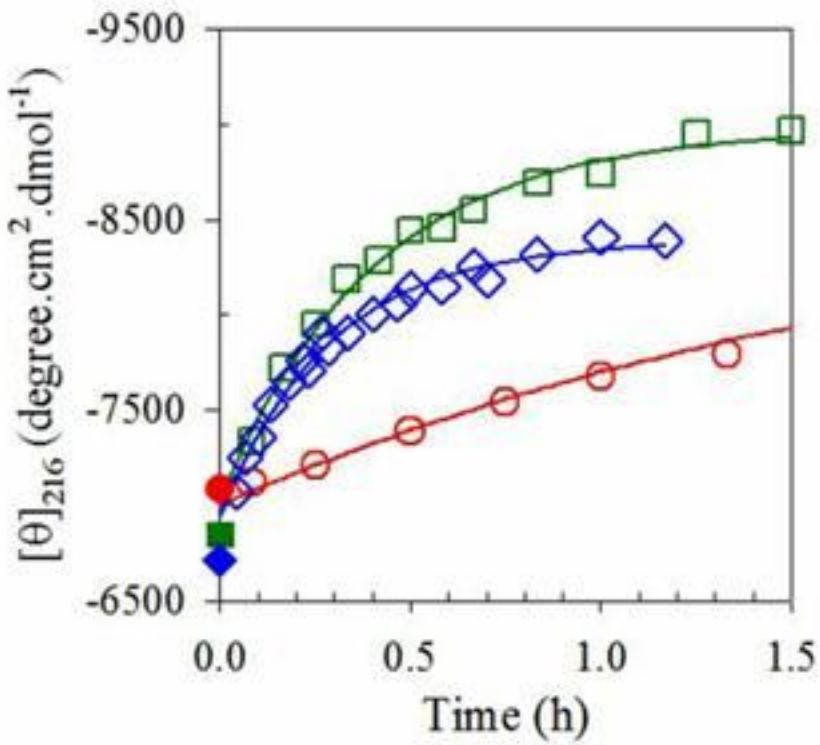

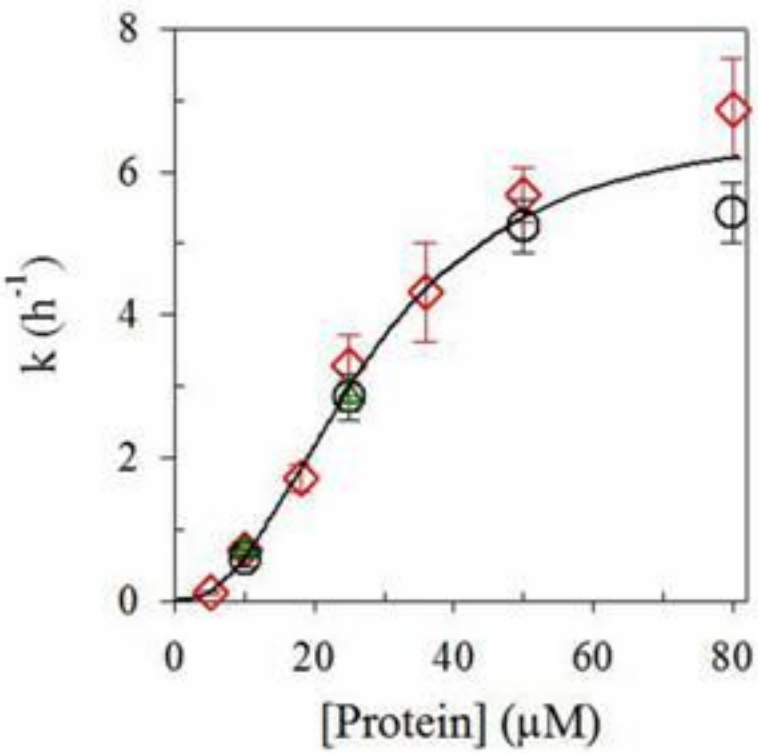

Conversion of the β-rich oligomer into worm-like amyloid fibrils occurs through higher order oligomers

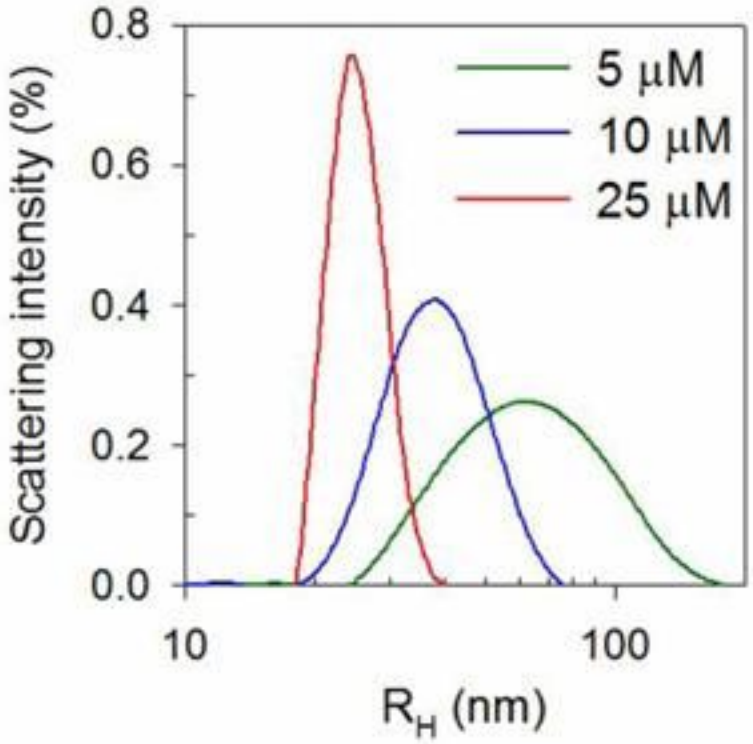

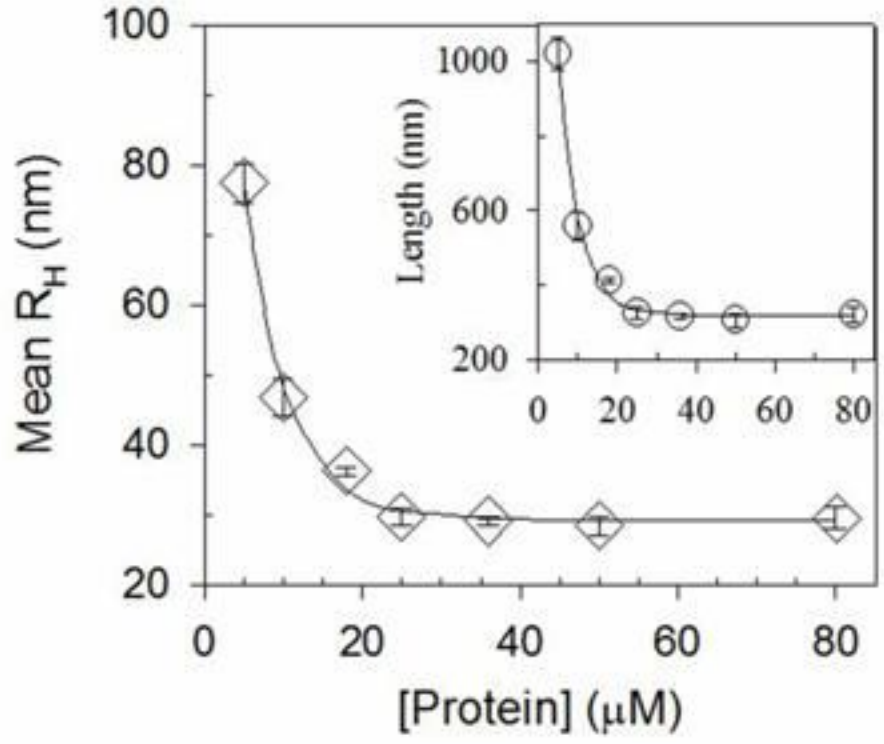

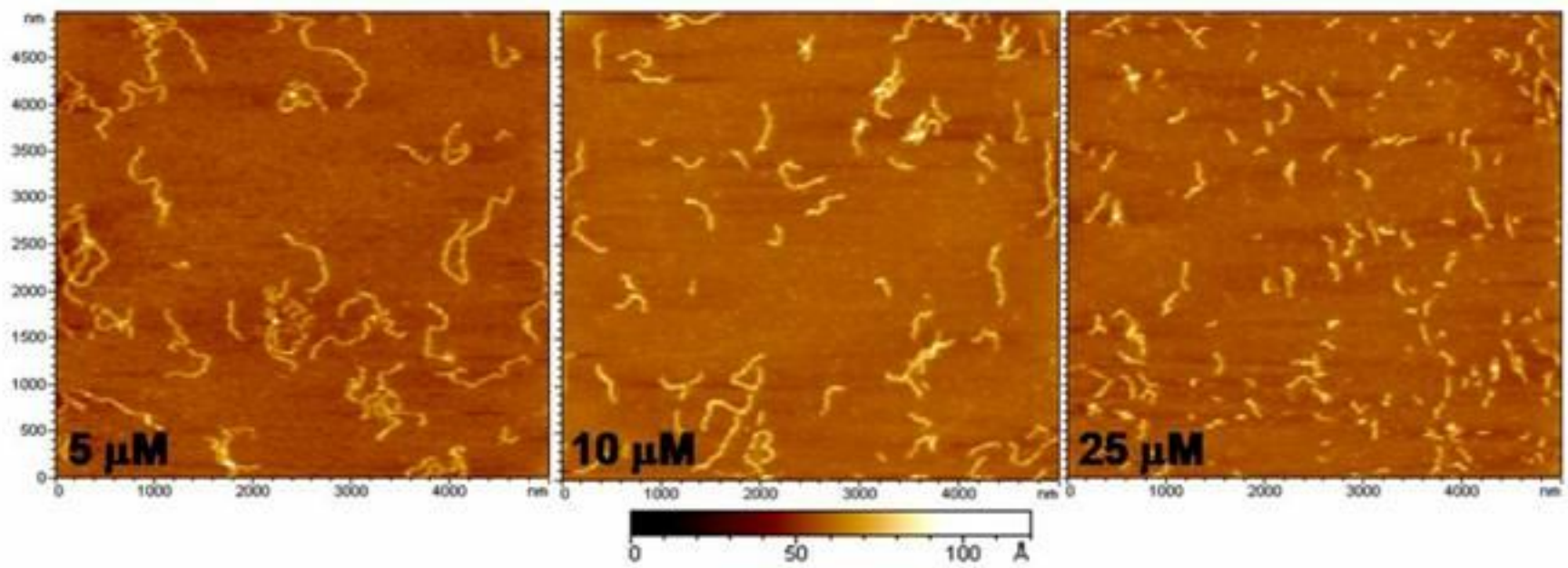

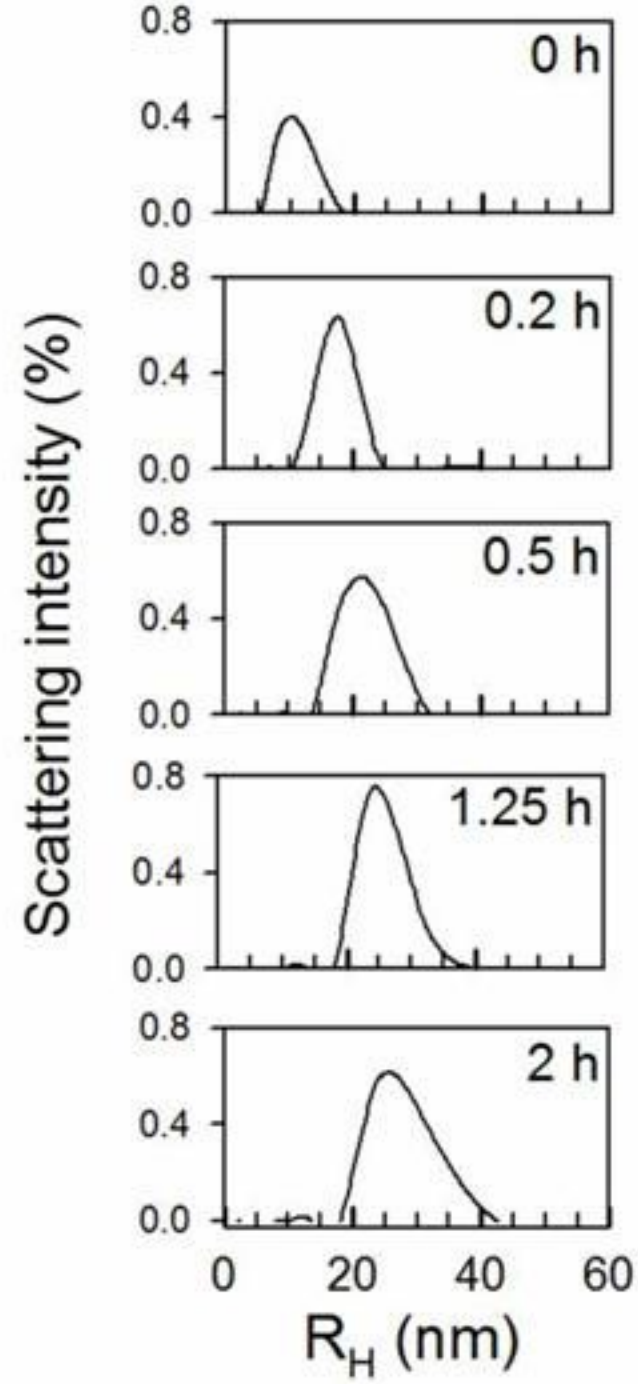

Kinetics of amyloid fibrillation monitored by multiple probes

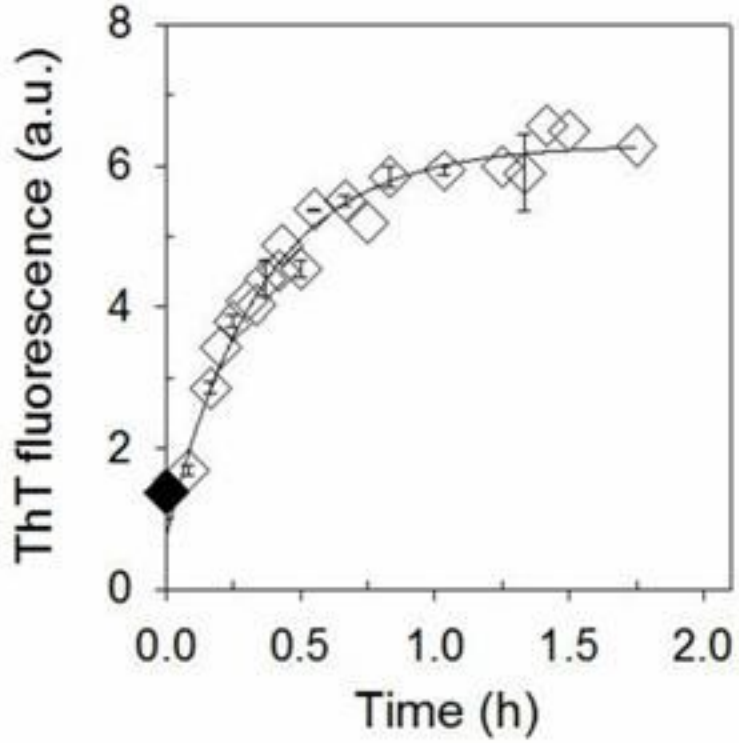

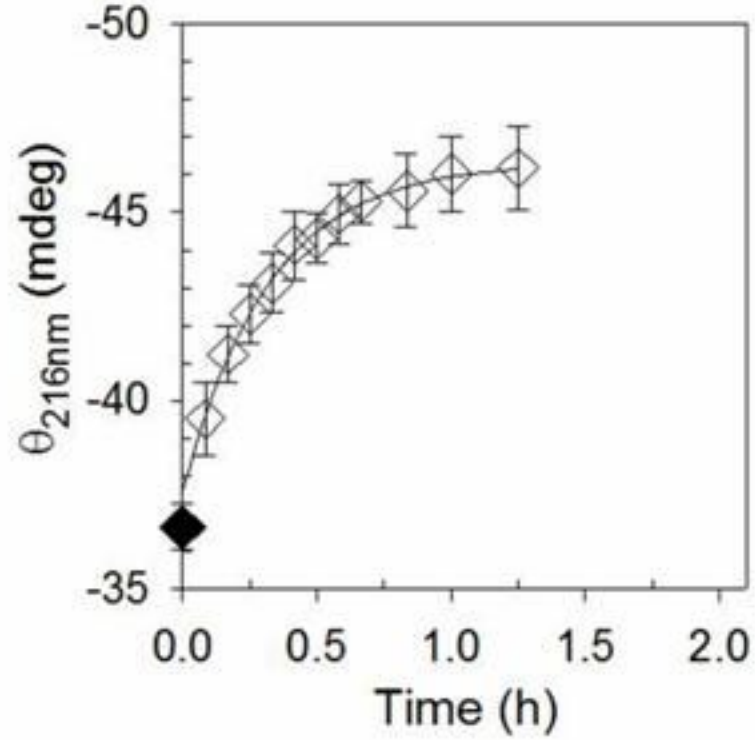

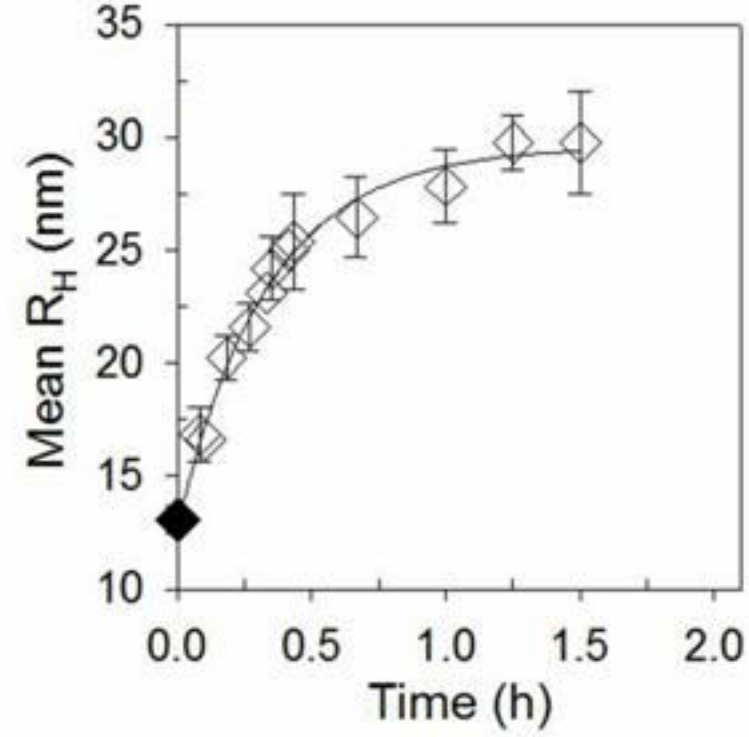

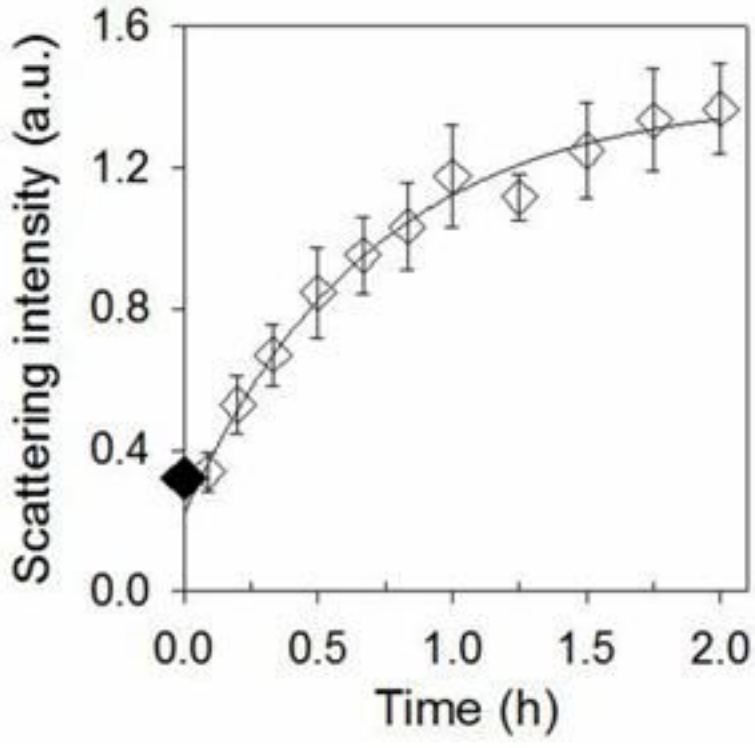

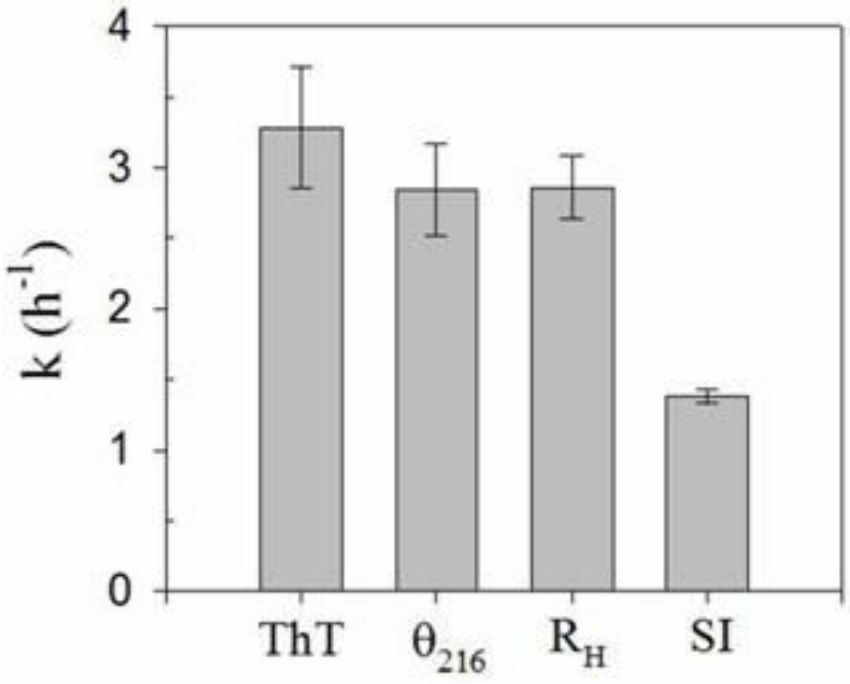

Evidence for Stepwise Formation of Amyloid Fibrils by the Mouse Prion Protein

Shweta Jain and Jayant B. Udgaonkar*

J. Mol. Biol. (2008) **382**, 1228–1241

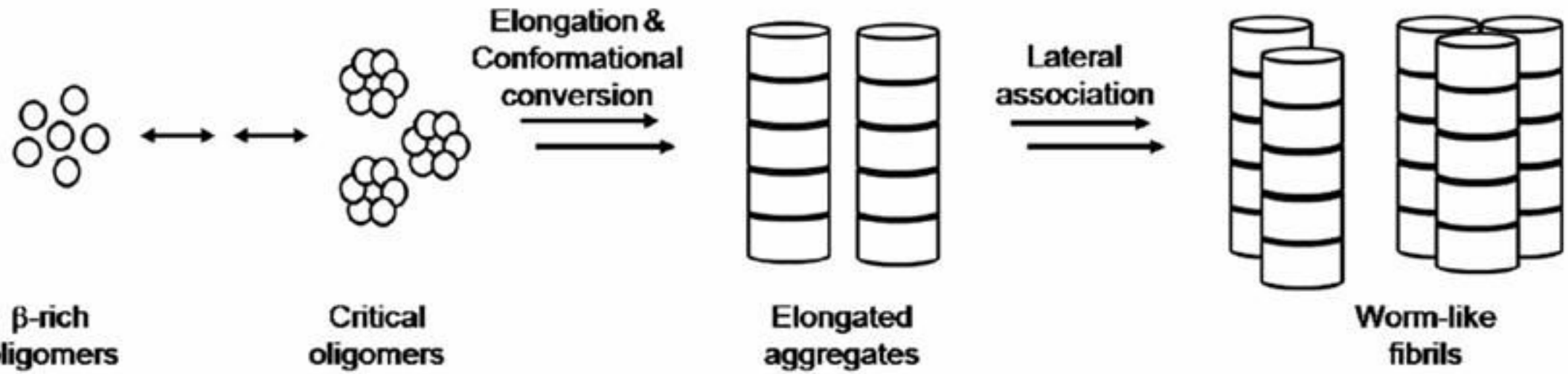

Fig. 7. Model for the formation of worm-like amyloid fibrils by the moPrP. The β-rich oligomers equilibrate with large oligomers, including elongation-competent critical oligomers. The critical oligomer grows by addition of smaller oligomers. Elongation occurs simultaneously with conformational change during fibrillation. Finally, the elongated aggregates appear to associate laterally to form mature worm-like fibrils.

Mutations alter extent of oligomer formation

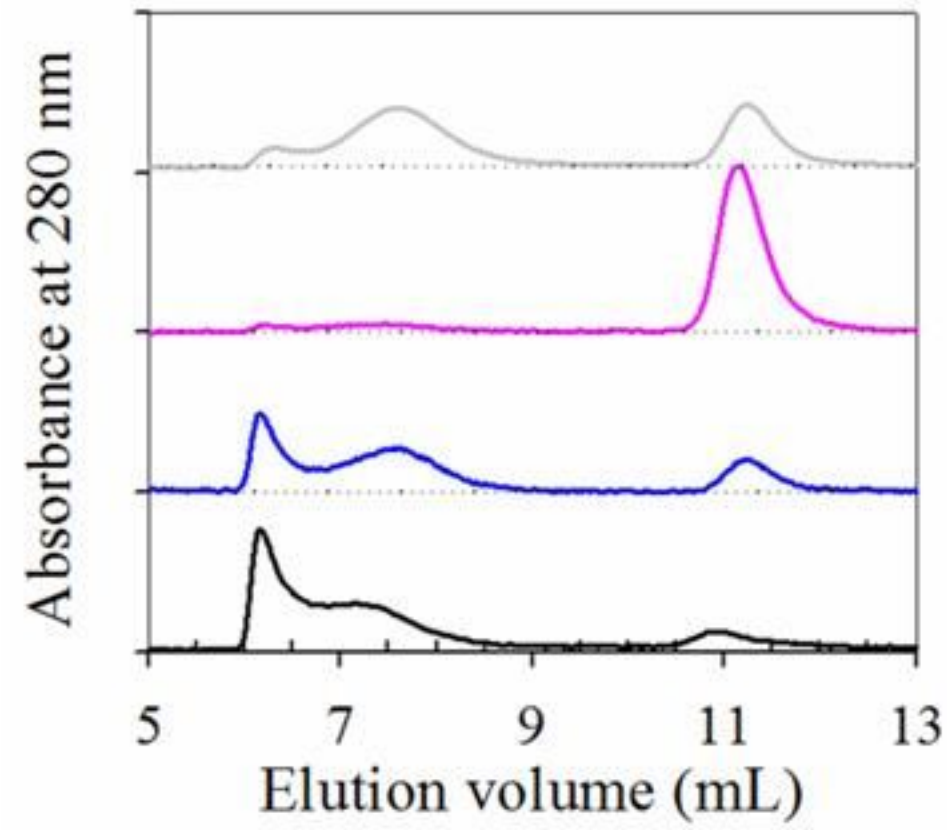

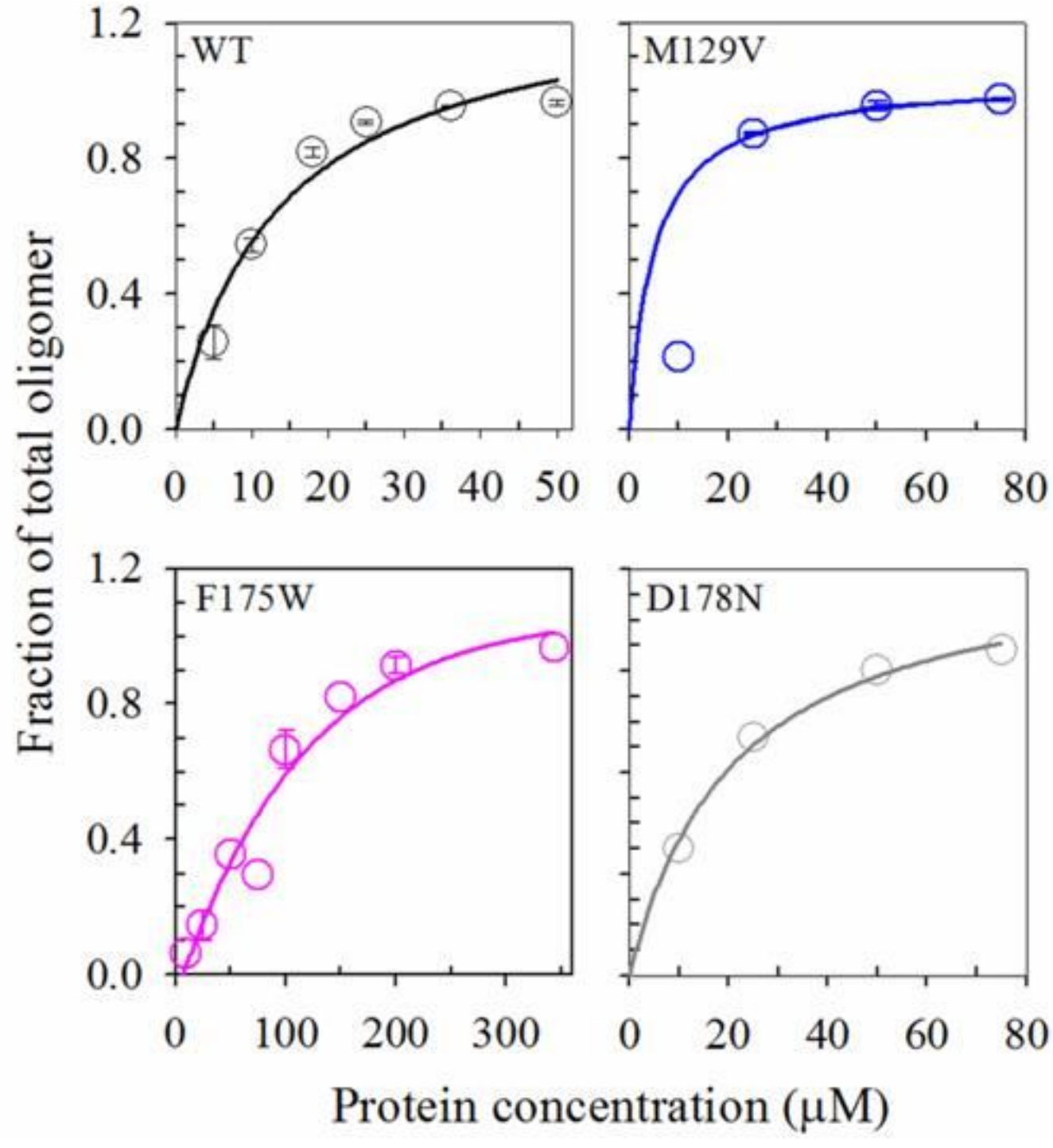

Mutations alter the rate of protofibril formation by affecting the extent of β-rich oligomer formation

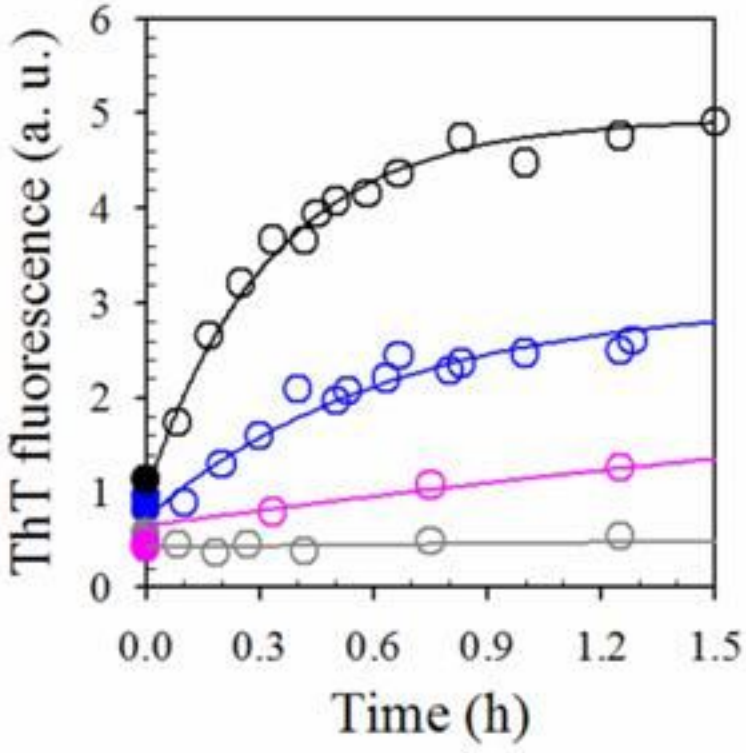

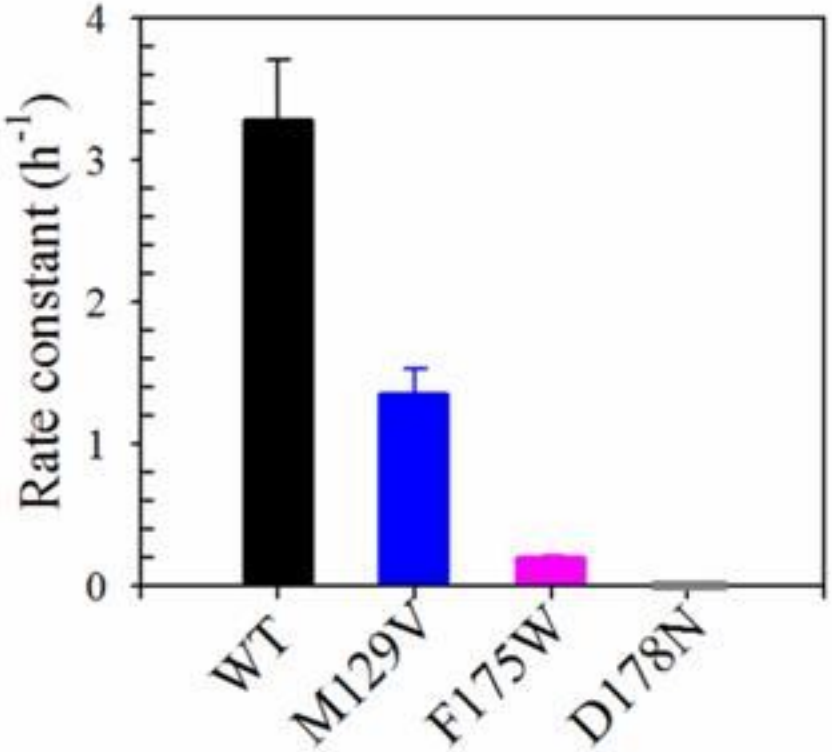

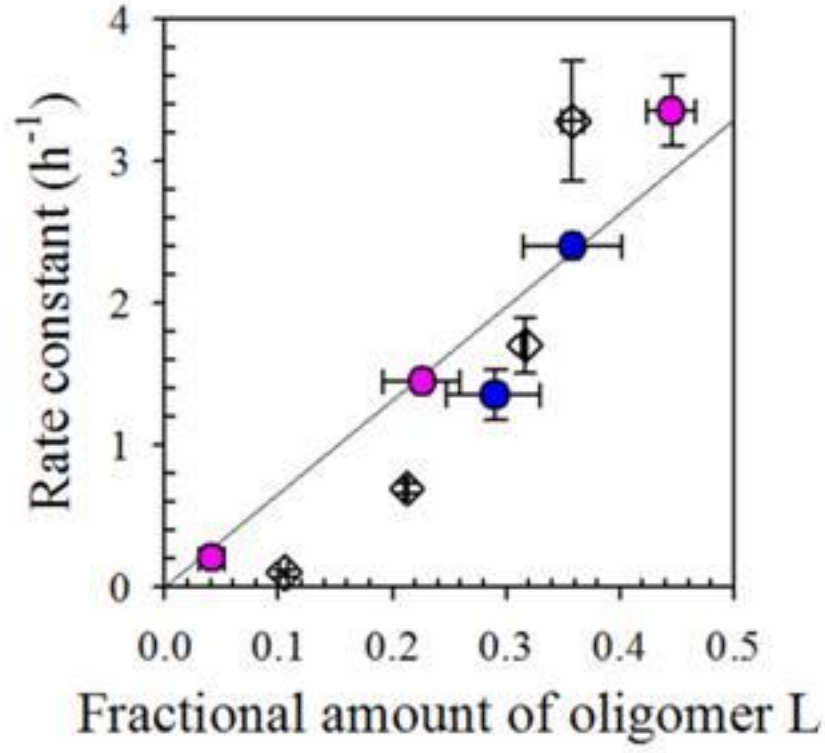

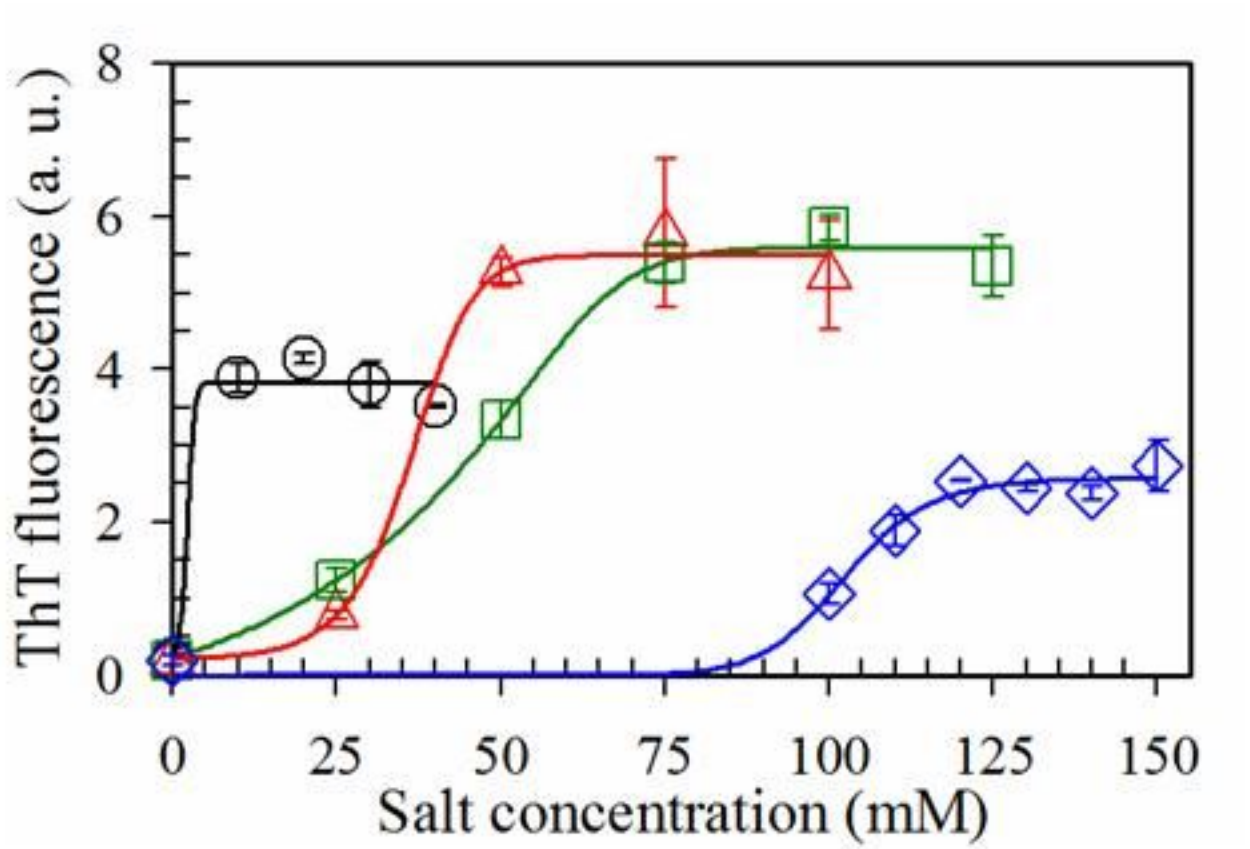
ThT fluorescence (a. u.)
0
2
4
6
8
0
25
50
75
100
125
150
Salt concentration (mM)

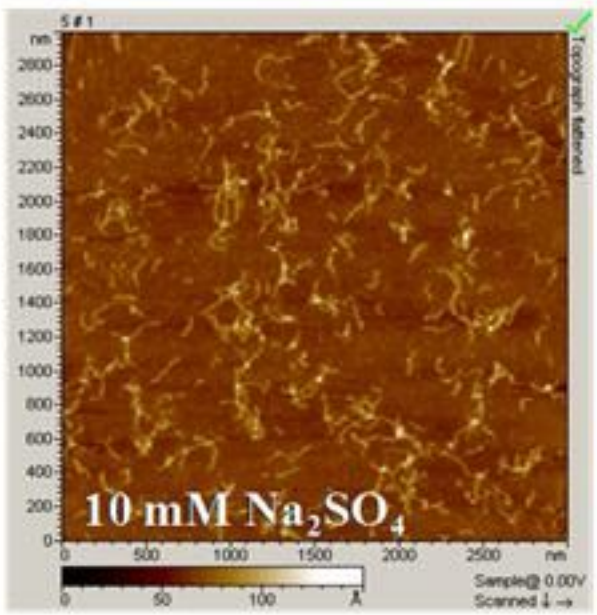
10 mM Na_2SO_4

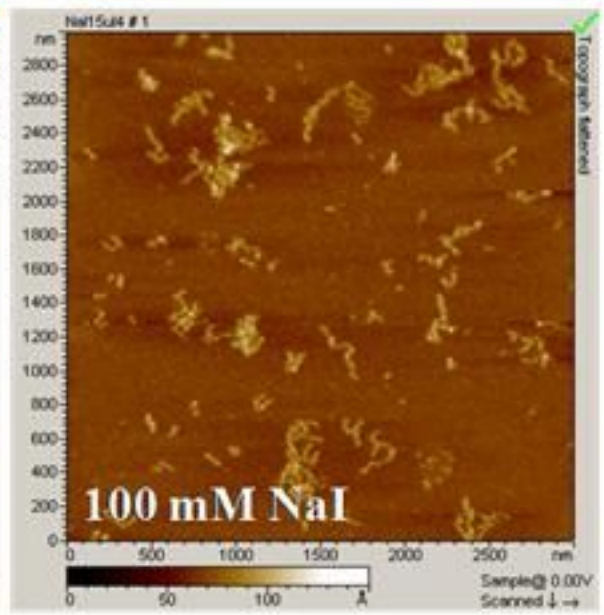
100 mM NaI

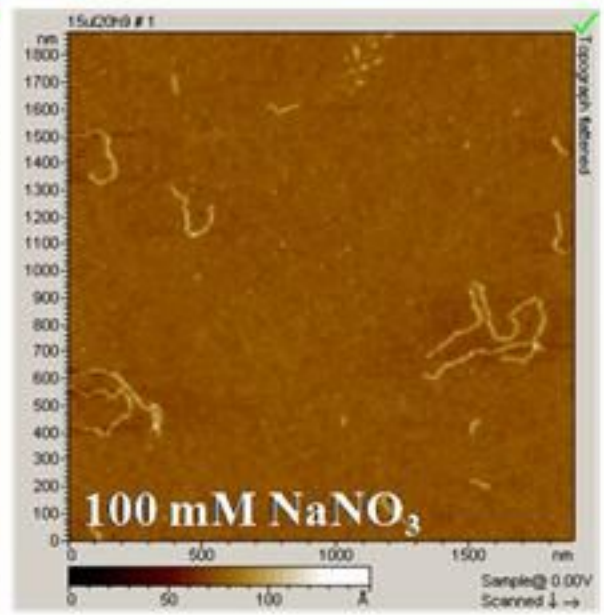
100 mM $NaNO_3$

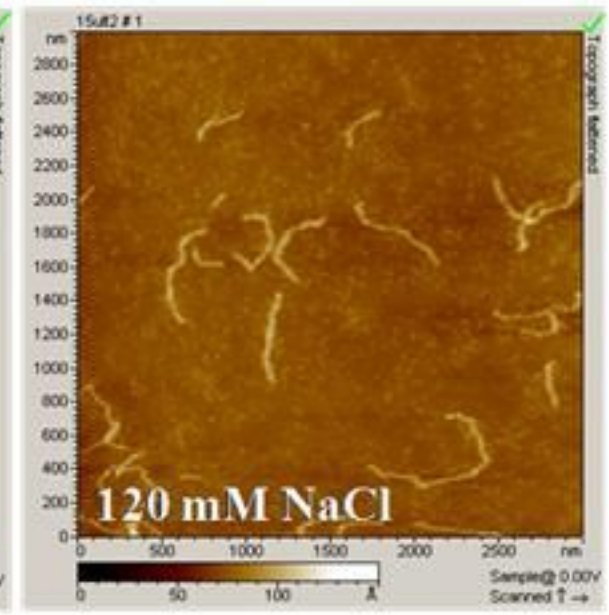
120 mM NaCl

Pathway I

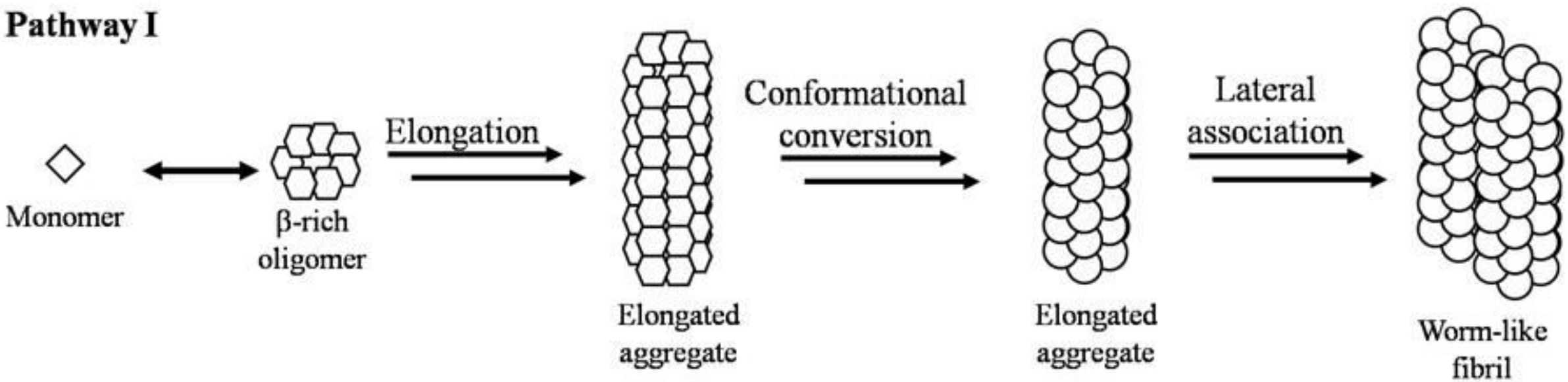

Pathway II

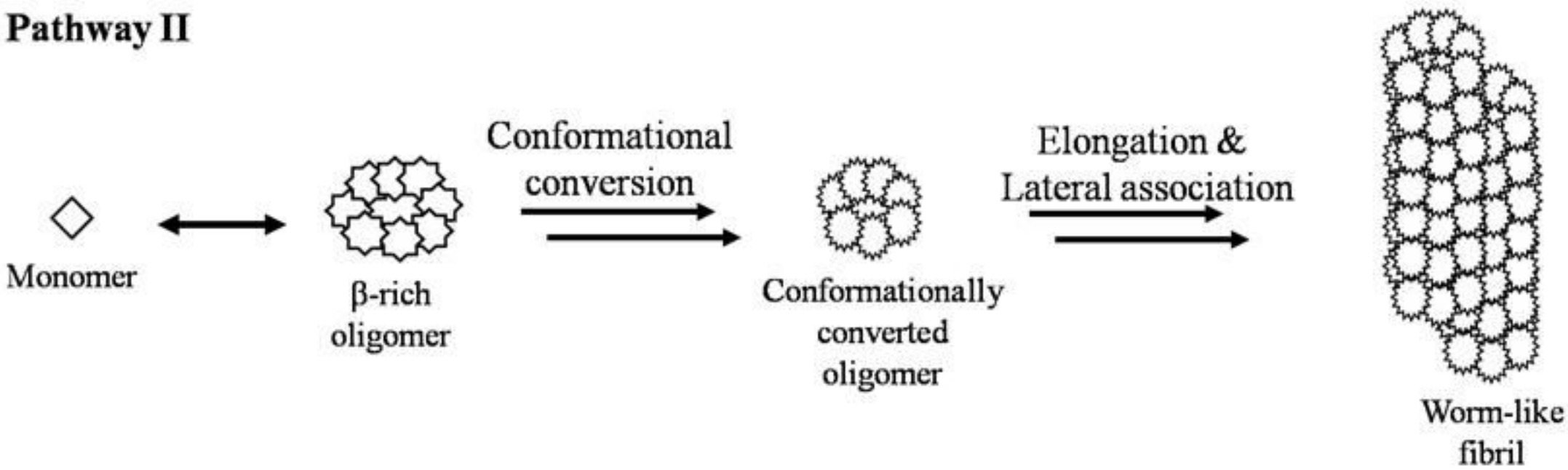

The Prion protein also forms long straight fibrils

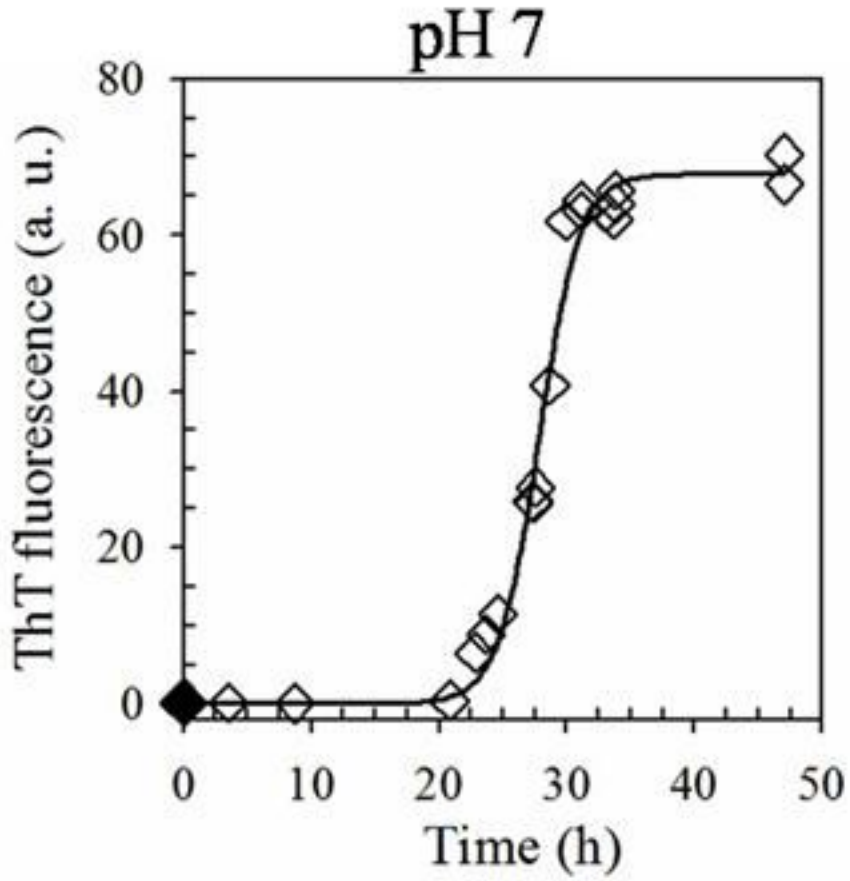

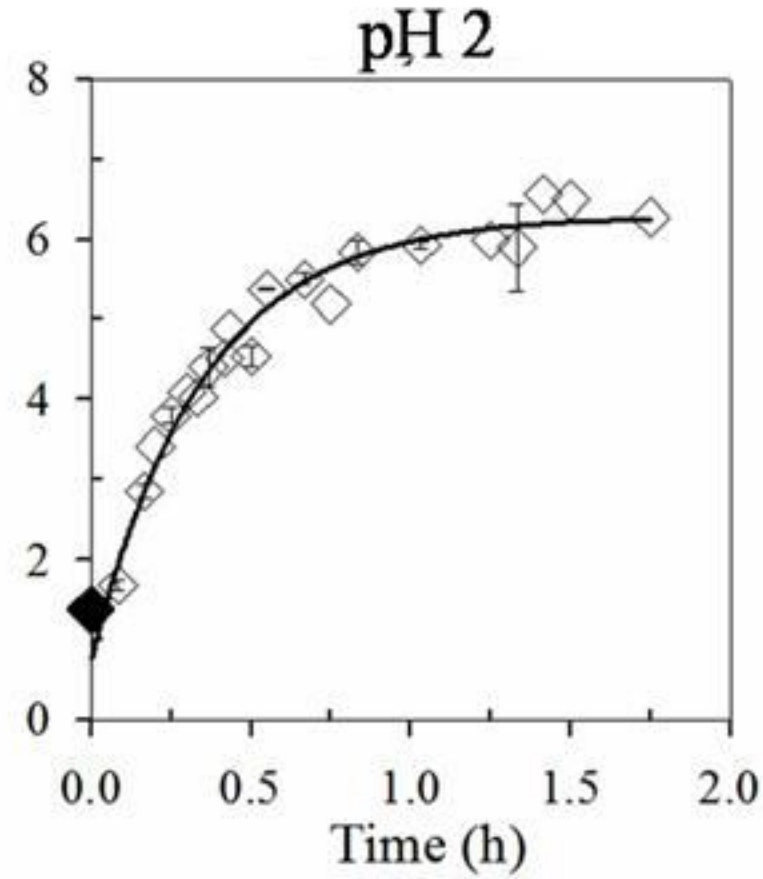

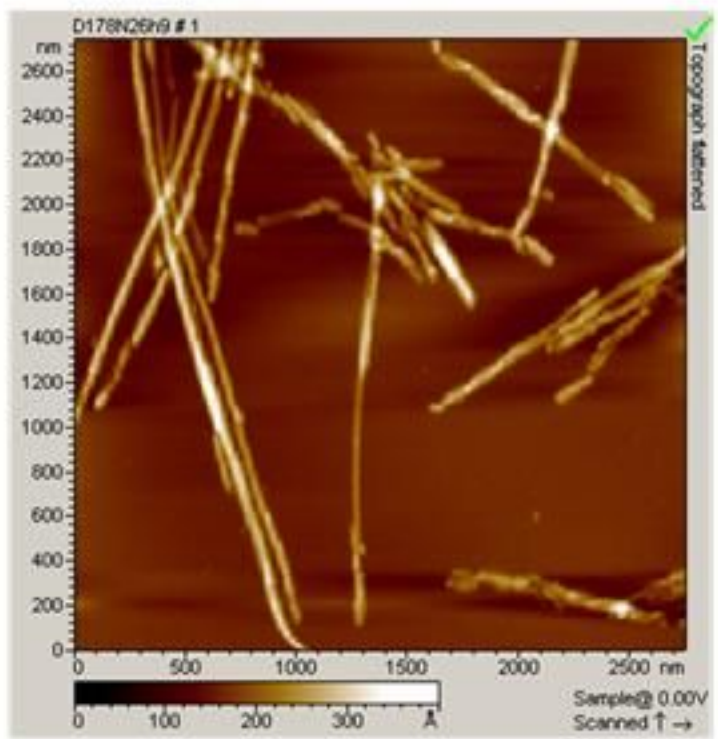

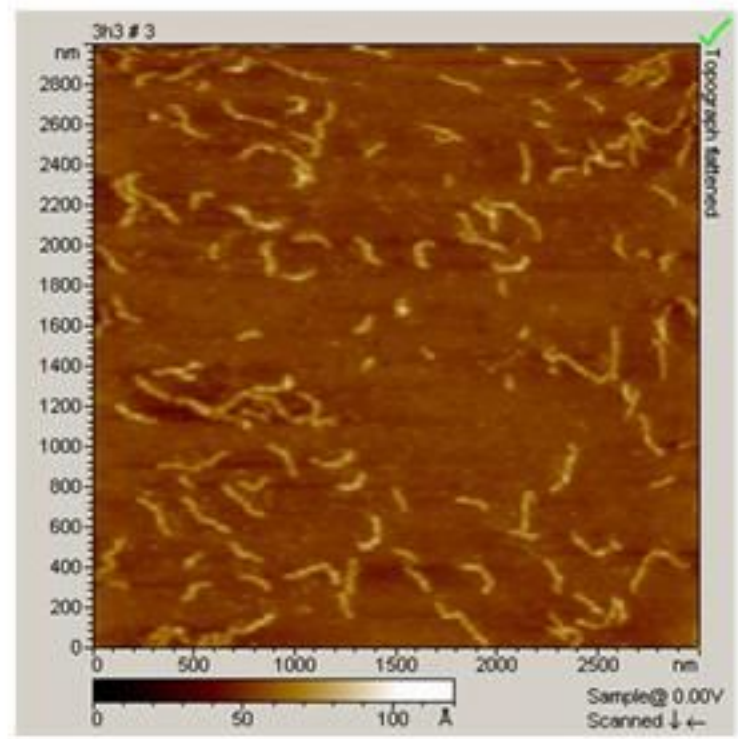

Alternative pathways for amyloid formation

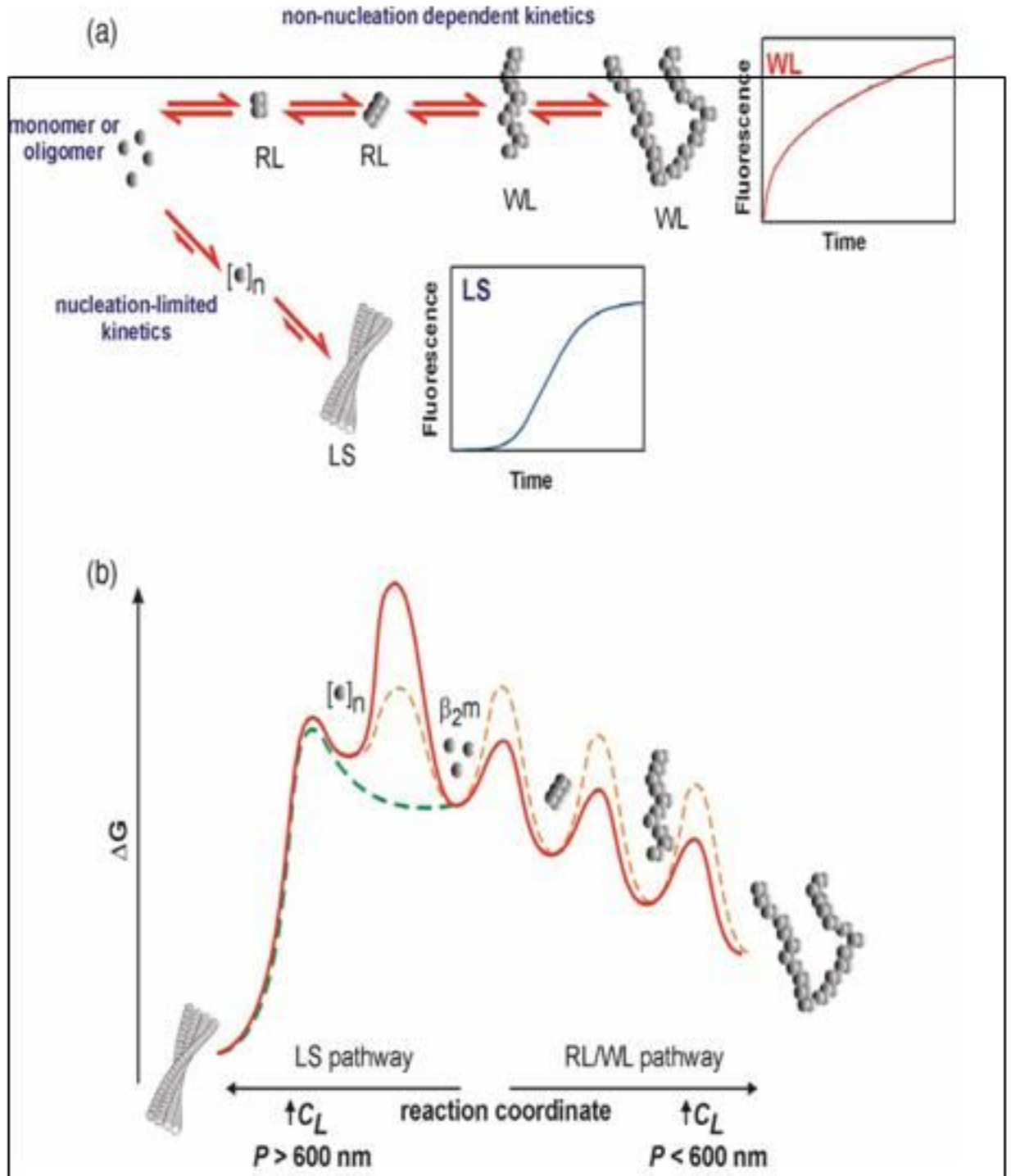

Gosal et al. (2005) JMB

The long straight fibrils are ribbons

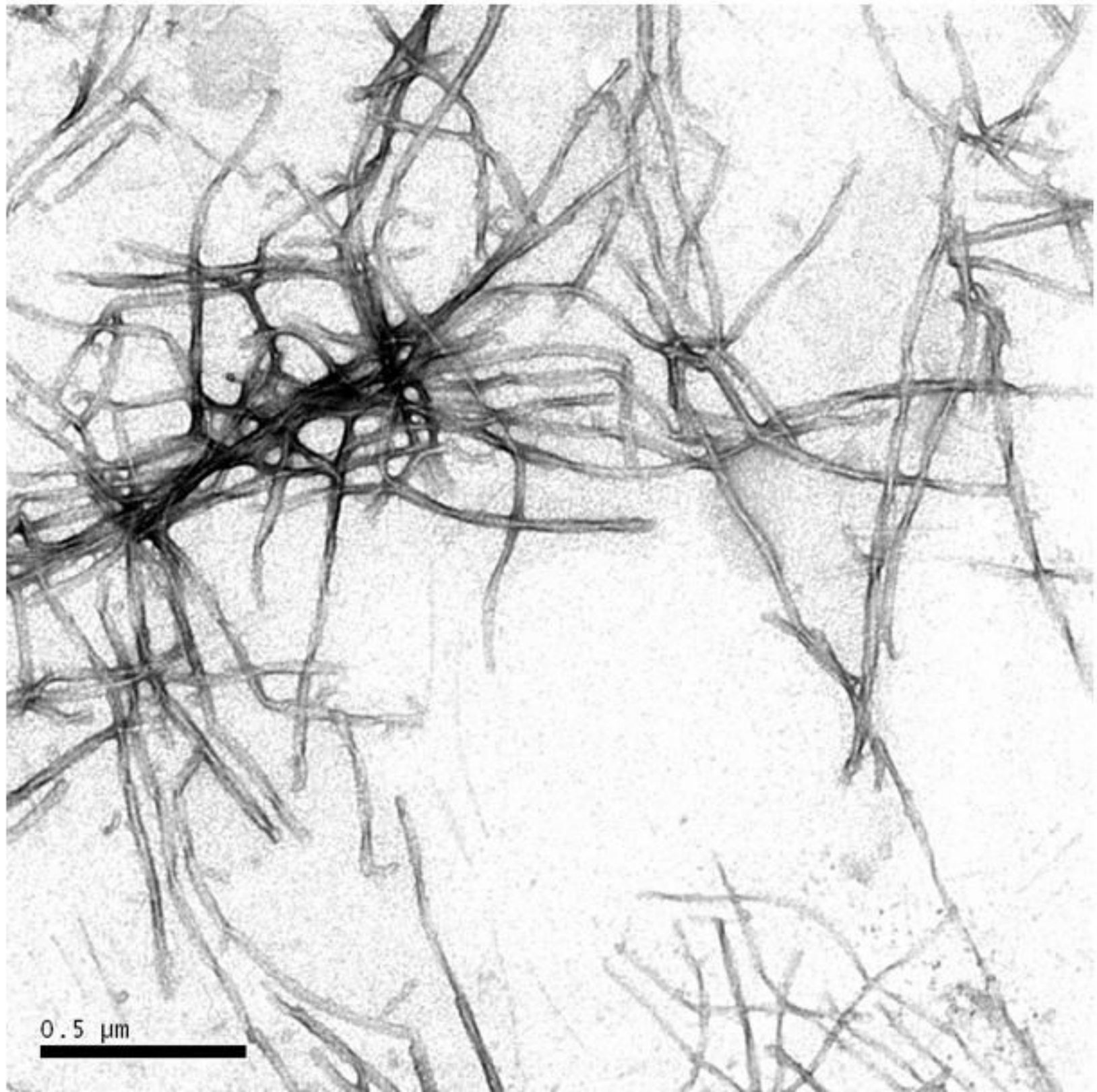

Oligomers are formed during the lag phase of prion protein aggregation

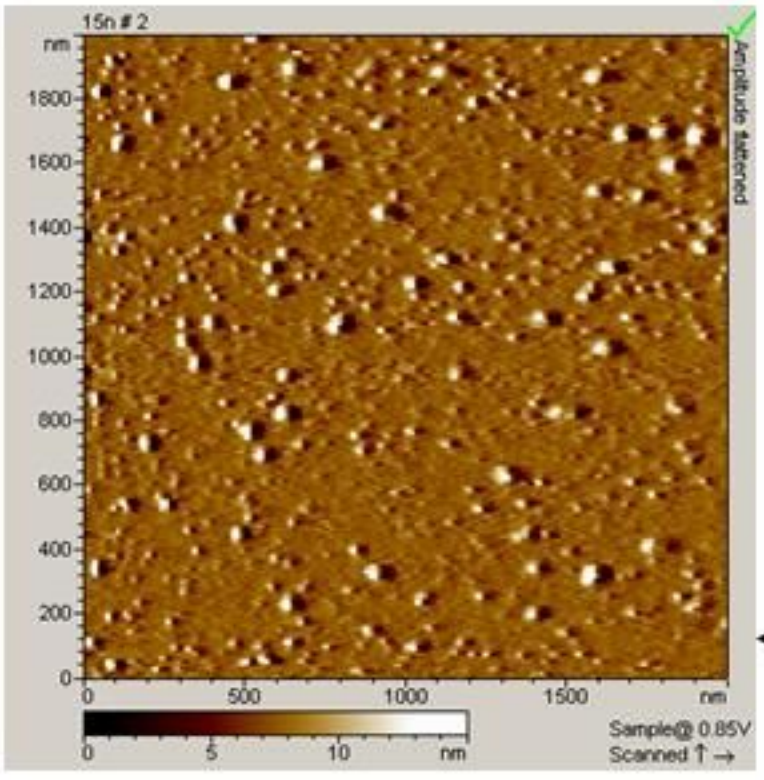

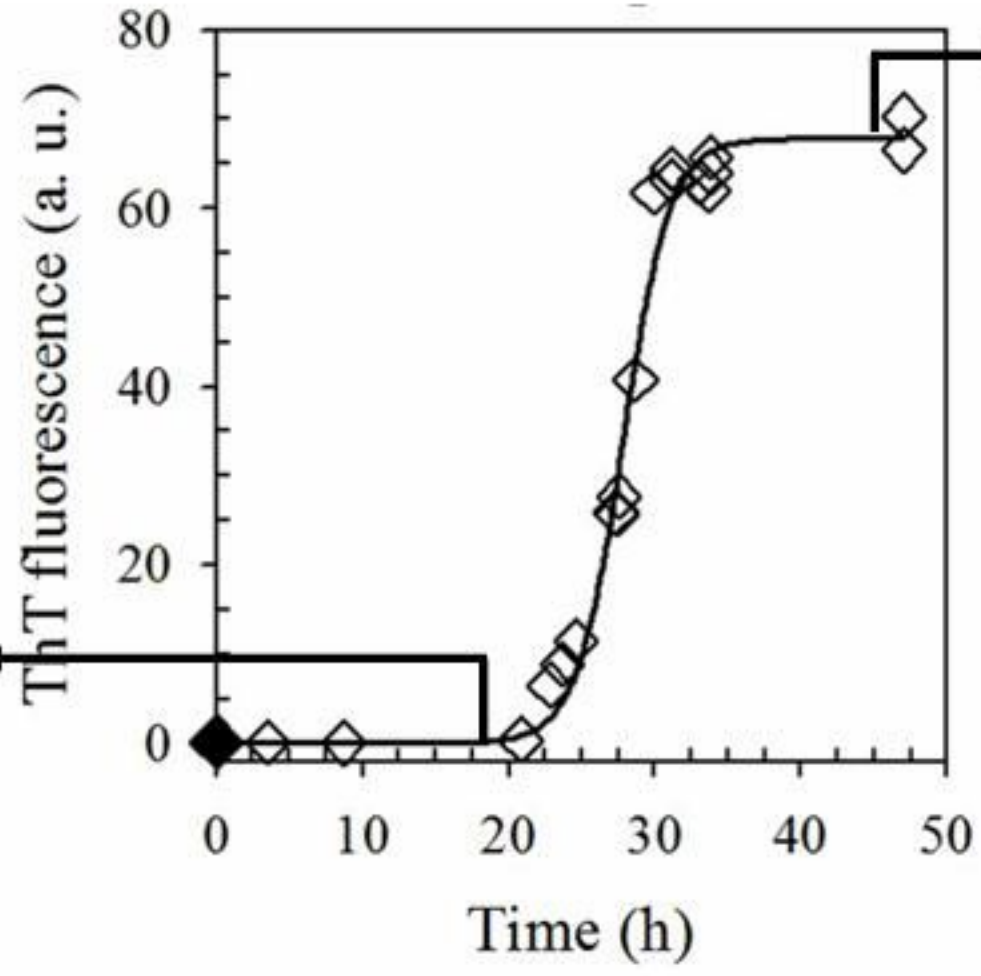

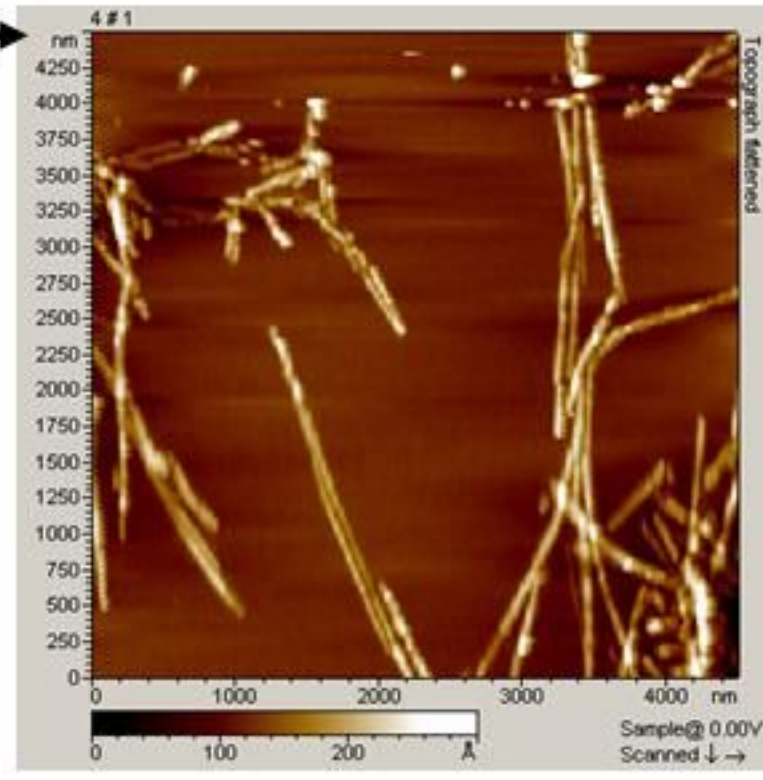

The model system-tau

- Tau is an **intrinsically disordered protein** as determined by CD, FTIR spectroscopy, EM etc.

Mandelkow *et. al., 2007*

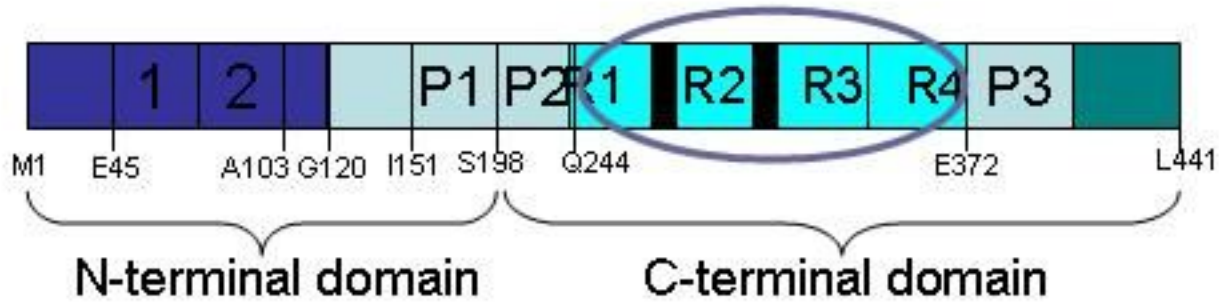

- The repeat domain of tau **(tau4RD)** is the microtubule-binding domain

- 144 amino acids
- Isoelectric point- 9.68
- MW- 15607 Da
- Sequence information
  - No Trp, 1 Tyr, 2 Phe, 2 Cys

Kinetics of aggregation as well as the fibrils formed are different in Tris and PBS buffers

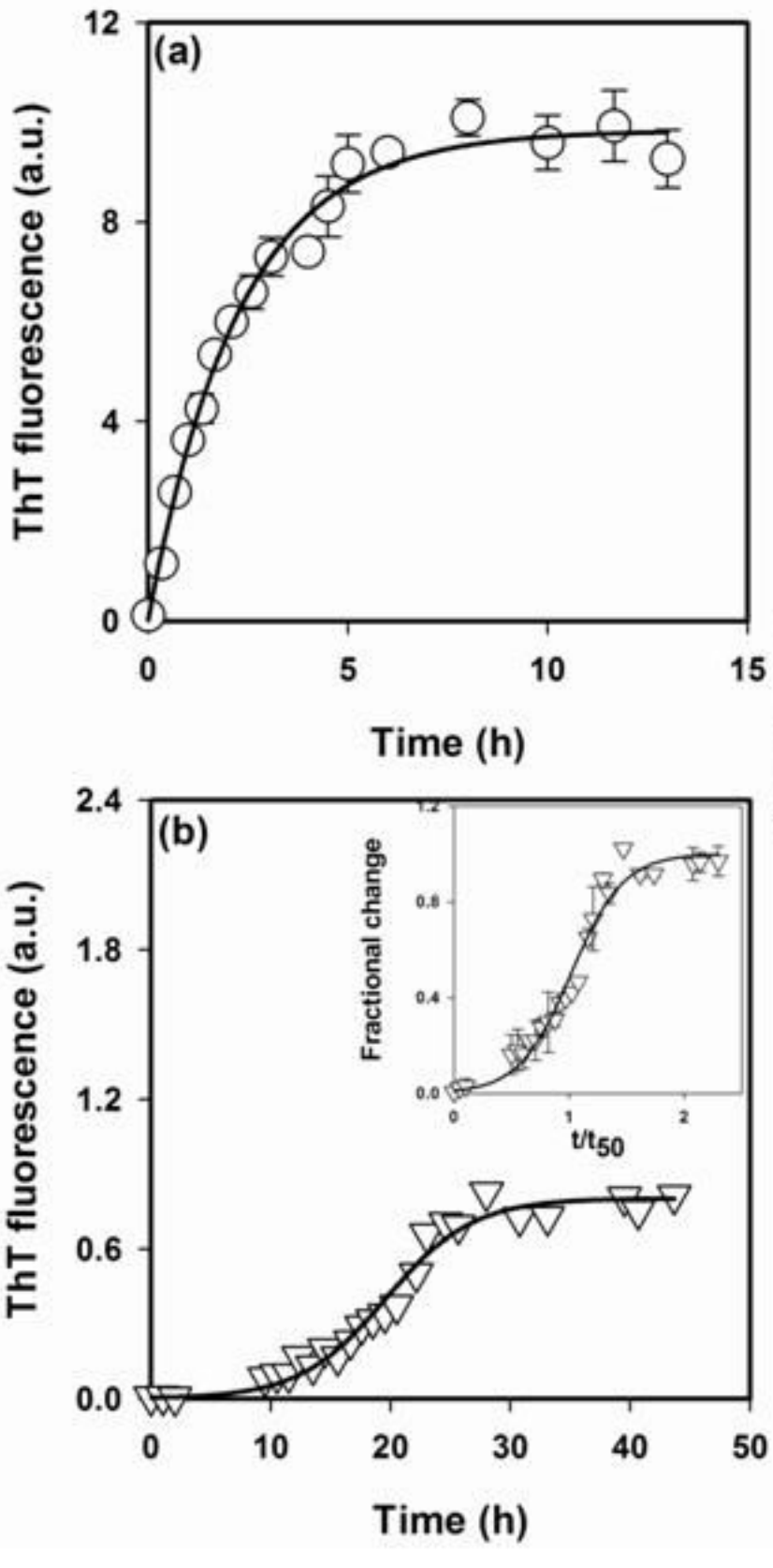

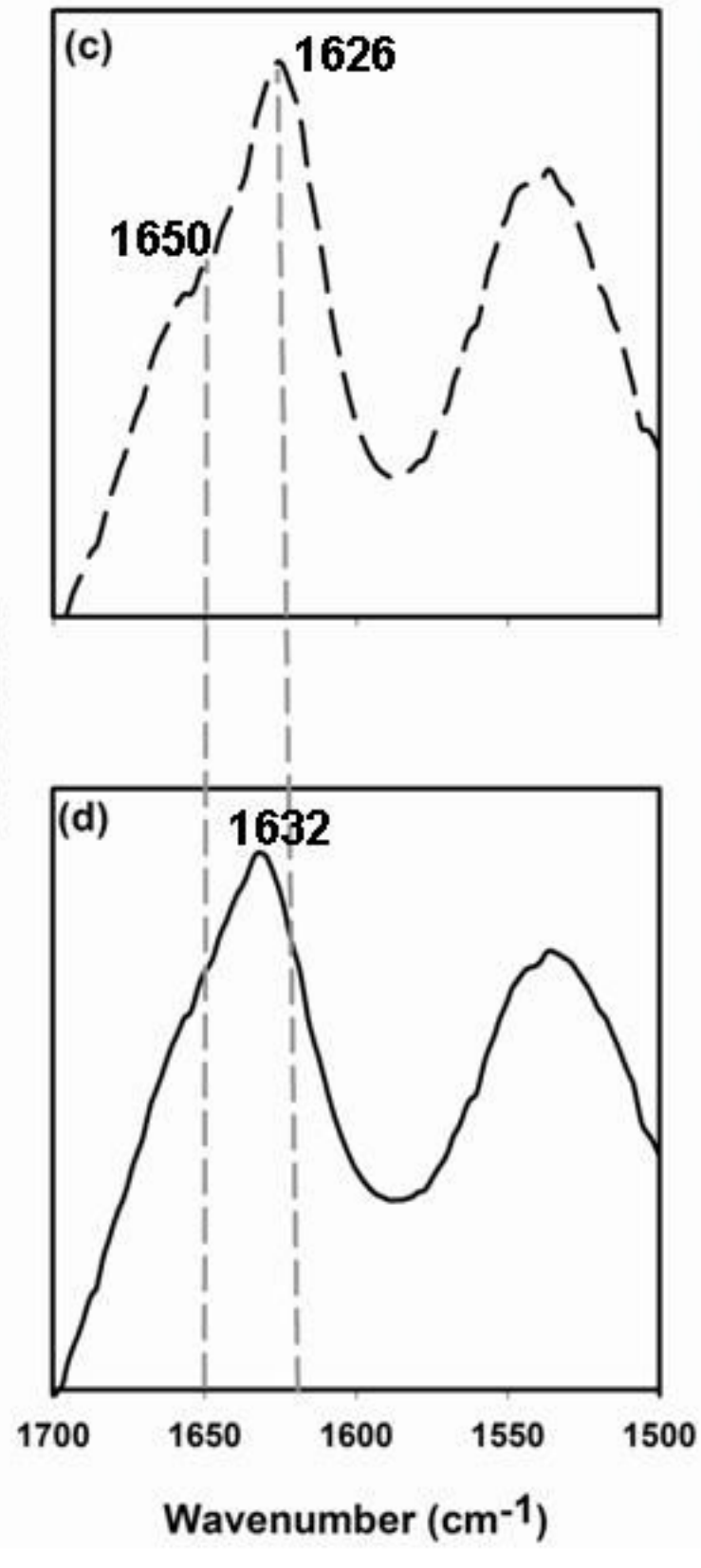

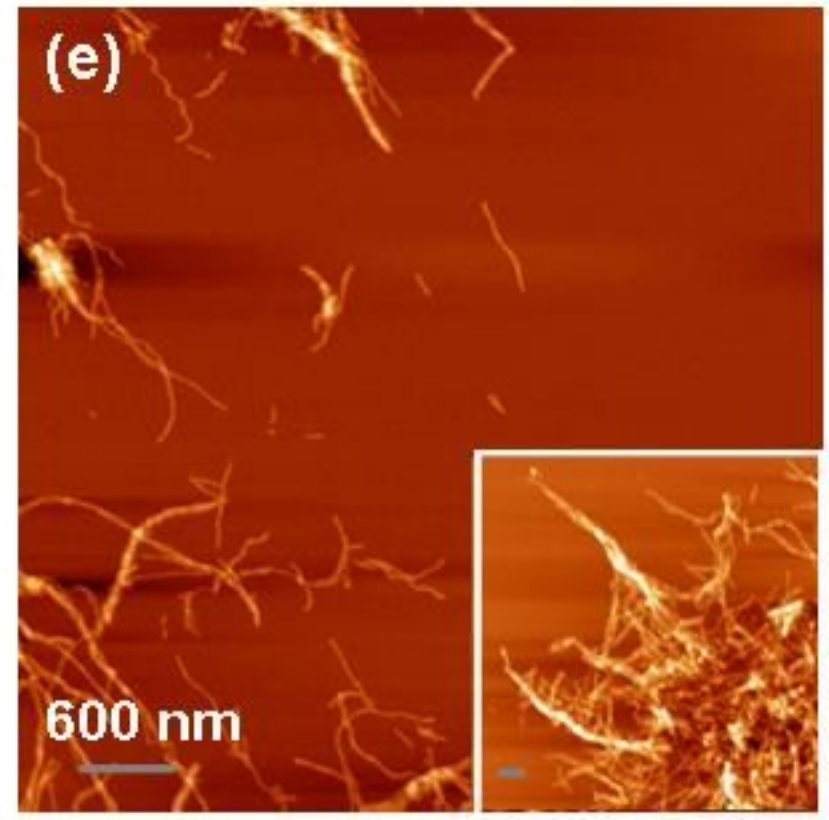

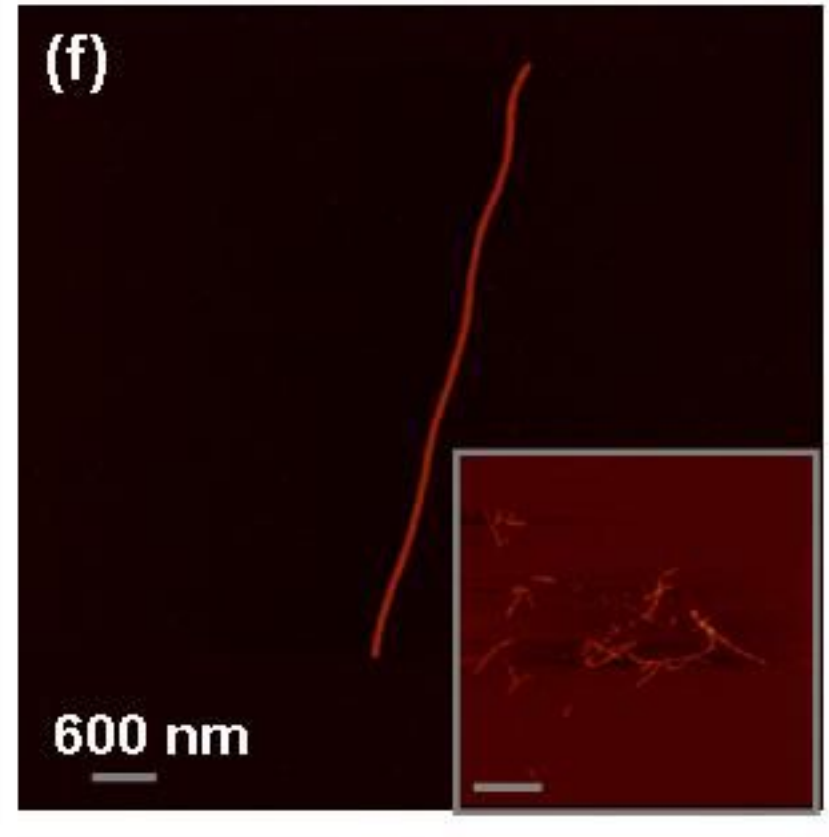

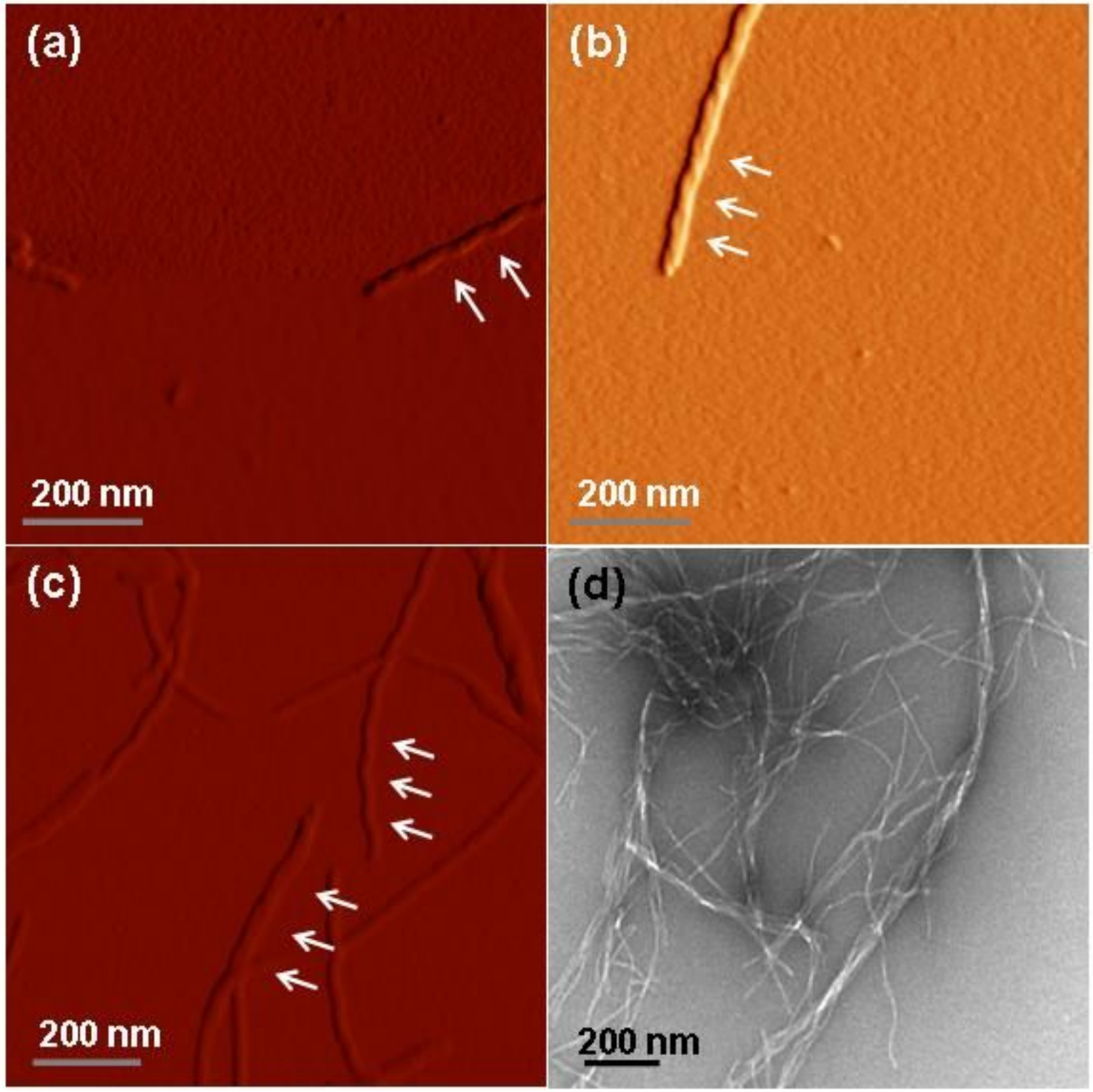

Tau fibrils are paired helical filaments with a characteristic 80 nm twist

Heparin-induced fibrillation of the tau protein

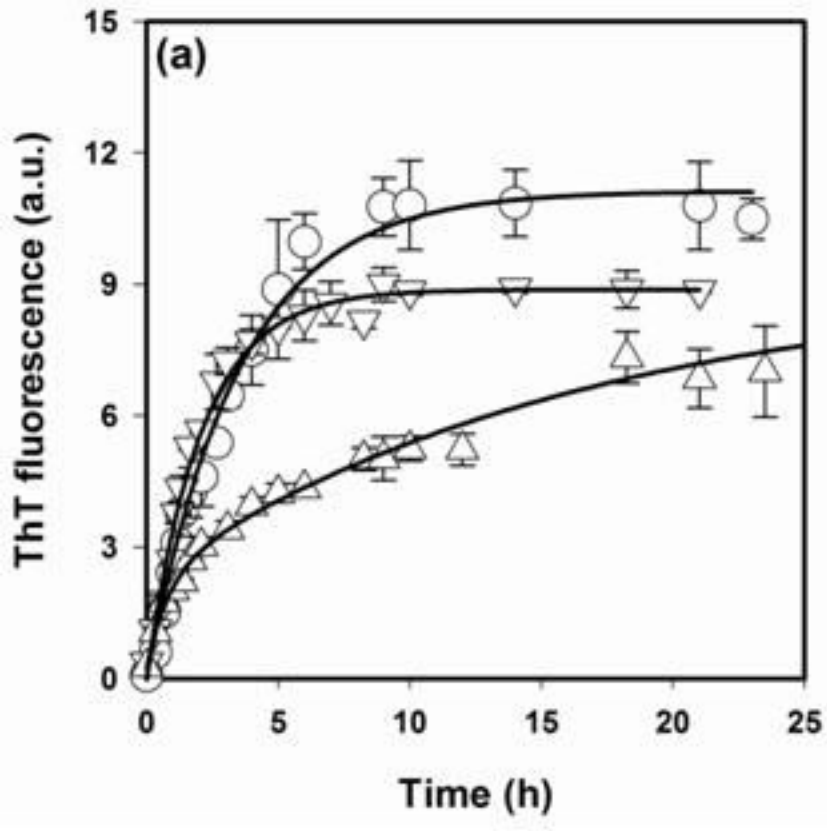

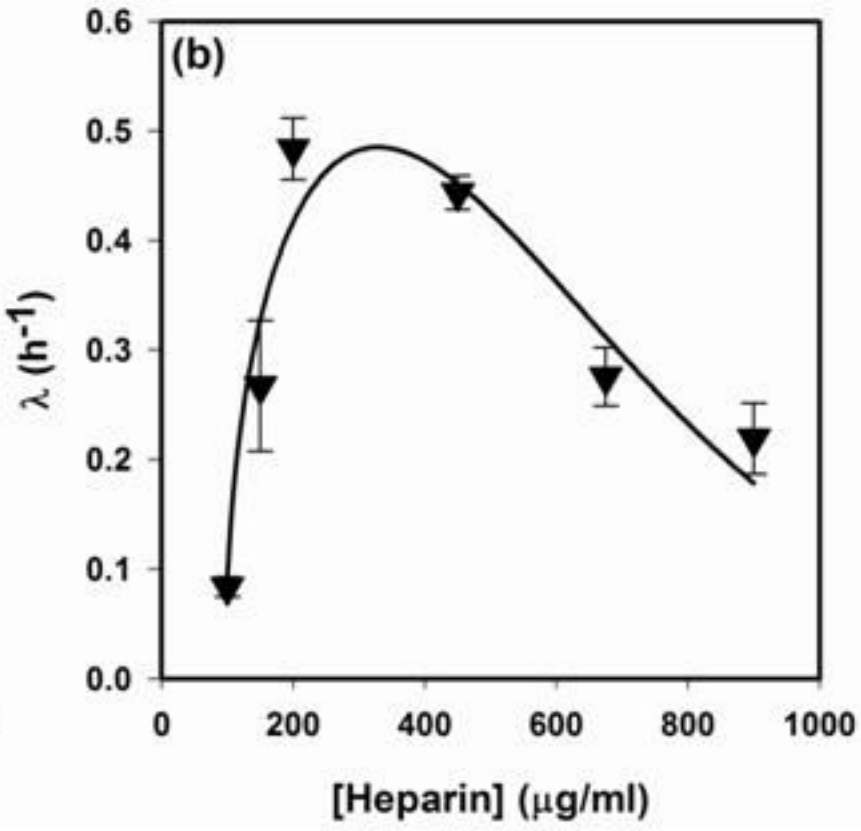

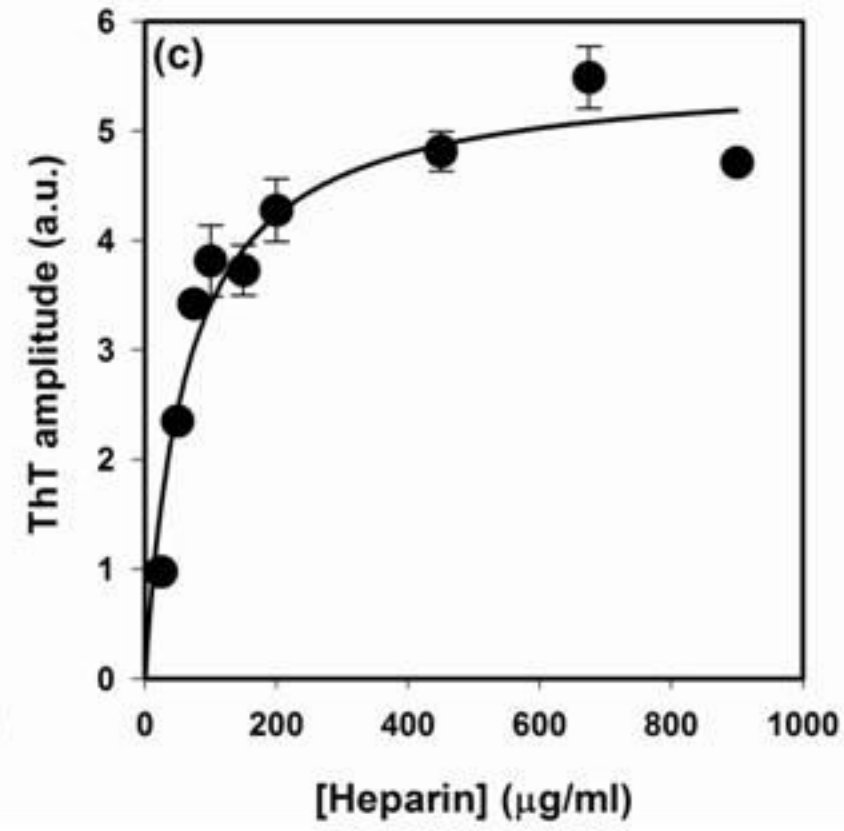

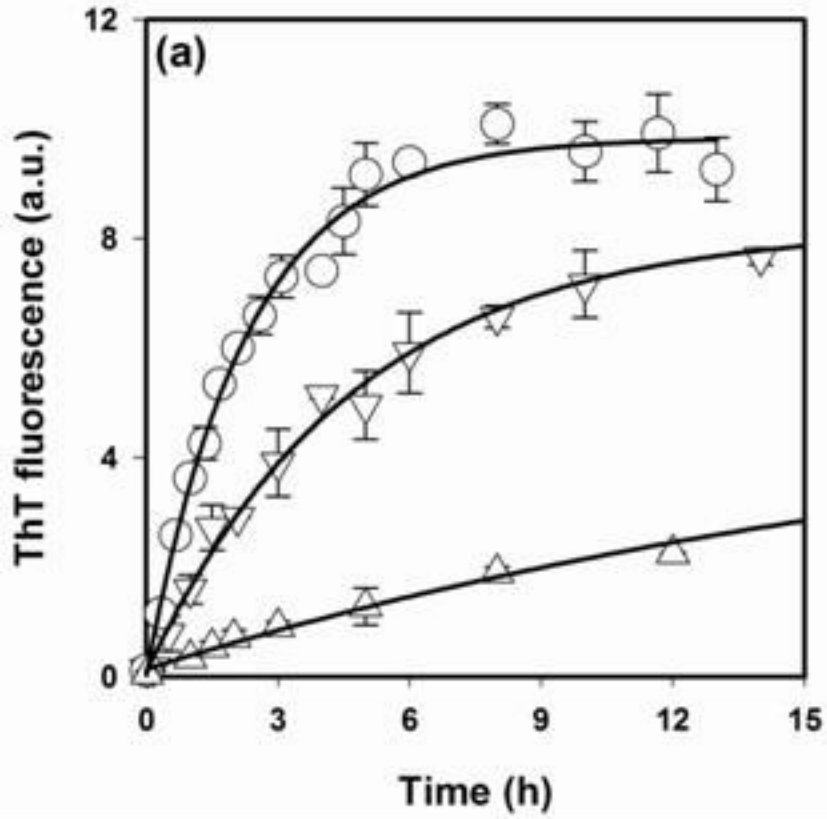
(a)
ThT fluorescence (a.u.)
Time (h)
0
4
8
12
0
3
6
9
12
15

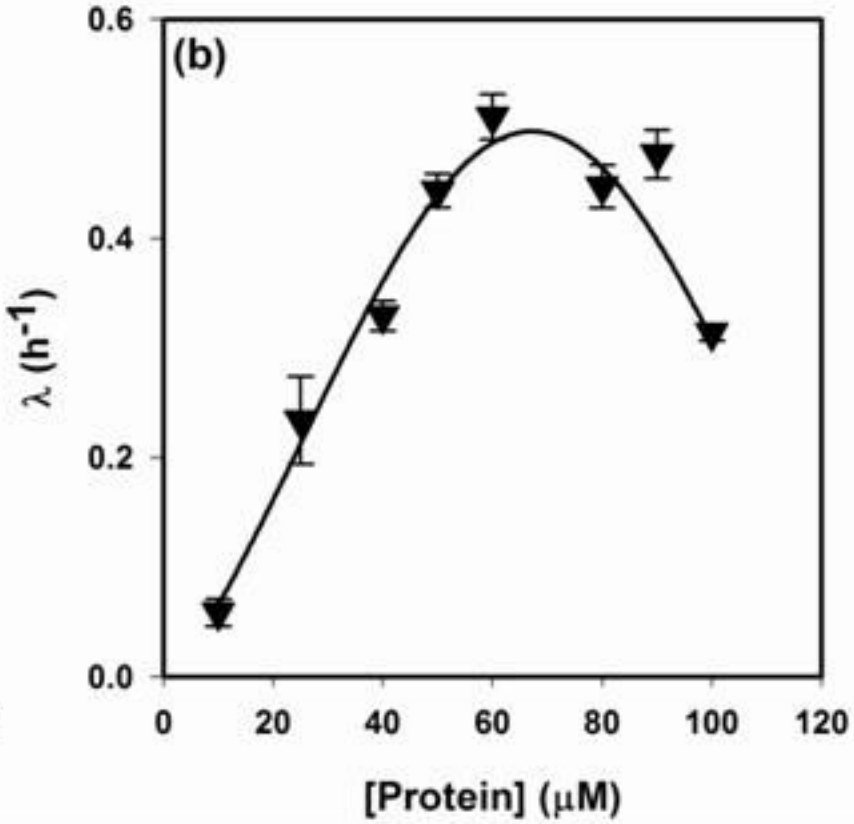
(b)
λ (h-1)
[Protein] (μM)
0.0
0.2
0.4
0.6
0
20
40
60
80
100
120

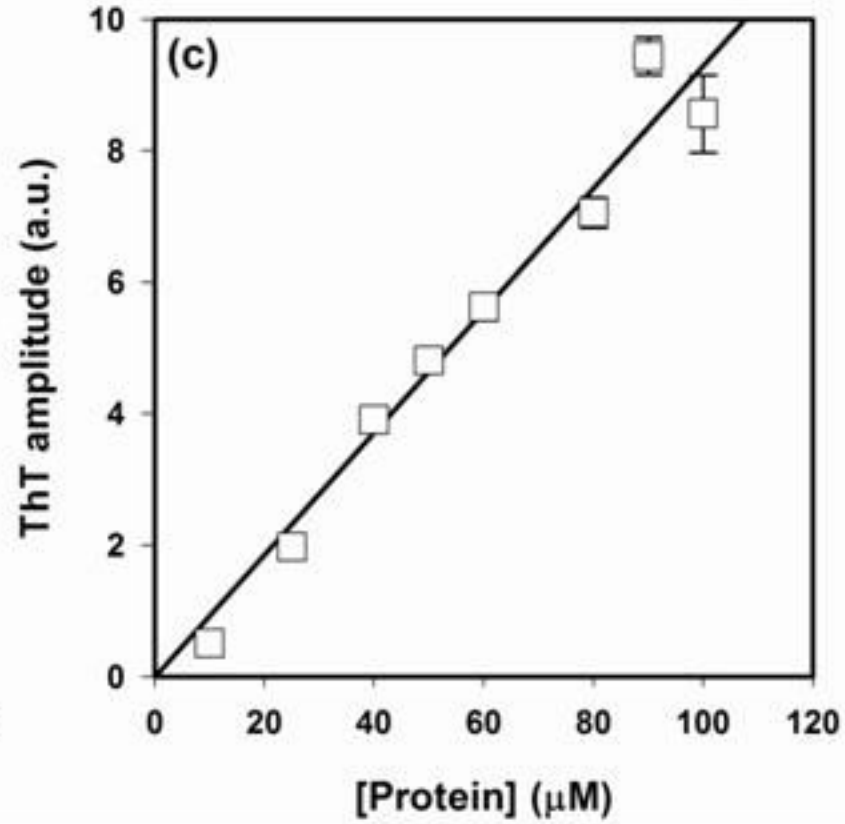
(c)
ThT amplitude (a.u.)
[Protein] (μM)
0
2
4
6
8
10
0
20
40
60
80
100
120

Short rod-like protofibrils are observed during fibril formation

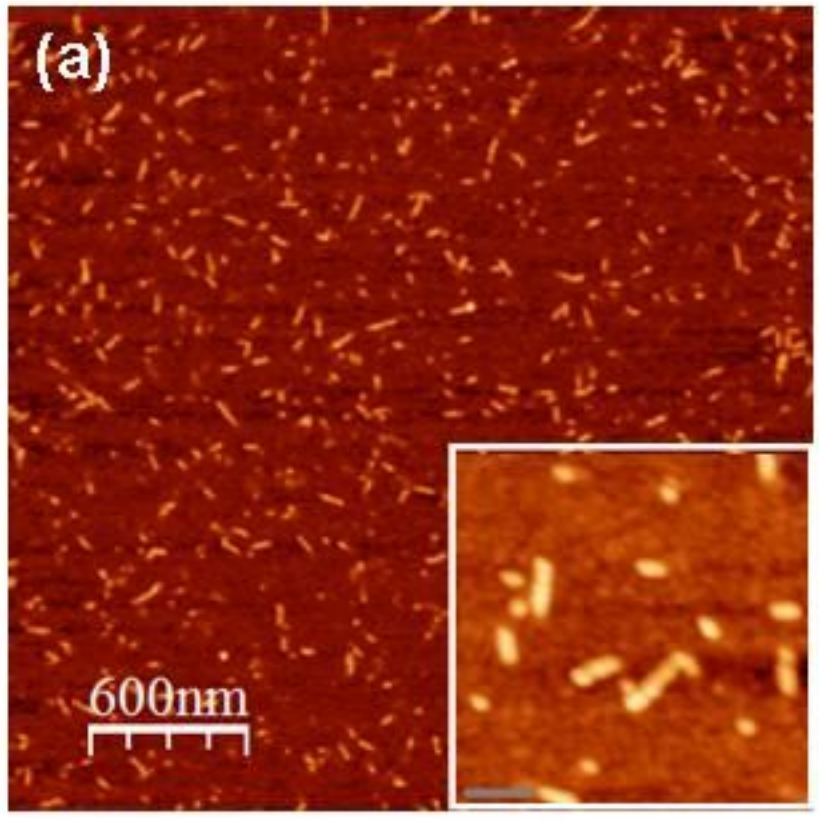

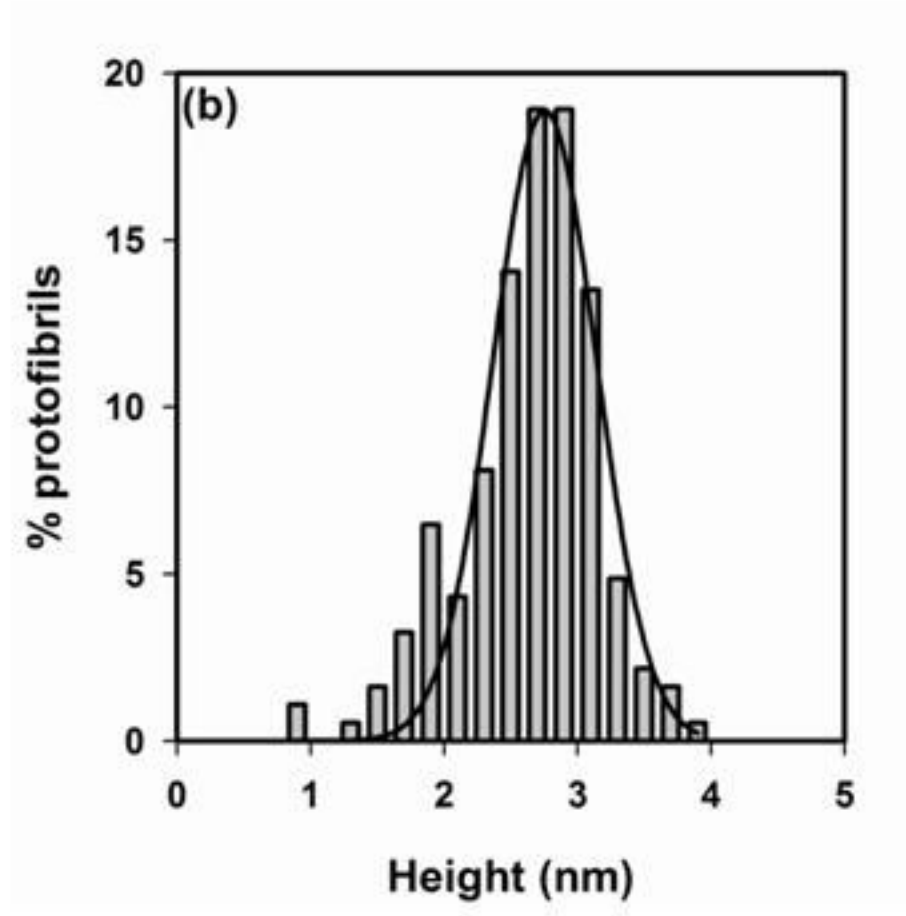

How do amyloid fibrils form?

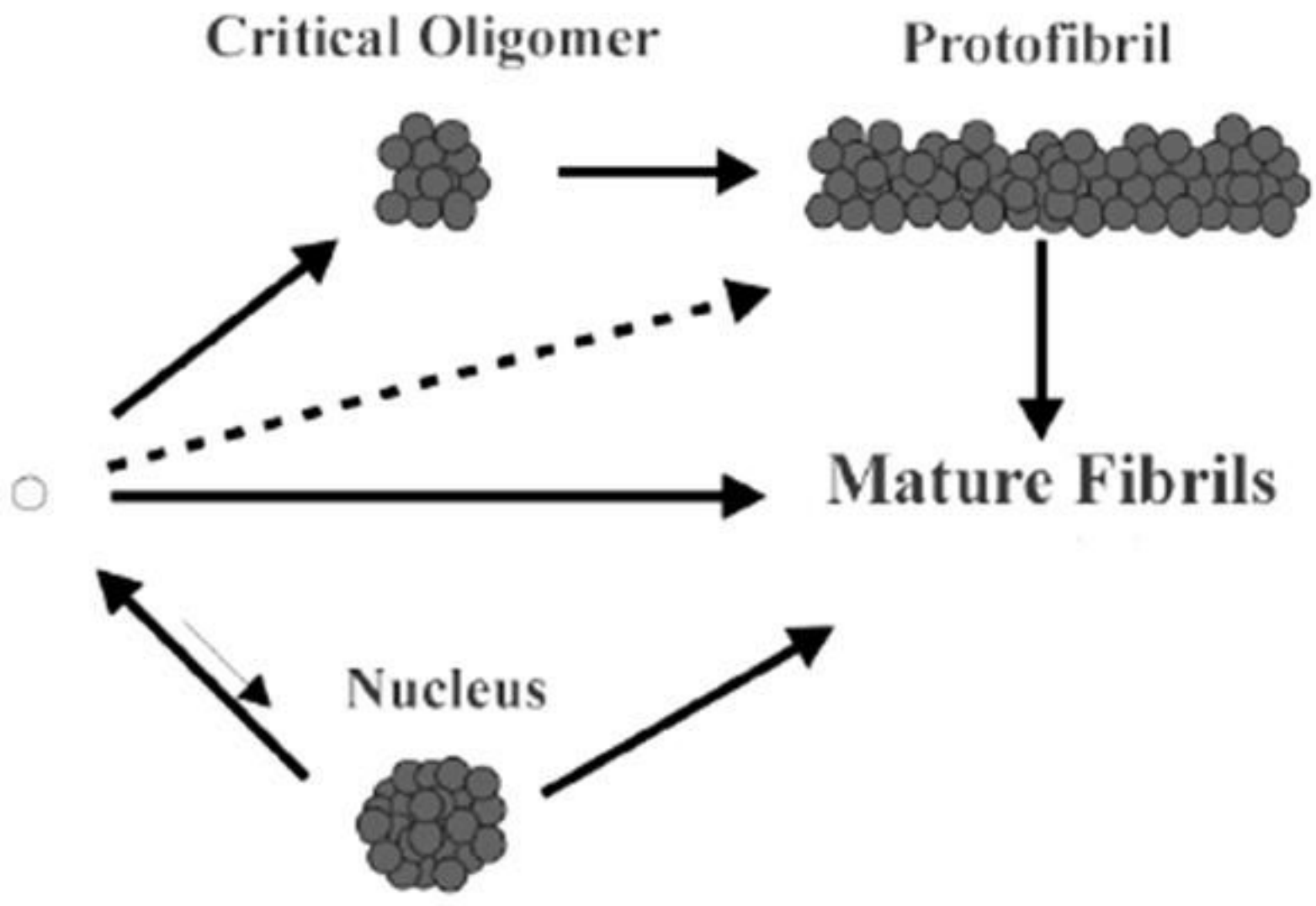

J. Mol. Biol. (2003), 325, 135-148

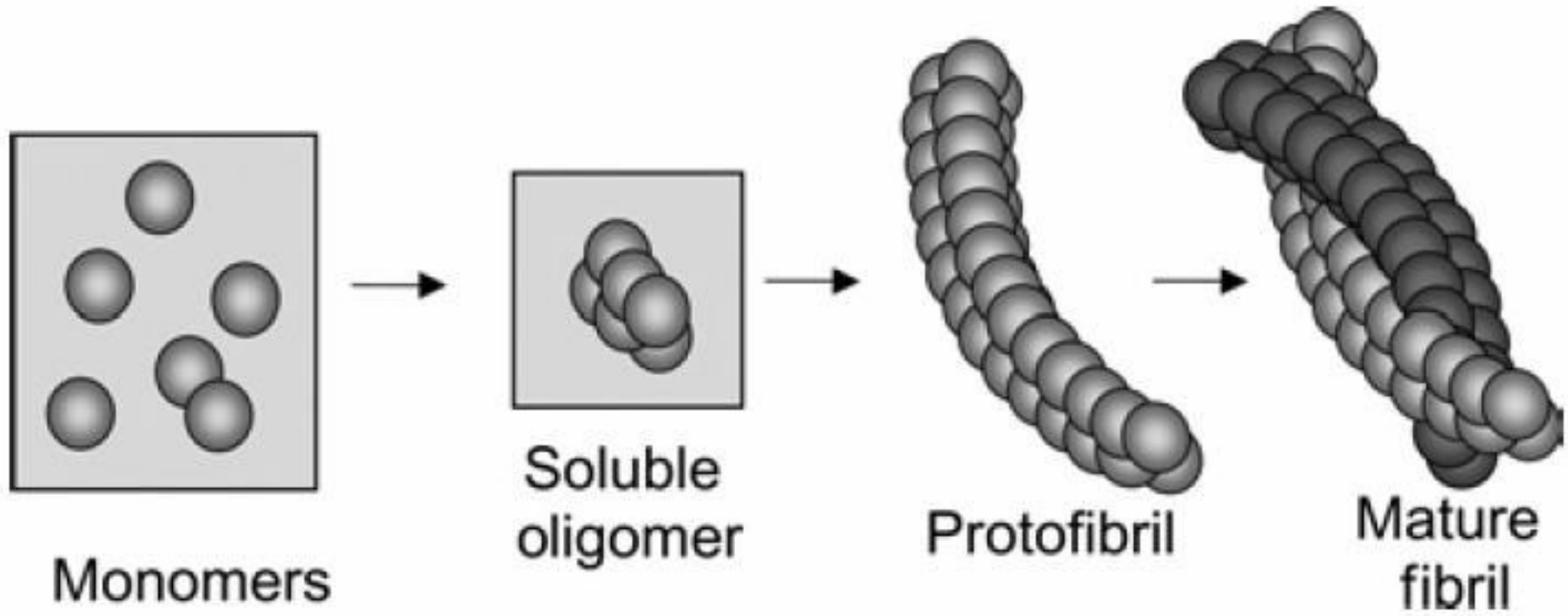

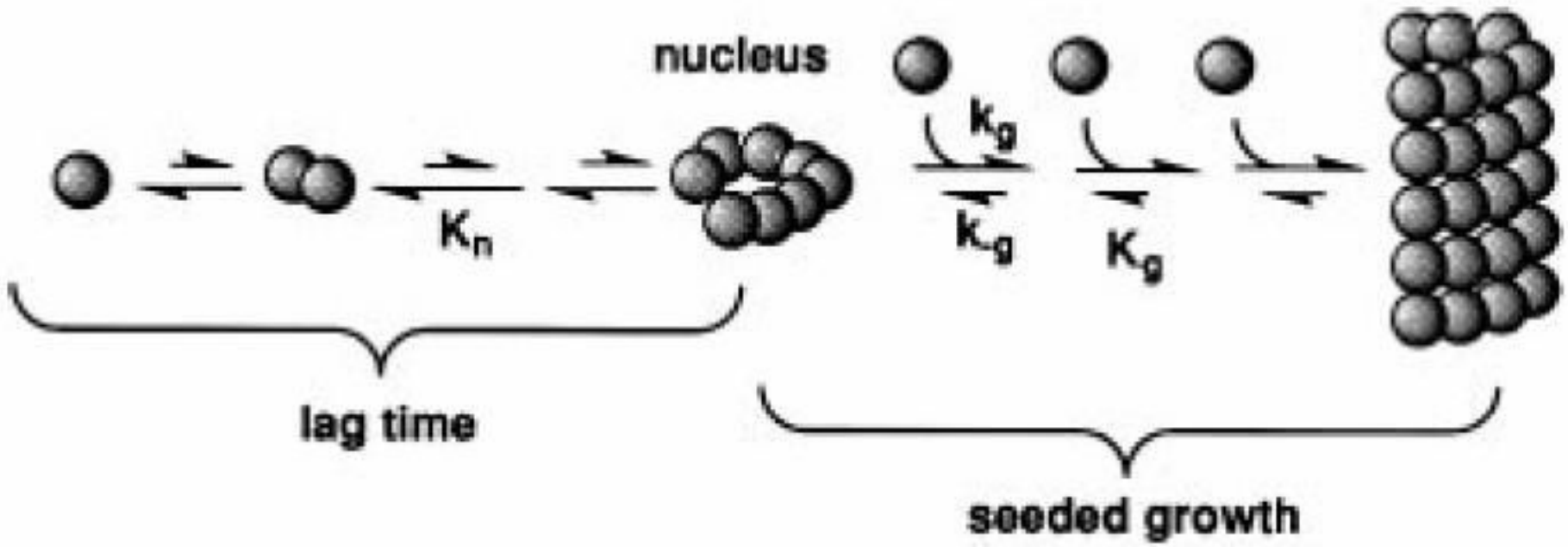

Figure 2 The simplest possible nucleation-dependent mechanism, showing a series of unfavorable protein-protein association equilibria (K_n) leading to an unstable nucleus, followed by a series of favorable equilibria (K_g), culminating in fibril formation. The critical concentration phenomenon results from the shift from unfavorable (K_n) to favorable (K_g) equilibria.